Biodiesel production from municipal waste using lipase catalysis

JB van der Merwe

orcid.org/0000-0001-5752-6394

Dissertation accepted in fulfilment of the requirements for the degree *Master of Engineering in Chemical Engineering* at the North-West University

Supervisor: Dr RJ Venter

Co-supervisor: Prof S Marx

Graduation: May 2022

Student number: 25882996

ACKNOWLEDGEMENTS

'Winners never quit, and quitters never win' – Vince Lombardi

I would like to express my appreciation to the following people for their contribution to this study and support throughout the year:

- Our Heavenly Father without whom nothing would be possible.
- My husband, Jean-Otto Smit, for his patience and support throughout my studies.
- My parents, Hendrik and Elana van der Merwe, for always reminding us of the saying that winners never quit, and quitters never win.
- My best friend, Vian van der Merwe, for all the long hours spent on campus and support throughout my studies.
- Prof. Sanette Marx for her advice and guidance.
- René Becker for her assistance, support, and kindness towards students in the laboratory.
- Dr Roelf Venter for his leadership, support, advice, and guidance.
- Dr LC Muller for the use of the GPC and assistance with the NMR.
- NRF for their financial support.

ABSTRACT

Municipal solid waste (MSW) and sewage sludge are attractive feedstocks for biofuel production through hydrothermal liquefaction (HTL) due to high moisture content, availability, and low costs. HTL has the advantage of not requiring any energy-intensive dewatering and drying processes compared to some other processes. HTL-biocrude has unwanted properties, such as a high water content, high viscosity, high ash, and high oxygen content, which limit the application thereof. Enzymatic esterification and transesterification are promising methods for the upgrading of biocrude that need to be further investigated. Enzymatic esterification of biocrude oil should be studied in detail to evaluate the effect of lipase catalysis on other biocrude components, not only on fatty acids; and the effectiveness of the overall fatty acid methyl ester (FAME) conversion should be determined.

The HTL experiments were conducted in a high-pressure batch type autoclave reactor with simulated municipal solid waste and sewage sludge as feedstock and solvent. The reaction temperature chosen was 300 °C with a residence time of 20 minutes. For each esterification experiment, a 50 mL pear-shaped reaction flask was used in which 0.1 g of lipase (Novozym 435) and 1 g of biocrude oil (2.63 mmol) were weighed to obtain a 10 mass % enzyme loading. A magnet for stirring and an appropriate amount of methanol was added to the reaction flask to obtain the desired methanol to oil molar ratio. Methanolysis continued for 6 hours under constant stirring at 12.5 Hz.

The results of the HTL of municipal waste (MW) showed the following product yields for: biocrude (6.80 mass %), biochar (14.82 mass %), biogas (9.52 mass %), and aqueous product (57.84 mass %). The biocrude was further characterised and a higher heating value (HHV) of 31.20 MJ/kg, a moisture content of 3.98 ± 0.85 mass %, a methyl ester and fatty acid content of 1.2 ± 0.21 % and 41.5 ± 3.38 % were obtained. The enzymatic esterification resulted in the following optimum conditions: reaction time of 6 hours at 30 °C and an oil to methanol molar ratio of 1:3 with a constant loading of 10 mass % Novozym 435 (N435). At the optimum conditions, a FAME conversion of 95.83 % was achieved with a HHV of 34.95 ± 1.22 MJ/kg and a methyl ester yield of 48.66 ± 5.40 %.

Various esterification conditions were investigated to observe their effect on the FAME conversion. The FAME conversion increased as the reaction time increased until the optimum reaction time was reached. Furthermore, a decrease in the FAME conversion was observed due to alcohol inhibition that was attributed to the denaturation of the enzyme. No significant difference in the FAME conversion was observed at the different temperatures.

The boiling range distribution of the biocrude oil was investigated and compared with the produced biodiesel for different reaction conditions. There was a slight decrease in the kerosene fraction and a significant increase in the diesel fraction due to the conversion of fatty acids to FAME. There was also a significant decrease in the heavy fraction that could be explained by the fact that the boiling point of the methyl ester of a fatty acid was lower than the boiling point of the fatty acid itself. This resulted in the fatty acids with boiling points in the heavy fractions boiling range to be observed in the diesel fraction boiling range. The only significant increase observed for each fraction was the esters.

Used N435 catalyst, acetone-regenerated N435 catalyst, as well as - tetrahydrofuran (THF), hexane-, dimethylsulfoxide- (DMSO), tert-butanol- and acetonitrile regenerated N435 catalyst were reused, and the results demonstrated that used N435 catalyst could be reused without solvent regeneration. However, acetone-regenerated N435 catalyst obtained insignificantly higher conversions. The reusability of N435 catalyst and acetone-regenerated N435 catalyst obtained a FAME conversion of 83.60 % and 86.34 %, respectively, after four cycles.

The results obtained for lipase-catalysed esterification indicated that it is a promising route for MW generated biocrude oil upgrading using mild reaction conditions compared to thermochemical routes. It was also observed that N435 catalyst was highly stable in the reaction environment and could be reused and still obtain high FAME conversions.

Keywords: municipal waste, hydrothermal liquefaction, enzymatic esterification, Novozym 435, lipase regeneration

TABLE OF CONTENTS

NOMENCLATURE

Abbreviation	Description
daf	dry, ash-free
HTL	hydrothermal liquefaction
MSW	municipal solid waste
MW	municipal waste
N435	Novozym 435
N_2	nitrogen gas
DMSO	dimethyl sulfoxide
THF	tetrahydrofuran
FAME	fatty acid methyl ester
Mn	number averaged molecular weight
PDI	polydispersity index
%	percent
mass %	mass percent
°C	degrees Celsius
mm	millimetre
m	metre
min	minute
h	hour
K	Kelvin

Hz	Hertz
Vol	volume
mL	millilitre
µL	microlitre
L	litre
g	gram
mg	milligram
mol	Mole
kg	kilogram
mmol	Millimole
MW	molecular weight
MPa	Mega Pascal
MJ	Mega Joule
SANS	South African National Standards
$CDCl_3$	deuterated chloroform
^1H NMRS	proton nuclear magnetic resonance spectroscopy
GCMS	gas chromatography mass spectrometry
GPC	gel permeation chromatography
FTIR	Fourier-transform infrared spectroscopy
HHV	higher heating value

LIST OF TABLES

LIST OF FIGURES

CHAPTER 1: INTRODUCTION

Chapter 1 provides a general overview of the contents of this study. The background and motivation are discussed in Section 1.1 and the problem statement is provided in Section 1.2. Section 1.4 lists the aim and objectives while the project scope is discussed in Section 1.4.

1.1 Background and motivation

The increase in urbanisation, globalisation, and industrialisation has led to a significant increase in the demand for food security, energy, and water. In 2016 the Paris Agreement was signed by 175 states, including South Africa due to fossil fuel emissions that have led to global climate change (Falkner, 2016). Fossil fuels, such as petroleum, heavy oils, coal, and natural gas are used to produce energy for industrial, transportation, and domestic use (Huang *et al.*, 2012). Fossil fuel emissions will decrease significantly if biofuels are used as an alternative to conventional fuels (Huang *et al.*, 2012; Karavalakis *et al.*, 2011).

Biofuels are classified as either primary or secondary biofuels as discussed in Section 2.2 (Alam *et al.*, 2015; Rodionova *et al.*, 2017). First-, second- and third-generation biofuels are classified as secondary biofuels based on the production technology used, type of biomass, and limitations of the biofuels produced (Huang *et al.*, 2012; Guo *et al*., 2015; Rodionova *et al.*, 2017). First-generation biofuel is produced by transesterification of edible oil such as animal fats, palm- ,soya- , rapeseed-, and sunflower oil (Huang *et al.*, 2012; Guo *et al*., 2015; Rodionova *et al.*, 2017). Second-generation biofuel is produced by the processing of inedible biomass such as municipal waste, used cooking oil, lignocellulosic materials, and agricultural wastes. Third-generation biofuel is produced by the processing of microbes and microalgae (Huang *et al.*, 2012; Guo *et al*., 2015; Rodionova *et al.*, 2017).

Recent studies show that developments on the feasibility of second-generation biofuel production have gained interest; particularly, the use of lignocellulosic biomass consisting of agricultural or municipal waste as sustainable feedstock that does not affect food security (Dong *et al.*, 2019). Second-generation biofuels are produced by thermochemical processes such as HTL and pyrolysis that have been extensively studied (Wang *et al.*, 2018). Furthermore, HTL is a thermal depolymerization process that converts liquid biomass into biocrude oil in a high temperature and high pressure environment. South Africa's agricultural sector are consuming a significant amount of the available water resources (Pradhan & Mbohwa, 2014). The unpredictable rainfall patterns and increasing population growth impact negatively on food security. It is unfeasible to use crops, such as sugarcane and maize, for the production of biofuels due to the limited availability of arable land, increasing crop prices, and production and processing costs (Pradhan & Mbohwa, 2014).

Therefore, alternative feedstocks, such as wastewater, mining water, municipal solid waste (MSW) and sewage sludge, should be considered for the viable production of advanced biofuels.

Large quantities of MSW are discarded by households and food processing industries year-round, where only small quantities are recycled, with the vast non-recycled waste landfilled (Klemetsrud *et al.*, 2016; Minowa *et al.*, 1995; Zastrow & Jennings, 2013). Landfilled material mainly consists of organic waste and occupies valuable space, generates odours, diseases, and emits greenhouse gases (Klemetsrud *et al.*, 2016; Minowa *et al.*, 1995). Sewage contains energy and valuable nutrients that can be converted to biofuel and usable products (Capodaglio & Callegari, 2018). MSW and sewage sludge are attractive feedstocks for biofuel production through HTL due to their high moisture contents, availability, low costs, and an established infrastructure for collection and handling (Huang *et al.*, 2011; Klemetsrud *et al.*, 2016).

HTL and pyrolysis are thermochemical processes used for biofuel production (Wang *et al.*, 2018). The operating conditions for the pyrolysis process are atmospheric pressure and temperatures ranging between 300 ºC and 700 ºC. Pre-drying of the biomass is essential for high heating rates and temperature control (Wang *et al.*, 2018). Pyrolysis of MSW and sewage sludge is an energy-intensive process due to the need for high operating temperatures and pre-drying of the biomass (Capodaglio & Callegari, 2018; Minowa *et al.*, 1995). Thus, for MSW as feedstock, it is not feasible due to the requirement of an energy-intensive dewatering and pre-drying process.

The HTL process converts biomass into biocrude and other reactor products at temperatures ranging from 280 ºC to 370 ºC and pressures ranging from 10 MPa to 25 MPa (Wang *et al.*, 2018). Processing of the feedstock takes place at subcritical or critical conditions of water allowing for the breakdown of the solid biopolymeric structure yielding biocrude, biogas, hydrochar, and an aqueous effluent as reactor products (Elliott *et al.*, 2015). HTL has the advantage of not requiring energy-intensive dewatering and drying process in contrast to the requirements of pyrolysis (Capodaglio & Callegari, 2018).

The HTL-biocrude oil typically contains phenols, alcohols, naphthols, acids, methoxy-phenols, cyclic ketones, and benzofurans (Elliott *et al.*, 2015; Kumar *et al.*, 2018). Compared to petroleum fuel, HTL-biocrude oil has unwanted properties such as low heating value, high water content, high viscosity, high corrosiveness, high ash and oxygen content (Xiu & Shahbazi, 2012). These properties also limit the application of the HTL-biocrude as a high-value fuel without being upgraded. Biocrude oil is generally upgraded through biological, chemical or thermochemical processes (Hansen *et al.*, 2020; Manurung *et al.*, 2017).

Thermochemical upgrading processes consist of hydrocracking and hydrotreating (Hansen *et al.*, 2020). Hydrocracking takes place under severe operating conditions of temperatures above 350 °C and pressures ranging between 7 bar and 138 bar which require complex processing equipment (Xiu & Shahbazi, 2012). The main disadvantages associated with hydrocracking are catalyst deactivation, reactor clogging, and the high costs associated with the process (Baloch *et al.*, 2018; Xiu & Shahbazi, 2012). The main advantages of hydrotreating are the milder operating conditions, lower costs and that it is already commercialised compared to hydrocracking (Xiu & Shahbazi, 2012). Hydrotreating produces a poor quality renewable diesel with a high cold filter plugging point which makes it an inadequate technique for the direct upgrading of biocrude oil to fuel (Baloch *et al.*, 2018; Xiu & Shahbazi, 2012).

Esterification and transesterification are promising methods for industrial application from a process cost point of view (Lin *et al.*, 2011). Esterification decreases the viscosity, acidity and corrosiveness of the biocrude oil, while improving its volatility, stability, and heating value (Baloch *et al.*, 2018; Gui *et al.*, 2008; Lin *et al.*, 2011; Xiu & Shahbazi, 2012).

Chemical processes for upgrading biocrude oil consist of esterification and transesterification reactions using biological, alkali or acid catalysts (Gog *et al.*, 2012; Guldhe *et al.*, 2015). Acid and alkali catalysts have the disadvantage of having high energy requirements, toxicity, corrosiveness and difficult recovery compared to biological catalysts (Karmee *et al.*, 2018). As an alternative, biological catalysts, like lipase, have the advantages of operating under moderate conditions, being environmentally friendly, reducing waste and purification costs, being relatively easy to recover, requiring low energy input, and being free fatty acid tolerant (Guldhe *et al.*, 2015; Hansen *et al.*, 2020; Karmee *et al.*, 2018; Manurung *et al.*, 2017). Esterification uses an alcohol-based solvent to convert carboxylic acids to esters, whereas transesterification uses alcohol to substitute triglycerides with small carbon chains (Amini *et al.*, 2017; Hansen *et al.*, 2020).

Karmee *et al.* (2018) investigated the production of biodiesels from spent coffee ground oil by using lipase catalysis. Different lipases were used for biodiesel production under solvent-free conditions. The immobilised catalyst, N435, obtained the highest conversion among the lipases investigated and was further used for the optimisation of reaction conditions achieving a biodiesel yield of 96 %. Similarly, Köse *et al*., (2002) investigated the influence of enzyme loading, oil to methanol molar ratio, temperature, and reaction time on methanolysis of refined cotton seed oil. The optimum FAME yield of 91.5 % was obtained at a 30 mass % enzyme loading, oil to methanol molar ratio of 1:4, 50 °C, and a reaction time of 7 hours.

A disadvantage associated with enzymatic esterification is the high costs of the lipase enzymes (Ghaly *et al.*, 2010) which can be mitigated by the reusability of N435 (Gog *et al.*, 2012; Leung *et*

al., 2010). Karmee (2016) investigated the reusability of N435 by using n-pentane as a solvent for regeneration and obtained a FAME conversion of 86 % after the fifth cycle.

1.2 Problem statement

HTL is a thermal process converting a high moisture content biomass into biocrude oil and energy without feedstock dewatering (Mulchandani & Westerhoff, 2016). Compared to petroleum fuel, HTL-biocrude has a low heating value, high water content, high viscosity, high corrosiveness, and high ash and oxygen content that limit the application of the biocrude oil without upgrading (Xiu & Shahbazi, 2012). As stated in the previous section, biocrude oil is generally upgraded through chemical, thermochemical or biological processes (Hansen *et al.*, 2020; Manurung *et al.*, 2017).

According to the feasibility study by Jiang *et al*. (2019:110), the minimum selling price of the biocrude oil is high due to the high feedstock costs resulting in an uneconomically process. The minimum selling price of the biocrude oil would be significantly lower if MSW and sewage sludge are used as feedstock in conjunction with government subsidies.(Jiang *et al.*, 2019).

Biofuels are used as an alternative to conventional fuels due to their low toxicity, high biodegradability, and ease of blending with conventional fuels resulting in reduced carbon dioxide emissions (Amini *et al.*, 2017). Emissions reduction is facilitated by the presence in biodiesel of ester compounds containing oxygen which promote cleaner burning (Huang *et al.*, 2012). Biodiesel is a liquid biofuel that consists of a mixture of esters produced through esterification and transesterification of FFAs and triglycerides, respectively (Amini *et al.*, 2017).

For esterification and transesterification, biocatalysts are used specifically to mitigate the disadvantages associated with the use of chemical catalysts (Amini *et al.*, 2017). The upgrading of biocrude oil through lipase catalysis need to be studied in detail to determine if the enzyme will be affected by components such phenolics, ketones and heterocyclic nitrogen, oxygen and sulphur compounds in the biocrude oil. Current studies on lipase catalysis only investigates conversion efficency. Therefore, lipase catalysis, enzyme reusablity and the effect of the enzyme on other components should also be further investigated.

1.3 Aim and objectives

This study aims to investigate the upgrading of biocrude oil obtained from the HTL of MSW and sewage sludge through enzymatic esterification. The FAME conversion of lipase-catalysed esterification will be evaluated and compared with additional methods such as chemical esterification and transesterification.

This will be done through the achievement of the following objectives:

- Synthesisation of biocrude oil by the HTL of a synthetic mixture of organic MSW in the presence of sewage sludge as a solvent.
- Production of biodiesel through the lipase-catalysed esterification of the prepared biocrude oil.
- Quantification of the effectiveness of lipase-catalysed esterification of biocrude oil based on product yield, biodiesel quality, and enzyme reusability.
- Evaluate the selectivity of methyl ester conversion of lipase-catalysed esterification in the presence of other biocrude oil components.

1.4 Scope of this study

To achieve the aims and objectives listed in Section 1.3, the scope of the study was determined to be the following.

Chapter 1: Introduction
This chapter provides the background of and the motivation for the study and an introduction into biofuels, municipal waste (MW) as biomass, HTL, biocrude upgrading, and biodiesel. It also contains the problem statement, aim, objectives and scope of this study.

Chapter 2: Literature review
The literature review contains an investigation into waste management in South Africa, operating conditions of HTL, upgrading of biocrude oil, and parameters affecting biocatalytic transesterification. Subheadings of this chapter include: Waste management, Biofuels, Hydrothermal liquefaction, Biodiesel, Feedstock for biodiesel production, Method of biodiesel production, Transesterification, and Parameters affecting biocatalytic transesterifications.

Chapter 3: Materials and methods
This chapter provides detail regarding the experimental procedures, analytical techniques and reagents used in this study. Subheadings in this chapter include: Materials, Experimental procedures, Analyses, and Experimental error.

Chapter 4: Results and discussion
This chapter provides the results of the characterisation of the MW, HTL product yields, characterisation of the biocrude oil, and enzymatic esterification. The effect of the methanol to oil ratio, reaction temperature, and residence time on the FAME yield, and characterisation of the biodiesel produced in this study are also communicated and discussed.

Chapter 5: Conclusion and recommendations

This chapter provides the conclusion of this study as well as several recommendations for future studies.

1.5 References

Amini, Z., Ilham, Z., Ong, H.C., Mazaheri, H. & Chen, W.H. 2017. State of the art and prospective of lipase-catalyzed transesterification reaction for biodiesel production. *Energy Conversion and Management*, 141:339-353.

Baloch, H.A., Nizamuddin, S., Siddiqui, M.T.H., Riaz, S., Jatoi, A.S., Dumbre, D.K., … Griffin, G.J. 2018. Recent advances in production and upgrading of bio-oil from biomass: a critical overview. *Journal of Environmental Chemical Engineering*, 6(4):5101-5118.

Capodaglio, A.G. & Callegari, A. 2018. Feedstock and process influence on biodiesel produced from waste sewage sludge. *Journal of Environmental Management*, 216:176-182. doi:10.1016/j.jenvman.2017.03.089

Department of Environmental Affairs. 2018. *South Africa State of Waste Report: first draft report*. http://sawic.environment.gov.za/documents/8635.pdf Date of access: 20 Feb. 2020

Dimitriadis, A. & Bezergianni, S. 2017. Hydrothermal liquefaction of various biomass and waste feedstocks for biocrude production: a state of the art review. *Renewable & Sustainable Energy Reviews*, 68:113-125. doi:10.1016/J.RSER.2016.09.120

Dong, C., Wang, Y., Wang, H., Lin, C.S.K., Hsu, H.Y. & Leu, S.Y. 2019. New generation urban biorefinery toward complete utilization of waste derived lignocellulosic biomass for biofuels and value-added products. *Energy Procedia*, 158:918-925.

Elliott, D.C., Biller, P., Ross, A.B., Schmidt, A.J. & Jones, S.B. 2015. Hydrothermal liquefaction of biomass: developments from batch to continuous process. *Bioresource Technology*, 178:147-156. doi:10.1016/j.biortech.2014.09.132

Falkner R. 2016. The Paris Agreement and the new logic of international climate politics. *International Affairs*, 92(5):1107-1125. doi:10.1111/1468-2346.12708

Ghaly, A.E., Dave, D., Brooks, M.S. & Budge, S. 2010. Production of biodiesel by enzymatic transesterification: review. *American Journal of Biochemistry & Biotechnology*, 6(2):54-76. doi:10.3844/ajbbsp.2010.54.76

Gog, A., Roman, M., Toşa, M., Paizs, C. & Irimie, F.D. 2012. Biodiesel production using enzymatic transesterification: current state and perspectives. *Renewable Energy*, 39(1):10-16. doi:10.1016/j.renene.2011.08.007

Gui, M.M., Lee, K.T. & Bhatia, S. 2008. Feasibility of edible oil vs. non-edible oil vs. waste edible oil as biodiesel feedstock. *Energy*, 33(11):1646-1653. doi:10.1016/j.energy.2008.06.002

Guldhe, A., Singh, B., Mutanda, T., Permaul, K. & Bux, F. 2015. Advances in synthesis of biodiesel via enzyme catalysis: novel and sustainable approaches. *Renewable & Sustainable Energy Reviews*, 41:1447-1464.

Guo, M., Song, W. & Buhain, J. 2015. Bioenergy and biofuels: history, status, and perspective. *Renewable and Sustainable Energy Reviews*, 42:712-725. doi:10.1016/j.rser.2014.10.013

Hansen, S., Mirkouei, A. & Diaz, L.A. 2020. A comprehensive state-of-technology review for upgrading bio-oil to renewable or blended hydrocarbon fuels. *Renewable and Sustainable Energy Reviews*, 118:109548. doi:10.1016/j.rser.2019.109548

Huang, D., Zhou, H. & Lin, L. 2012. Biodiesel: an alternative to conventional fuel. *Energy Procedia*, 16:1874-1885. doi:10.1016/j.egypro.2012.01.287

Huang, H., Yuan, X., Zeng, G., Zhu, H., Li, H., Liu, Z., … Bi, W. 2011. Quantitative evaluation of heavy metals' pollution hazards in liquefaction residues of sewage sludge. *Bioresource Technology*, 102(22):10346-10351. doi:10.1016/j.biortech.2011.08.117

Jiang, Y., Jones, S.B., Zhu, Y., Snowden-Swan, L.L., Schmidt, A.J., Billing, J.M. & Anderson, D. 2019. Techno-economic uncertainty quantification of algal-derived biocrude via hydrothermal liquefaction. *Algal Research*, 39:101450. doi:10.1016/j.algal.2019.101450

Karavalakis, G., Boutsika, V., Stournas, S. & Bakeas, E. 2011. Biodiesel emissions profile in modern diesel vehicles. Part 2: Effect of biodiesel origin on carbonyl, PAH, nitro-PAH and oxy-PAH emissions. *The Science of the Total Environment*, 409(4):738-747. doi:10.1016/j.scitotenv.2010.11.010

Karmee, S.K. 2016. Preparation of biodiesel from nonedible oils using a mixture of used lipases. *Energy Sources, Part A Recover. Util. Environ. Eff. Taylor & Francis*. 38(18):2727–2733.

Karmee, S.K., Swanepoel, W. & Marx, S. 2018. Biofuel production from spent coffee grounds via lipase catalysis. *Energy Sources, Part A: Recovery, Utilization and Environmental Effects*, 40(3):294-300. doi:10.1080/15567036.2017.1415394

Klemetsrud, B., Ukaew, S., Thompson, V.S., Thompson, D.N., Klinger, J., Li, L., Eatherton, D.,

… & Shonnard, D. 2016. Characterization of products from fast micropyrolysis of municipal solid waste biomass. *ACS Sustainable Chemistry & Engineering*, 4(10):5415-5423. doi:10.1021/Acssuschemeng.6B00610

Köse, O., Tüter, M. & Aksoy, H.A. 2002. Immobilized Candida antarctica lipase-catalyzed alcoholysis of cotton seed oil in a solvent-free medium. *Bioresource Technology*, 83(2):125–129. doi:10.1016/s0960-8524(01)00203-6

Kumar, M., Olajire Oyedun, A. & Kumar, A. 2018. A review on the current status of various hydrothermal technologies on biomass feedstock. *Renewable and Sustainable Energy Reviews*, 81:1742-1770. doi:10.1016/j.rser.2017.05.270

Leung, D.Y.C., Wu, X. & Leung, M.K.H. 2010. A review on biodiesel production using catalyzed transesterification. *Applied Energy*, 87(4):1083-1095.

Lin, L., Cunshan, Z., Vittayapadung, S., Xiangqian, S., & Mingdong, D. 2011. Opportunities and challenges for biodiesel fuel. *Applied Energy*, 88(4):1020-1031.

Manurung, R., Sutarman, W. & Taslim, T. 2017. Optimization of enzymatic process in biodiesel production for green process development. *Journal of Engineering and Applied Sciences*, 12(9):2485-2491. doi:10.36478/jeasci.2017.2485.2491

Minowa, T., Murakami, M., Dote, Y., Ogi, T. & Yokoyama, S. 1995. Oil production from garbage by thermochemical liquefaction. *Biomass and Bioenergy*, 8(2):117-120. doi:10.1016/0961-9534(95)00017-2

Mulchandani, A. & Westerhoff, P. 2016. Recovery opportunities for metals and energy from sewage sludges. *Bioresource Technology*, 215:215-226. doi:10.1016/j.biortech.2016.03.075

Pradhan, A. & Mbohwa, C. 2014. Development of biofuels in South Africa: challenges and opportunities. *Renewable and Sustainable Energy Reviews*, 39:1089-1100. doi:10.1016/j.rser.2014.07.131

Rodionova, M.V., Poudyal, R.S., Tiwari, I., Voloshin, R.A., Zharmukhamedov, S.K., Nam, H.G., Zayadan, B.K., Bruce, B.D., Hou, H.J.M. & Allakhverdiev, S.I. 2017. Biofuel production: challenges and opportunities. *International Journal of Hydrogen Energy*, 42(12):8450-8461. doi:10.1016/j.ijhydene.2016.11.125

Wang, F., Tian, Y., Zhang, C.C., Xu, Y.P., & Duan, P.G. 2018. Hydrotreatment of bio-oil distillates produced from pyrolysis and hydrothermal liquefaction of duckweed: a comparison

study. *The Science of the Total Environment*, 636:953-962. doi:10.1016/j.scitotenv.2018.04.363

Xiu, S. & Shahbazi, A. 2012. Bio-oil production and upgrading research: a review. *Renewable and Sustainable Energy Review*, 16(7):4406-4414. doi:10.1016/j.rser.2012.04.028

Zastrow, D.J. & Jennings, P.A. 2013. Hydrothermal liquefaction of food waste and model food waste compounds. *2013 American Institute of Chemical Engineers (AIChE) Annual Meeting Online Proceedings*, (336978):1-9.

CHAPTER 2: LITERATURE REVIEW

The literature review of HTL and lipase catalysis is provided in this chapter.

Waste management in South Africa is discussed in Section 2.1 followed by the classification of biofuels in Section 2.2.

Section 2.3 investigates HTL operating conditions and their effect on the biocrude yield. Biodiesel and the specification of the established South African National Standards for a fuel to be classified as a biodiesel are discussed in Section 2.4.

Sections 2.5 and 2.6 investigate the different feedstocks used for biodiesel production and biocrude upgrading methods for biofuel production. The different catalysts used during transesterification and the parameters affecting transesterification and the biodiesel yield are discussed in Section 2.7.

2.1 Waste management

The population of South Africa increased by 17 million people between 1994 and 2019 which requires municipalities to make provision for a greater demand for services (Worldometer, 2021). South Africa's significant population growth increases the demand for clean drinking water, waste management facilities and sustainable sanitation. Waste management is mandatory and based on South Africa's 2017 state of waste report approximately 43 million tonnes of waste were generated (Department of Environmental Affairs, 2018). It is estimated that only 4.9 million tonnes were recycled while 38 million tonnes were landfilled (Department of Environmental Affairs, 2018).

Landfill material mainly consists of organic waste that occupies valuable space, generates odours, emits greenhouse gases, but is a source of renewable energy (Klemetsrud *et al.*, 2016; Minowa *et al.*, 1995; Zastrow & Jennings, 2013). Zastrow and Jennings (2013) proposed the utilisation of HTL technology to produce renewable fuel from MSW to reduce landfill waste.

The treatment of municipal wastewater results in large amounts of sewage sludge that increases with population growth (Pathak *et al.*, 2009). Furthermore, the disposal of sewage sludge has serious safety and environmental concerns. Sewage is disposed of through land application , irrigation, or placements in landfills (Mulchandani & Westerhoff, 2016; Pathak *et al.*, 2009; Weng *et al.*, 2014). Disposal of sewage wastewater through irrigation of agricultural land results in the improvement of chemical, biological and physical properties of the soil (Pathak *et al.*, 2009). However, the amount of heavy metals in sewage restricts its use as fertiliser since the metals accumulate in the plants and vegetables (Pathak *et al.*, 2009; Tóth *et al.*, 2016). Landfilling faces

several disadvantages such as odour, the release of greenhouse gases, the limiting of space due to the increase in urbanisation, and the potential of underground water contamination (Mulchandani & Westerhoff, 2016). Due to several health and environmental concerns, alternative methods should be considered (Dufreche *et al.*, 2007). Sewage sludge contains nutrients and energy that make it a valuable feedstock in the production of biofuel (Capodaglio & Callegari, 2018).

The production of biofuel through the processing of MSW and sewage sludge is a potentially feasible and environmentally-friendly alternative method of waste management (Dufreche *et al.*, 2007; Melero *et al.*, 2015; Siddiquee & Rohani, 2011; Zastrow & Jennings, 2013).

2.2 Biofuels

Biofuels are classified as either primary or secondary biofuels (Alam *et al.*, 2015; Rodionova *et al.*, 2017). The difference is that primary (natural) biofuels are used in their unprocessed form, whereas secondary biofuels are produced by further processing of the feedstock (Nigam & Singh, 2011). Primary biofuel involves the burning of dry animal waste, cellulosic plant material, and wood in their unprocessed form to generate heat (Rodionova *et al.*, 2017). Secondary biofuels are classified into three generations, namely: first-, second-, and third-generation biofuels. These are characterised according to the production technology, biomass, and the limitations of the biofuels produced (Alam *et al*., 2012; Naik *et al*., 2010; Nigam & Singh, 2011; Rodionova *et a*l., 2017).

Second-generation biofuels are classified according to their method of production, i.e. thermochemical or biochemical processes (Naik *et al.*, 2010; Nigam & Singh, 2011). Recent developments in the economic feasibility of second-generation biofuel production and large scale biorefining have stimulated some interest, particularly, in lignocellulosic biomass consisting of agricultural or municipal waste that is a sustainable biomass not affecting food security (Dong *et al.*, 2019). Biofuel generations are characterised according to the biomass used, production technology, and the limitations of the biofuel products, as shown in Table 2.1.

Table 2.1:Characterisation of the biofuel generations (Alam *et al.*, 2012; Nigam & Singh, 2011; Rodionova *et al.*, 2017; S.N. Naik *et al.*, 2010).

	First-generation	Second-generation	Third-generation
Biomass	Animal fats, vegetable oils, starch- and sugar-rich biomass	Non-food lignocellulosic biomass, waste oils and municipal wastes	Cyanobacterial microalgae, and seaweeds
Technology	Transesterification	HTL and pyrolysis	Fermentation, HTL, anaerobic digestion pyrolysis, gasification, and transesterification
Products	Biodiesel, corn ethanol, and sugar alcohol	Hydrotreated oil, biocrude, lignocellulosic ethanol, butanol, and mixed alcohols	Bioethanol, butanol, methane, hydrogen, syngas, and biocrude
Advantages	Locally distributed and environmentally friendly	Environmentally friendly, reduction in landfill sites, and not affecting food security	Cultivated in saline water and requiring less water than terrestrial crops
Disadvantages	Limited biomass; high production costs, storage facilities, land-use change; and necessity of mixing fuel with conventional fuel	Storage facilities, land-use change, advanced technology is still underdeveloped to ensure economic feasibility, and procurement of subsidies	Procurement of government subsidies, storage facilities, and land-use change

Transesterification converts triglycerides of oil-based biomass to FAME by displacing alcohol from an ester by another alcohol (Guldhe *et al.*, 2015; Hassan & Kalam, 2013). Catalytic transesterification is used for the production of biodiesel and can either be a homogeneous or heterogeneous catalyst (Gog *et al.*, 2012; Hassan & Kalam, 2013). Homogeneous catalysts consist of alkali and acid catalysts whereas heterogeneous catalysts consist of enzymes, titanium

silicates, alkali earth metal compounds and anion exchange resins (Hassan & Kalam, 2013). Guldhe *et al.* (2015) proposed that the recent advances in the enzyme catalysis of biodiesel resulted in a greener and sustainable approach that could be implemented on a large scale.

Pyrolysis, HTL, and lipid extraction are second-generation processes used in the production of biofuel (Wang *et al.*, 2018). Pre-drying of the biomass is essential to ensure economic feasibility during lipid extraction and pyrolysis (Siddiquee & Rohani, 2011; Wang *et al.*, 2018).

Lipid extraction has the following disadvantages: catalysts used are highly sensitive, polar solvents used are not environmentally-friendly, a variety of side reactions could occur and a significant amount of organic solvent are required making it expensive (Kwon *et al.*, 2012; Mulchandani & Westerhoff, 2016; Siddiquee & Rohani, 2011).

Pyrolysis is an environmentally-friendly process with the disadvantages of being an energy-intensive process, for having a complex product stream, with the potential for corrosion occurring in downstream equipment, and the production of gases requiring further treatment (Capodaglio & Callegari, 2018; Chen *et al.*, 2003; Guo *et al*., 2015; Serio *et al.*, 2000).

HTL operations are based on pyrolytic mechanisms; however, its biocrude oil is different from the biocrude oil produced by pyrolysis (Elliott *et al.*, 2015). The HTL-biocrude occurs in a hydrophobic phase that is more viscous, has a lower density, and less dissolved water compared to the pyrolysis biocrude oil (Elliott *et al.*, 2015). HTL has the main advantages of not requiring energy-intensive dewatering and drying processes compared to pyrolysis and lipid extraction (Capodaglio & Callegari, 2018; Mulchandani & Westerhoff, 2016).

2.3 Hydrothermal liquefaction

HTL takes place at temperatures ranging between 200 °C and 450 °C and pressures ranging between 40 bar and 220 bar resulting in the production of biocrude oil, biogas, biochar and an aqueous effluent (Dimitriadis & Bezergianni, 2017; Elliott *et al.*, 2015; Mulchandani & Westerhoff, 2016). The biomass composition, operating conditions, and the reactor configuration affect the oxygen content, moisture content, higher heating values, and the yield of the biocrude oil (Mathimani & Mallick, 2019). Processing of the biomass takes place in the presence of a water environment at elevated temperature and pressure for the breakdown of the solid biopolymeric structure (Elliott *et al.*, 2015). Water in the biomass serves as a chemical reagent and reaction medium for decomposing of reactions (Dimitriadis & Bezergianni, 2017; Yuliansyah *et al*., 2019).

According to Mathimani & Mallick, (2019), biomass with a high lipid content is preferred over a high carbohydrate content since the protein-rich biomass can be converted efficiently to biocrude

oil. Sewage sludge contains a significant amount of lipids that includes phospholipids, diglycerides, triglycerides, monoglycerides, and FFAs (Kargbo, 2010). Furthermore, sewage sludge is an excellent biomass for the production of biofuel due to the high lipid and fatty acid content thereof (Kargbo, 2010). The membranes of the microorganisms inside sewage sludge consists of phospholipids and are converted to FAME through acid and base catalysed transesterification (Dufreche *et al.*, 2007). The composition of the MSW depends on the time, place of sampling, and the specific municipality (Alibardi & Cossu, 2015). The organic fraction of the MSW mainly consists of carbohydrate-rich materials, protein and lipids; which can therefore be used as a feedstock for HTL (Alibardi & Cossu, 2015; Kobayashi *et al.*, 2012; Toor *et al.*, 2011)

The conversion of biomass into biocrude oil depends on the following operating conditions: temperature, pressure, catalyst, biomass to water ratio, solvent, and residence time (Akhtar & Amin, 2011; Dimitriadis & Bezergianni, 2017; Kumar *et al.*, 2018). The operating temperature influences the yield and quality of the biocrude (Dimitriadis & Bezergianni, 2017; Kumar *et al.*, 2018). The biocrude yield increases as the operating temperature increases until the temperature reaches a point where it suppresses liquefaction and the yield decreases (Dimitriadis & Bezergianni, 2017; Kumar *et al.*, 2018). The macromolecules of the biomass produce amino acids from glycerol, protein, and reducing and non-reducing sugars of carbohydrates, and long-chain fatty acids of lipids through hydrolysis at a temperature range between 0 °C and 100 °C (Mathimani & Mallick, 2019). Deamination, degradation, and decarboxylation processes take place in compounds such as fatty acids, amino acids and sugars at a temperature range between 100 °C and 200 °C (Mathimani & Mallick, 2019). Furthermore, at reaction temperatures above 200 °C long-chain fatty acids produce amide products.

At reaction temperatures above 250 °C, the biocrude yield decreases and the hydrolysed products are hydrophilic (Akhtar & Amin, 2011; Mathimani & Mallick, 2019). On the further increase of the operating temperature approaching or exceeding the critical point of water, gas formation takes place, the macromolecules of the biocrude polymerise to form coke, and the reduction of the organic product in the aqueous phase occurs (Cao *et al.*, 2017; Mathimani & Mallick, 2019). This increased reaction temperature leads to a reduction in the biocrude oil yield, and an increase in the biochar and gas yield (Cao *et al.*, 2017).

According to the literature, there is no optimum operating temperature for HTL (Cao *et al.*, 2017), as it depends on the feedstock, the solvent, and the catalyst used (Cao *et al.*, 2017; Kumar *et al.*, 2018; Mathimani & Mallick, 2019). Reaction temperatures of 300 °C and 340 °C are recommended for the increased production of biocrude and biochar, respectively (Kumar *et al.*, 2018). Depending on the feedstock the biocrude yield will be at a maximum at a temperature range between 280 °C and 300 °C and gradually decrease as the temperature increases (Akhtar

& Amin, 2011; Cao *et al.*, 2017). Xu *et al.* (2018) investigated the HTL of sewage sludge at different temperatures showing that by increasing the reaction temperature, the biocrude yield increased to a maximum yield at 340 °C. Minowa *et al.* (1995) compared the biocrude yield at different temperatures and obtained a higher yield at 300°C than at 250 °C, as can be seen in Table 2.2.

The operating pressure reduces high energy costs by preventing a two-phase system and maintains the water in the liquid phase (Akhtar & Amin, 2011; Cao *et al.*, 2017; Mathimani & Mallick, 2019). High pressures keep water in a single phase at supercritical and subcritical states, preventing phase transition (Akhtar & Amin, 2011; Cao *et al.*, 2017; Dimitriadis & Bezergianni, 2017). An increase in pressure will increase water density and result in effective biomass extraction (Cao *et al.*, 2017; Elliott *et al.*, 2015; Mathimani & Mallick, 2019). An increase in temperature will increase the pressure, thereby increasing polymerisation of the HTL products and coke formation (Cao *et al.*, 2017). If the reaction temperature decreases the pressure will also decrease resulting in a decrease in the biocrude yield and incomplete HTL reactions (Cao *et al.*, 2017; Elliott *et al.*, 2015).

The residence time influences the HTL conversion efficiency and product yield (Cao *et al.*, 2017; Elliott *et al.*, 2015; Mathimani & Mallick, 2019). Residence time is the period of time for which the desired temperature is maintained in the reactor (Kumar *et al.*, 2018; Mathimani & Mallick, 2019). The threshold of the residence time depends on the biomass, operating conditions, and the catalyst (Dimitriadis & Bezergianni, 2017). A residence time of 5 to 30 minutes is recommended; if the residence time goes beyond this threshold the biocrude yield will decrease (Wang *et al.*, 2018). Shorter residence times significantly reduces costs and increases high biocrude yields, whereas longer residence times increase the production of biochar, aqueous product and biogas, thereby reducing the biocrude yield (Dimitriadis & Bezergianni, 2017; Elliott *et al.*, 2015; Kumar *et al.*, 2018; Mathimani & Mallick, 2019). Minowa *et al.* (1995) investigated the biocrude yield at a temperature of 300 °C at different residence times and the results indicated that the yield was the highest at a residence time of 6 minutes, as seen in Table 2.2.

The addition of a catalyst reduce reaction temperature and pressure, inhibits side reactions, increase reaction rates, reduces the biochar yield, and improves the quality and yield of the biocrude oil (Cao *et al.*, 2017; Dimitriadis & Bezergianni, 2017; Kumar *et al.*, 2018). The catalyst loading influences HTL effectiveness and suppresses the formation of the biochar while increasing the biocrude yield (Cao *et al.*, 2017; Dimitriadis & Bezergianni, 2017). Both heterogeneous and homogeneous catalysts are used during HTL. There are two types of heterogeneous catalysts, namely metal catalysts, and supported catalysts. Heterogeneous catalysts are also used for thermal gasification as they are more resistant to harsh reaction

conditions (Kumar *et al.*, 2018; Mathimani & Mallick, 2019). Homogeneous catalysts includes both acid and alkali catalysts. According to Cao *et al.*, (2017), biocrude oil has a higher oxygen content when acid catalysts are used. Alkali catalysts decreases biochar formation, inhibit biological molecule dehydration, increases the pH of the liquid, and promote decarboxylation and water-gas conversion (Cao *et al.*, 2017; Kumar *et al.*, 2018). It is expensive and difficult to recover homogeneous catalysts (Kumar *et al.*, 2018; Mathimani & Mallick, 2019).

Water is the most common solvent used in HTL; it stabilises free radicals, is environmentally friendly, and improve the quality of the biocrude oil (Dimitriadis & Bezergianni, 2017; Xue *et al.*, 2016). Organic solvents used include ethanol and methanol. Ethanol and methanol have a lower critical point compared to water, and therefore milder reaction conditions are required (Dimitriadis & Bezergianni, 2017). High water to biomass ratios increase the biocrude yield and as the reaction reaches or goes beyond the critical point of the liquid the yield will decrease due to hydrolysis and repolymerisation reactions (Dimitriadis & Bezergianni, 2017; Xue *et al.*, 2016). According to Xue *et al*. (2016), although an increase in water will not always increase the biocrude yield, it will reduce the formation of biochar and increase HTL costs. Various operating conditions of organic waste and sewage sludge were investigated as shown in Table 2.2.

For this study, a reaction temperature of 300 °C was chosen with a residence time of 20 minutes.

Table 2. 2: Various operating conditions of organic waste and sewage sludge during HTL

Biomass	Solvent	Temperature (°C)	Residence time (min)	Biomass: water	Biocrude yield (mass %)	Source
Pinus (leaves of pine tree)	water	300	30	1:10	33	(Cao *et al.*, 2016)
Pinus (bark of pine tree)	water	300	30	1:10	43	(Cao *et al.*, 2016)
Household (organic waste)	-	300	6	-	17	(Minowa *et al.*, 1995)
Household (organic waste)	-	250	6	-	5	(Minowa *et al.*, 1995)
Household (organic waste)	-	250	30	-	9	(Minowa *et al.*, 1995)
Household (organic waste)	-	300	30	-	16	(Minowa *et al.*, 1995)
Sewage sludge (dry)	methanol	280	20	-	32.78	(Huang *et al.*, 2014)
Sewage sludge (dry)	methanol	300	20	-	30.96	(Huang *et al.*, 2014)
Wet sewage sludge	water	300	20	70 g sewage and 200 ml of water	33.2	(Li *et al.*, 2018)
Wet sewage sludge	water	340	20	70 g sewage and 200 ml of water	37.1	(Li *et al.*, 2018)
Sewage sludge (dry)	water	300	40	1:5	46	(Malins *et al.*, 2015)

The composition of the HTL products are determined using chemical analysis techniques such as quantitative and qualitative gas chromatography/mass spectrometry (GCMS) analysis, total acid number, total organic carbon, total nitrogen, and elemental analysis (Madsen *et al.*, 2018; Madsen *et al.*, 2017a, Zhang, *et al.*, 2017). GCMS analysis is used to identify different components in the biocrude oil such as alcohols, carboxylic acids, amines, cyclic oxygenates, phenolics, benzenediols, fatty acids, hydrocarbons, and monoglycerides (Madsen *et al.*, 2018). For this study, the biocrude will be analysed using the following analysis techniques: GCMS, calorific value, Karl Fischer coulometric titration, gel permeation chromatography (GPC), Fourier-transform infrared spectroscopy (FTIR), and proximate and elemental analyses.

According to the literature, the following analyses are conducted to determine the composition of the biochar: thermogravimetric analysis (TGA), HHV, FTIR, proximate and elemental analyses (Lai *et al.*, 2018; Leng *et al.*, 2015). For this study, the biochar will be characterised by means of the following analyses: higher heating value (HHV), proximate and elemental analyses.

HTL produces a biocrude product consisting of phenols, acids, cyclic ketones, alcohols, methoxy-phenols, naphthols and benzofurans (Elliott *et al.*, 2015; Kumar *et al.*, 2018). Compared to petroleum fuel, biocrude has the following unwanted properties: high water content, high viscosity, corrosiveness, and a high ash and oxygen content (Xiu & Shahbazi, 2012). Furthermore, these unwanted properties have limited the application of biocrude oil unless upgraded (see discussion in Section 2.6).

2.4 Biodiesel

Biodiesel is used as an alternative to conventional fuel to reduce environmental impact, improve lubricity, and does not require any engine modifications (Hassan & Kalam, 2013). Furthermore, biodiesel is safe, biodegradable, non-toxic, has a high flash point and does not contain sulphur and aromatic components (Azócar *et al.*, 2010; Vyas *et al.*, 2010). Biodiesel is a term used to refer to a diesel fuel that consists of monoalkyl esters of long-chain fatty acids that are derived from a biological source (Hassan & Kalam, 2013). The main disadvantages of biodiesel are that it is corrosive, has high NOx emissions, a high pour and cloud point, high viscosity, and that it is not cost-competitive compared to conventional diesel (Hassan & Kalam, 2013). Furthermore, the high pour and cloud point result in the freezing of the biodiesel during winter.

Biodiesel quality is determined according to its chemical and physical properties (Robles-Medina *et al.*, 2009). In South Africa, fuel is classified as biodiesel once it meets the specification of the established South African national standard for automotive biodiesel (South African National Standards, 1935) The biodiesel standard is shown in Table 2.3.

Table 2.3: South African National Standards for FAME (South African National Standards, 2011)

Property	Unit	Minimum	Maximum	Test Method
FAME content	% (m/m)	96.5	-	EN 14103
Density at 15 °C	kg/m^3	860	900	EN ISO 3675 EN ISO 12185
Kinematic viscosity at 40 °C	mm^2/s	3.5	5.0	EN ISO 3104
Flash point	°C	101	-	EN ISO 2719 EN ISO 3679
Sulphur content	mg/kg	-	10	EN ISO 20846 EN ISO 20884
Cetane number	-	51	-	EN ISO 5165
Water content	mg/kg	-	500	EN ISO 12937
Oxidation stability at 110 °C	hour	6.0	-	EN 15751 EN 14112
Acid value	mg KOH/g	-	0.50	EN 14104
Methanol content	% (m/m)	-	0.20	EN 14110
Monoglyceride content	% (m/m)		0.8	EN 14105
Diglyceride content	% (m/m)	-	0.2	EN 14105
Triglyceride content	% (m/m)		0.2	EN 14105
Free glycerol	% (m/m)	-	0.02	EN 14105 EN 14106

2.5 Feedstock for biodiesel production

Vegetable oils, waste cooking oils, and animal fat are the primary feedstocks used in the production of biodiesel (Azócar *et al.*, 2010; Banković-Ilić *et al.*, 2012). The feedstock choice depends on the oil content, feasibility, and process chemistry (Ghaly *et al.*, 2010; Karmakar *et al.*, 2010). The chemical and physical properties of the feedstock that affect the biodiesel production and its quality are the FFA content, impurities, moisture, unsaponifiable and calorific content (Karmakar *et al.*, 2010). The FFA content refers to the number of fatty acids in the feedstock which is not connected to triglyceride molecules (Karmakar *et al.*, 2010). Additionally, the FFA reacts with alkali that leads to soap formation during transesterification. The calorific content of the biodiesel refers to the energy content (Karmakar *et al.*, 2010). Furthermore, the moisture content, impurities and unsaponifiable content refer to the filterable solids, amount of water, and non-triglycerides that cannot be converted into monoalkyl fatty esters.

Edible oils used in the production of biodiesel include sunflower, palm, rapeseed and soybean oils (Azócar *et al.*, 2010; Karmakar *et al.*, 2010). The main advantage of using edible oils as feedstock in biodiesel production is their low saturation level and low FFA content (Azócar *et al.*, 2010). However, their main disadvantage is the high feedstock costs, inferior storage, and production of inadequate amounts for both human consumption and biodiesel production (Ashraful *et al.*, 2014; Banković-Ilić *et al.*, 2012). Additionally, non-edible oils are less expensive compared to edible oils with plantation costs as their main disadvantage (Azócar *et al.*, 2010; Gui *et al.*, 2008). Other promising feedstocks considered for biodiesel production include waste grease, waste frying oil, microalgae, and biocrude (Azócar *et al.*, 2010; Karmakar *et al.*, 2010). Biocrude is a biofuel used as a combustion fuel in boilers, burners and furnaces or as an alternative to conventional fuel after upgrading (Xiu & Shahbazi, 2012). Biocrude is upgraded through esterification, transesterification, hydrotreating or hydrocracking.

2.6 Biocrude upgrading methods for biofuel production

Biocrude oil has a high viscosity, low heating value, high corrosiveness, and high water and ash content preventing it from being directly used as a transportation fuel (Xiu & Shahbazi, 2012). The chemical composition of biocrude depends on the following HTL reaction conditions: temperature, feedstock type, residence time, solvent used, and gas used for the reaction (Ramirez *et al.*, 2015). In addition, the choice of biomass has a significant effect on the chemical composition of biocrude compared to the other conditions. The methods used for the upgrading of biocrude oil, including advantages as well as disadvantages, are listed in Table 2.4.

Table 2.4: Advantages and disadvantages of various biocrude upgrading methods

Method	Advantages	Disadvantages	Source
Hydrotreating	Inexpensive, mild reaction conditions and commercialised	Poor quality fuel, low biodiesel yield, and high coking tendencies	(Baloch *et al.*, 2018; Xiu & Shahbazi, 2012)
Hydrocracking	Produces large quantities of light product	Expensive, reactor clogging, severe reaction conditions; catalyst deactivation, and requiring complicated equipment	(Baloch *et al.*, 2018; Xiu & Shahbazi, 2012)
Esterification and transesterification	Most practical, high biodiesel yield, inexpensive, fuel properties closer to those of diesel and can be used for industrial applications	Side reactions, low water and FFA content required, and mechanisms involved with solvent addition needs further research	(Baloch *et al.*, 2018; Gui *et al.*, 2008; Lin *et al.*, 2011; Xiu & Shahbazi, 2012)
Emulsification	Simple and less corrosion	Expensive, time-consuming, and requiring high amounts of energy	(Baloch *et al.*, 2018; Xiu & Shahbazi, 2012)

According to Lin *et al.* (2011), of the available methods, transesterification is the most promising technique for industrial application, is inexpensive, and decreases the high viscosity of the biocrude. The addition of polar solvents during esterification and transesterification reduces the viscosity, acidity and corrosiveness and improves the volatility, stability and heating value of the biocrude (Baloch *et al.*, 2018; Xiu & Shahbazi, 2012). The viscosity decreases due to the chemical reactions between the solvent and biocrude, changing the biocrude microstructure and physical dilution that affect the reaction rate (Xiu & Shahbazi, 2012). Also, the heating value increases due to the HHV of the solvent used during esterification and transesterification.

2.7 Transesterification

During transesterification, the triglycerides react with an alcohol in the presence of a catalyst to form monoalkyl esters and glycerol (Guldhe *et al.*, 2015). In addition, transesterification is also known as alcoholysis. Methanol is the most inexpensive alcohol frequently used as an acyl-acceptor that are stoichiometrically added to the biocrude oil (Ghaly *et al.*, 2010; Guldhe *et al.*, 2015; Leung *et al.*, 2010). For the conversion of one mole triglycerides into FAME, the reaction requires three moles of methanol, but excess methanol drives the reaction forward (Guldhe *et al.*, 2015). The catalysts used for transesterification are divided into the following categories: acidic, alkali, and biological (Gog *et al.*, 2012). The three different catalysts and their advantages, as well as disadvantages, are listed in Table 2.5.

Table 2.5: The advantages and disadvantages of the alkali, acidic and biological catalysts used in transesterification

Category	Type	Advantages	Disadvantages	Source
Alkali	Homogenous	High catalytic activity and yield, favourable kinetics, fast reaction rate, inexpensive and mild operating conditions	Requires low FFA content, saponification, anhydrous conditions, generates wastewater, difficult catalyst recovery, product purification required, and emulsion formation	(Gog *et al.*, 2012; Guldhe *et al.*, 2015; Leung *et al.*, 2010)
	Heterogenous	Long catalyst life, non-corrosive, recyclable; high selectivity and yield, reusability, and	More severe reaction conditions and energy requirements, saponification, expensive, large amount of wastewater, and	(Gog *et al.*, 2012; Guldhe *et al.*, 2015; Leung *et al.*, 2010)

		environmentally friendly	requirement of high alcohol to oil molar ratios	
Acidic	Homogenous	No soap formation, medium yield and reaction rate, inexpensive and simultaneous esterification, and transesterification	Corrosion of equipment, requirement of product purification, difficult to recycle, more severe reaction conditions and energy requirements, long reaction residence time, and weak catalyst activity	(Gog *et al.*, 2012; Guldhe *et al.*, 2015; Leung *et al.*, 2010)
	Heterogenous	Recyclable, environmentally friendly, high yield, reusability, simultaneous esterification, and transesterification	Expensive, diffusion limitations, corrosion of equipment, high energy requirements, low microporosity, and low acid site concentrations	(Gog *et al.*, 2012; Guldhe *et al.*, 2015; Leung *et al.*, 2010)
Biological	Enzymes	No soap formation, high yield, low energy requirements, high product purity, reusability, and environmental friendliness	Expensive, alcohol inhibition and denaturation	(Gog *et al.*, 2012; Guldhe *et al.*, 2015; Leung *et al.*, 2010)

The acidic and alkali catalysts include heterogeneous and homogenous catalysts (Gog *et al.*, 2012; Leung *et al.*, 2010). Biological catalysts require mild operating conditions, has a lower energy consumption and the separation and purification of the product are easier compared to chemical catalysts (Guldhe *et al.*, 2015). However, biological catalysts are less used for industrial application due to their high costs and long reaction times (Guldhe *et al.*, 2015; Leung *et al.*, 2010). The high cost and long reaction time associated with the enzyme catalysts are mitigated by the reusability and operational stability of the newly developed biological catalyst known as immobilised lipase (Gog *et al.*, 2012; Leung *et al.*, 2010). The different immobilisation methods used in biodiesel production consist of adsorption, entrapment, cross-linkage, encapsulation, and covalent bonding (Amini *et al.*, 2017a; Ghaly *et al.*, 2010; Tan *et al.*, 2010). However, adsorption

is the most widely used technique, is inexpensive and has less mass transfer limitations compared to entrapment and crosslinking (Guldhe *et al.*, 2015). The advantages and disadvantages of the different immobilisation methods are listed in Table 2.6.

Table 2.6: Comparing the advantages and disadvantages of the various immobilisation techniques (Tan *et al.*, 2010)

Method	Advantages	Disadvantages
Adsorption	Inexpensive, mild preparation conditions, most widely used technique and carrier can be regenerated for reuse	Weak interaction between carrier and lipase, sensitive to pH and temperature, small adsorption capacity and a possibility that the protein can be stripped from the carrier
Covalent bond	Stable	Rigorous preparation conditions, some of the coupling agents are toxic
Entrapment	Mild preparation conditions, the method is used for a variety of carriers and lipases	Mass transfer limitations
Crosslinking	Stable with a strong interaction between the lipase and carrier	Low mechanical strength, harsh conditions

Adsorption consists of the attachment of an enzyme to the surface of a carrier by weak hydrophobic interactions, and van der Walls and dispersion forces (Ghaly *et al.*, 2010; Tan *et al.*, 2010). The main limitations associated with adsorption is low enzyme stability resulting in low conversions when the enzyme is reused, and the risk of the enzyme being stripped off the support (Ghaly *et al.*, 2010). The enzyme is stripped of the support during the transesterification reaction due to high amounts of glycerol and direct shear between the support and impeller since the adsorption involves weak forces (Ghaly *et al.*, 2010; Jegannathan *et al.*, 2008). N435 is the most thoroughly investigated and commonly used immobilised lipase which provides significantly high reaction yields (Amini *et al.*, 2017a; Fukuda *et al.*, 2001; Gog *et al.*, 2012).

As discussed in literature, N435 is immobilised through adsorption on a microporous acrylic resin that can absorb polar compounds when it is regenerated, which leads to enzyme deactivation (Amini *et al.*, 2017; Chen & Wu, 2003; Gog *et al.*, 2012). Laszlo *et al.* (2011), investigated lipase regeneration and indicated that immobilised lipases like N435 may be effectively reused and has a tolerance for polar and non-polar solvents. Regenerated N435 is provided with a protective shield by the regenerated solvent that minimises methanol deactivation (Nguyen *et al.* 2017).

2.8 Parameters affecting biocatalytic transesterification

The FAME yield is affected by several conditions such as reaction temperature, catalyst loading, alcohol to oil molar ratio, and reaction time (Amini *et al.*, 2017a). The effects of the operating conditions vary for each specific system and therefore the optimum operating conditions have to be determined for each system to ensure a high FAME yield (Amini *et al.*, 2017b; Motasemi & Ani, 2012).

2.8.1 Oil to alcohol molar ratio

The transesterification reaction requires three moles of alcohol for the conversion of one mole of triglycerides to produce three moles of FAME and one mole of glycerol (Fukuda *et al.*, 2001; Leung *et al.*, 2010). An excess amount of alcohol drives the reaction forward which ensures a larger FAME yield and a shorter reaction time. Moreover, if the alcohol to oil molar ratio increases beyond the optimum ratio the yield will increase as well as the alcohol recovery costs (Fukuda *et al.*, 2001; Leung *et al.*, 2010). Transesterification experiments are conducted at a starting methanol to oil molar ratio of 3:1 (Rathore *et al.*, 2016).

A major obstacle for enzymatic transesterification is lipase inactivation due to excess methanol (Yan *et al.*, 2014). However, lipase inactivation can be avoided by the continuous or stepwise addition of methanol (Gog *et al.*, 2012; Norjannah *et al.*, 2017). Shimada *et al.* (1999) found that N435 was the most effective immobilised lipase for methanolysis. Karmee *et al.* (2018) investigated the influence of the methanol to oil molar ratio of spent coffee ground biocrude oil catalysed by N435. In addition, the ratios were varied from 1:1 to 1:10 until an optimum FAME yield of 96 % was obtained at a ratio of 1:5. The FAME yield gradually decreased at higher methanol to oil molar ratios due to the inactivation of the lipase catalyst caused by the increase in the polarity of the medium (Karmee *et al.*, 2018; Rodrigues *et al.*, 2008). Other authors also investigated the influence of the methanol to oil molar ratio as seen in Table 2.7.

Table 2.7 :The effect of methanol to oil molar ratio on FAME yield

Feedstock	Amount of N435 (mass %)	The molar ratio of oil to methanol	Temperature (°C)	Residence time (h)	Observation	Source
Spent coffee ground	10	1:1–1:10	40	6	The optimum yield was obtained at a molar ratio of 1:5	(Karmee *et al.*, 2018)
Lipid from food waste	10	1:3–1:10	40	6	The highest yield was observed at a molar ratio of 1:5	(Karmee *et al.*, 2015)
Sunflower oil	15	1:3–1:12	30	6	The optimum yield was obtained at a molar ratio of 1:5	(Rodrigues *et al.*, 2008)
Cottonseed oil	30	1:1–1:6	40	7	The highest yield was observed at a molar ratio of 1:4	(Köse *et al.*, 2002)

The reaction rate and FAME yield of the transesterification reaction are both affected by the lipase catalyst loading (Mathiyazhagan & Ganapathi, 2011; Yadav & Devi, 2004). Furthermore, an increase in the catalyst loading will increase the FAME yield and the reaction rate until a limit is reached, then the loading will have no further effect on the conversion efficiency and the yield will decrease (Ribeiro *et al.*, 2011; Taher & Al-Zuhair, 2017; Tran *et al.*, 2012). It is not economically feasible to choose the highest catalyst loading since lipase catalyst is expensive and therefore the optimisation of catalyst loading is important (Taher & Al-Zuhair, 2017; Tran *et al.*, 2012).

Karmee (2018) studied the influence of varying the N435 catalyst loading on methanolysis of Manilkara zapota (L.) seed oil ranging from 5 mass % to 25 mass %. In addition, the reaction in his study took place at the operation conditions of 3:1 methanol to oil molar ratio, a temperature of 40 °C and a reaction time of 4 hours. The optimum FAME yield was obtained at a 10 mass % catalyst loading. According to Taher & Al-Zuhair (2017), studies on N435 indicated that the effect of catalyst loading becomes significantly less above 20 mass %.

2.8.2 Reaction temperature

Esterification and transesterification reactions are conducted at relatively low temperatures to prevent lipase inactivity (Gog *et al.*, 2012). The FAME yield is rarely influenced by fluctuations in reaction temperature between 20 °C and 70° C and therefore the optimum temperature for lipases esterification and transesterification is in general between 30 °C and 60 °C (Ghaly *et al.*, 2010; Gog *et al.*, 2012). Furthermore, the optimum temperature of immobilised lipases is higher than for free lipases (Ghaly *et al.*, 2010). The optimum temperature depends on lipase stability, type of organic solvent used, reaction rate, and the methanol to oil molar ratio (Ghaly *et al.*, 2010; Szczęsna Antczak *et al.*, 2009). Various authors have investigated the influence of the reaction temperature on the FAME yield as seen in Table 2.8. Most authors indicated that the optimum temperature is between 30 °C and 50 °C.

Table 2.8: The effect of reaction temperature on FAME yield

	Amount of N435 (mass %)	The molar ratio of oil to methanol	Temperature range (°C)	Residence time (h)	Observation	Source
A mixture of soybean and rapeseed oil	4	1:1	20–60	6	The optimum yield was obtained at a temperature of 50 °C	(Shimada *et al*., 1999)
Lipid from food waste	10	1:5	30–60	6	The highest yield was obtained at 40 °C	(Karmee *et al.*, 2015)
Sunflower oil	15	1:5	20–50	6	The optimum yield was obtained at a temperature of 30 °C	(Rodrigues *et al.*, 2008)
Cottonseed oil	30	1:4	20–60	7	The highest yield was observed at a temperature of 50 °C	(Köse *et al.*, 2002)

2.8.3 Reaction time

During transesterification the reaction rate is initially slow due to the dispersion of biocrude and alcohol (Mathiyazhagan & Ganapathi, 2011). Furthermore, as the reaction proceeds the fatty acid ester conversion increases as the reaction time increases. Once the reaction has reached the highest FAME yield at the optimum reaction time, a further extension of the reaction time will lead to a decrease in FAME yield due to the reversibility of the transesterification reaction (Leung *et al.*, 2010; Mathiyazhagan & Ganapathi, 2011).

Karmee *et al.* (2018) observed the influence of varying the reaction time from 0.5 to 24 hours on the transesterification reaction of spent coffee ground. In addition, the reaction in his study took place at the operating conditions of 5:1 methanol to oil molar ratio, a temperature of 40 °C and a catalyst loading of 10 mass %. Karmee *et al.* (2018) and other authors reported that optimal reaction time can vary between 7 and 72 hours (Amini *et al.*, 2017a; Karmee, 2018; Köse *et al.*, 2002; Kumar *et al.*, 2015; Shimada *et al.*, 1999).

2.9 References

Akhtar, J. & Amin, N.A.S. 2011. A review on process conditions for optimum bio-oil yield in hydrothermal liquefaction of biomass. *Renewable and Sustainable Energy Reviews*, 15(3):1615-1624. doi:10.1016/j.rser.2010.11.054

Alam, F., Date, A., Rasjidin, R., Mobin, S., Moria, H. & Baqui, A. 2012. Biofuel from algae: is it a viable alternative? *Procedia Engineering*, 49:221-227.

Alam, F., Mobin, S., & Chowdhury, H. 2015. Third generation biofuel from Algae. *Procedia Engineering*, 105:763-768. doi:10.1016/j.proeng.2015.05.068

Alibardi, L. & Cossu, R. 2015. Composition variability of the organic fraction of municipal solid waste and effects on hydrogen and methane production potentials. *Waste Management*, 36:147-155. doi:10.1016/j.wasman.2014.11.019

Amini, Z., Ilham, Z., Ong, C.H., Mazaheri, H. & Chen, W. 2017a. State of the art and prospective of lipase-catalyzed transesterification reaction for biodiesel production. *Energy Conversion and Management*, 141:339-353.

Amini, Z., Ong, H.C., Harrison, M.D., Kusumo, F., Mazaheri, H. & Ilham, Z. 2017b. Biodiesel production by lipase-catalyzed transesterification of Ocimum basilicum L. (sweet basil) seed oil. *Energy Conversion and Management*, 132:82-90.

Ashraful, A.M., Masjuki, H.H., Kalam, M.A., Rizwanul Fattah, I.M., Imtenan, S., Shahir, S.A. & Mobarak, H.M. 2014. Production and comparison of fuel properties, engine performance, and emission characteristics of biodiesel from various non-edible vegetable oils: a review. *Energy Conversion Management*, 80:202-228.

Azócar, L., Ciudad, G., Heipieper, H.J. & Navia, R. 2010. Biotechnological processes for biodiesel production using alternative oils. *Applied Microbiology and Biotechnology*, 88(3):621-636. doi:10.1007/s00253-010-2804-z

Baloch, H.A., Nizamuddin, S., Siddiqui, M.T.H., Riaz, S., Jatoi, A.S., Dumbre, D.K., … Griffin, G.J. 2018. Recent advances in production and upgrading of bio-oil from biomass: a critical overview. *Journal of Environmental Chemical Engineering*, 6(4):5101-5118.

Banković-Ilić, I.B., Stamenković, O.S. & Veljković, V.B. 2012. Biodiesel production from non-edible plant oils. *Renewable and Sustainable Energy Reviews*, 16(6):3621-3647. doi:10.1016/j.rser.2012.03.002

Cao, L., Luo, G., Zhang, S. & Chen, J. 2016. Bio-oil production from eight selected green landscaping wastes through hydrothermal liquefaction. *RSC Advances*, 6(18):15260-15270.

Cao, L., Zhang, C., Chen, H., Tsang, D.C.W., Luo, G., Zhang, S. & Chen, J. 2017. Hydrothermal liquefaction of agricultural and forestry wastes: state-of-the-art review and future prospects. *Bioresource Technology*, 245(June):1184-1193. doi:10.1016/j.biortech.2017.08.196

Capodaglio, A.G. & Callegari, A. 2018. Feedstock and process influence on biodiesel produced from waste sewage sludge. *Journal of Environmental Management*, 216:176-182. doi:10.1016/j.jenvman.2017.03.089

Chen, G., Andries, J., Luo, Z. & Spliethoff, H. 2003. Biomass pyrolysis/gasification for product gas production: the overall investigation of parametric effects. *Energy Conversion Management*, 44(11):1875-1884. doi:10.1016/S0196-8904(02)00188-7

Department of Environmental Affairs. 2018. *South Africa State of Waste Report: first draft report*. http://sawic.environment.gov.za/documents/8635.pdf Date of access: 26 May. 2020

Dimitriadis, A. & Bezergianni, S. 2017. Hydrothermal liquefaction of various biomass and waste feedstocks for biocrude production: a state of the art review. *Renewable & Sustainable Energy Reviews*, 68:113-125. doi:10.1016/J.RSER.2016.09.120

Dong, C., Wang, Y., Wang, H., Lin, C.S.K., Hsu, H.Y. & Leu, S.Y. 2019. New generation urban biorefinery toward complete utilization of waste derived lignocellulosic biomass for biofuels and value-added products. *Energy Procedia*, 158:918-925.

Dufreche, S., Hernandez, R., French, T., Sparks, D., Zappi, M. & Alley, E. 2007. Extraction of lipids from municipal wastewater plant microorganisms for production of biodiesel. *Journal of the American Oil Chemists' Society*, 84(2):181-187.

Elliott, D.C., Biller, P., Ross, A.B., Schmidt, A.J. & Jones, S.B. 2015. Hydrothermal liquefaction of biomass: developments from batch to continuous process. *Bioresource Technology*, 178:147-156. doi:10.1016/j.biortech.2014.09.132

Fukuda, H., Kondo, A. & Noda, H. 2001. Biodiesel fuel production by transesterification of oils. *Journal of Bioscience and Bioengineering*, 92(5):405-416. doi:10.1263/jbb.92.405

Ghaly, A.E., Dave, D., Brooks, M.S. & Budge, S. 2010. Production of biodiesel by enzymatic transesterification: review. *American Journal of Biochemistry & Biotechnology*, 6(2):54-76.

doi:10.3844/ajbbsp.2010.54.76

Gog, A., Roman, M., Toşa, M., Paizs, C., & Irimie, F.D. 2012. Biodiesel production using enzymatic transesterification: current state and perspectives. *Renewable Energy*, 39(1):10-16. doi:10.1016/j.renene.2011.08.007

Gui, M.M., Lee, K.T. & Bhatia, S. 2008. Feasibility of edible oil vs. non-edible oil vs. waste edible oil as biodiesel feedstock. *Energy*, 33(11):1646-1653. doi:10.1016/j.energy.2008.06.002

Guldhe, A., Singh, B., Mutanda, T., Permaul, K. & Bux, F. 2015. Advances in synthesis of biodiesel via enzyme catalysis: novel and sustainable approaches. *Renewable & Sustainable Energy Reviews*, 41:1447-1464.

Guo, M., Song, W. & Buhain, J. 2015. Bioenergy and biofuels: history, status, and perspective. *Renewable and Sustainable Energy Reviews*, 42:712-725. doi:10.1016/j.rser.2014.10.013

Hassan, M.H. & Kalam, M.A. 2013. An overview of biofuel as a renewable energy source: development and challenges. *Procedia Engineering*, 56:39-53. doi:10.1016/j.proeng.2013.03.087

Huang, H.J., Yuan, X.Z., Li, B.T., Xiao, Y.D. & Zeng, G.M. 2014. Thermochemical liquefaction characteristics of sewage sludge in different organic solvents. *Journal of Analytical and Applied Pyrolysis*, 109:176-184. doi:10.1016%2Fj.jaap.2014.06.015

Jegannathan, K.R., Abang, S., Poncelet, D., Chan, E.S. & Ravindra, P. 2008. Production of biodiesel using immobilized lipase - a critical review. *Critical Reviews in Biotechnology*, 28(4):253-264. doi:10.1080/07388550802428392

Kargbo, D.M. 2010. Biodiesel production from municipal sewage sludges. *Energy & Fuels*, 24(5):2791-2794. doi:10.1021/ef1001106

Karmakar, A., Karmakar, S. & Mukherjee, S. 2010. Properties of various plants and animals feedstocks for biodiesel production. *Bioresource Technology*, 101(19):7201-7210. doi:10.1016/j.biortech.2010.04.079

Karmee, S.K. 2018. Enzymatic biodiesel production from Manilkara zapota (L.) seed oil. *Waste and Biomass Valorization*, 9(5):725-730. doi:10.1007/s12649-017-9854-8

Karmee, S.K., Linardi, D., Lee, J. & Lin, C.S.K. 2015. Conversion of lipid from food waste to biodiesel. Waste Management, 41:169-173. doi:10.1016/j.wasman.2015.03.025

Karmee, S.K., Swanepoel, W. & Marx, S. 2018. Biofuel production from spent coffee grounds via lipase catalysis. *Energy Sources, Part A: Recovery, Utilization and Environmental Effects*, 40(3):294-300. doi:10.1080/15567036.2017.1415394

Klemetsrud, B., Ukaew, S., Thompson, V.S., Thompson, D.N., Klinger, J., Li, L., Eatherton, D., … & Shonnard, D. 2016. Characterization of products from fast micropyrolysis of municipal solid waste biomass. *ACS Sustainable Chemistry & Engineering*, 4(10):5415-5423. doi:10.1021/Acssuschemeng.6B00610

Kobayashi, T., Xu, K.Q., Li, Y.Y. & Inamori, Y. 2012. Evaluation of hydrogen and methane production from municipal solid wastes with different compositions of fat, protein, cellulosic materials and the other carbohydrates. *International Journal of Hydrogen Energy*, 37(20):15711-15718.

Köse, O., Tüter, M. & Aksoy, H.A. 2002. Immobilized Candida antarctica lipase-catalyzed alcoholysis of cotton seed oil in a solvent-free medium. *Bioresource Technology*, 83(2):125–129. doi:10.1016/s0960-8524(01)00203-6

Kumar, M., Olajire Oyedun, A. & Kumar, A. 2018. A review on the current status of various hydrothermal technologies on biomass feedstock. *Renewable and Sustainable Energy Reviews*, 81:1742-1770. doi:10.1016/j.rser.2017.05.270

Kwon, E.E., Kim, S., Jeon, Y.J. & Yi, H. 2012. Biodiesel production from sewage sludge: new paradigm for mining energy from municipal hazardous material. *Environmental Science & Technology*, 46(18):10222-10228. doi:10.1021/es3019435

Lai, F.-Y., Chang, Y.-C., Huang, H.-J., Wu, G.-Q., Xiong, J.-B., Pan, Z.-Q. & Zhou, C.-F. 2018. Liquefaction of sewage sludge in ethanolwater mixed solvents for bio-oil and biochar products. *Energy*, 148:629-641. doi:10.1016/j.energy.2018.01.186

Laszlo, J.A., Jackson, M. & Blanco, R.M. 2011. Active-site titration analysis of surface influences on immobilized Candida antarctica lipase B activity. *Journal of Molecular Catalysis. B, Enzymatic*, 69(1-2):60-65.

Leng, L.-J., Yuan, X.-Z., Huang, H.-J., Wang, H., Wu, Z.-B, Fu, L.-H., … Zeng, G.-M. 2015. Characterization and application of bio-chars from liquefaction of microalgae, lignocellulosic biomass and sewage sludge. *Fuel Processing Technology*, 129:8-14. doi:10.1016%2Fj.fuproc.2014.08.016

Leung, D.Y.C., Wu, X. & Leung, M.K.H. 2010. A review on biodiesel production using catalyzed transesterification. *Applied Energy*, 87(4):1083-1095.

Li, R.D., Ma, Z.M, Yang, T.H., Li, B.S., Wei, L.H. & Sun, Y. 2018. Sub–supercritical liquefaction of municipal wet sewage sludge to produce bio-oil: effect of different organic–water mixed solvents. *Journal of Supercritical Fluids*, 138:115-123. doi:10.1016/j.supflu.2018.04.011

Lin, L., Cunshan, Z., Vittayapadung, S., Xiangqian, S., & Mingdong, D. 2011. Opportunities and challenges for biodiesel fuel. *Applied Energy*, 88(4):1020-1031.

Madsen, R.B., Anastasakis, K., Biller, P. & Glasius, M. 2018. Rapid determination of water, total acid number, and phenolic content in bio-crude from hydrothermal liquefaction of biomass using FT-IR. *Energy & Fuels*, 32(7):7660–7669. doi:10.1021/acs.energyfuels.8b01208

Madsen, R.B., Bernberg, R.Z.K., Biller, P., Becker, J., Iversen, B.B. & Glasius, M. 2017a. Hydrothermal co-liquefaction of biomasses – quantitative analysis of bio-crude and aqueous phase composition. *Sustainable Energy & Fuels*, 1(4):789-805. doi:10.1039/c7se00104e

Madsen, R.B., Zhang, H., Biller, P., Goldstein, A.H. & Glasius, M. 2017b. Characterizing semivolatile organic compounds of biocrude from hydrothermal liquefaction of biomass. *Energy & Fuels*, 31(4):4122-4134. doi:10.1021/acs.energyfuels.7b00160

Malins, K., Kampars, V., Brinks, J., Neibolte, I., Murnieks, R. & Kampare, R. 2015. Bio-oil from thermo-chemical hydro-liquefaction of wet sewage sludge. *Bioresource Technology*, 187:23-29. doi:10.1016/j.biortech.2015.03.093

Mathimani, T. & Mallick, N. 2019. A review on the hydrothermal processing of microalgal biomass to bio-oil: knowledge gaps and recent advances. *Journal of Cleaner Production*, 217:69-84. doi:10.1016/j.jclepro.2019.01.129

Mathiyazhagan, M. & Ganapathi, A. 2011. Factors affecting biodiesel production. *Research in Plant Biolology*, 1(2):1-5.

Melero, J.A., Sánchez-Vázquez, R., Vasiliadou, I.A., Castillejo, F.M., Bautista, L.F., Iglesias, J. … Molina, R. 2015. Municipal sewage sludge to biodiesel by simultaneous extraction and conversion of lipids. *Energy Conversion and Management*, 103:111-118. doi:10.1016/j.enconman.2015.06.045

Minowa, T., Murakami, M., Dote, Y., Ogi, T. & Yokoyama, S. 1995. Oil production from garbage by thermochemical liquefaction. *Biomass and Bioenergy*, 8(2):117-120. doi:10.1016/0961-9534(95)00017-2

Motasemi, F. & Ani, F.N. 2012. A review on microwave-assisted production of biodiesel.

Renewable and Sustainable Energy Reviews, 16(7):4719-4733. doi:10.1016/j.rser.2012.03.069

Mulchandani, A. & Westerhoff, P. 2016. Recovery opportunities for metals and energy from sewage sludges. *Bioresource Technology*, 215:215-226. doi:10.1016/j.biortech.2016.03.075

Naik, S.N., Goud, V. V., Rout, P.K. & Dalai, A.K. 2010. Production of first and second generation biofuels: a comprehensive review. *Renewable and Sustainable Energy Reviews*, 14(2):578-597. doi:10.1016/j.rser.2009.10.003

Nguyen, H.C., Liang, S.-H., Doan, T.T., Su, C.-H. & Yang, P.-C. 2017. Lipase-catalyzed synthesis of biodiesel from black soldier fly (Hermetica illucens): optimization by using response surface methodology. *Energy Conversion and Management*, 145:335-342.

Nigam, P.S. & Singh, A. 2011. Production of liquid biofuels from renewable resources. *Progress in Energy and Combustion Science*, 37(1):52-68. doi:10.1016/j.pecs.2010.01.003

Norjannah, B., Ong, H.C. & Masjuki, H.H. 2017. Effects of methanol and enzyme pretreatment to Ceiba pentandra biodiesel production. *Energy Sources, Part A: Recovery, Utilization, and Environmental Effects*, 39(14):1548–1555. doi:10.1080/15567036.2017.1344747

Pathak, A., Dastidar, M.G. & Sreekrishnan, T.R. 2009. Bioleaching of heavy metals from sewage sludge: a review. *Journal of Environmental Management*, 90(8):2343-2353. doi:10.1016/j.jenvman.2008.11.005

Ramirez, J.A., Brown, R.J. & Rainey, T.J. 2015. A review of hydrothermal liquefaction bio-crude properties and prospects for upgrading to transportation fuels. *Energies*, 8(7):6765-6794. doi:10.3390/en8076765

Rathore, V.N., Newalkar, B.L. & Badoni, R.P. 2016. Processing of vegetable oil for biofuel production through conventional and non-conventional routes. *Energy for Sustainable Development*, 31(1200):24-49.

Ribeiro, B.D., De Castro, A.M., Coelho, M.A.Z. & Freire, D.M.G. 2011. Production and use of lipases in bioenergy : a review from the feedstocks to biodiesel production. *Enzyme Research*, 2011:615803. doi:10.4061/2011/615803

Robles-Medina, A., González-Moreno, P.A., Esteban-Cerdán, L. & Molina-Grima, E. 2009. Biocatalysis: towards ever greener biodiesel production. *Biotechnology Advances*, 27(4):398-408. doi:10.1016/j.biotechadv.2008.10.008

Rodionova, M.V., Poudyal, R.S., Tiwari, I., Voloshin, R.A., Zharmukhamedov, S.K., Nam, H.G., … Allakhverdiev, S.I. 2017. Biofuel production: challenges and opportunities. *International Journal of Hydrogen Energy*, 42(12):8450-8461. doi:10.1016/j.ijhydene.2016.11.125

Rodrigues, R.C., Volpato, G., Wada, K. & Ayub, M. 2008. Enzymatic synthesis of biodiesel from transesterification reactions of vegetable oils and short chain alcohols. *Journal of the American Oil Chemists' Society*, 85(10):925-930. doi:10.1007/s11746-008-1284-0

Szczęsna Antczak, M., Kubiak, A., Antczak, T. & Bielecki, S. 2009. Enzymatic biodiesel synthesis: key factors affecting efficiency of the process. *Renewable Energy*, 34(5):1185-1194. doi:10.1016/j.renene.2008.11.013

Serio, M.A., Chen, Y., Wójtowicz, M.A. & Suuberg, E.M. 2000. Pyrolysis processing of mixed solid waste streams. *American Chemical Society, Division of Fuel Chemistry Preprints*, 45(3):466-474.

Shimada, Y., Watanabe, Y., Samukawa, T., Sugihara, A., Noda, H., Fukuda, H. & Tominaga, Y. 1999. Conversion of vegetable oil to biodiesel using immobilized Candida antarctica lipase. *Journal of the American Oil Chemists' Society*, 76:789-793.

Siddiquee, M.N. & Rohani, S. 2011. Lipid extraction and biodiesel production from municipal sewage sludges: a review. *Renew. Sustain. Energy Rev. Elsevier Ltd*. 15(2):1067–1072.

South African National Standards. 2011. *SANS 1935:2011 SOUTH AFRICAN NATIONAL STANDARD Automotive biodiesel — Fatty Acid Methyl Esters (FAME) for diesel engines — Requirements and test methods*. Pretoria: SABS.

Taher, H. & Al-Zuhair, S. 2017. The use of alternative solvents in enzymatic biodiesel production: a review. *Biofuels, Bioproducts and Biorefining*, 11(1):168-194. doi:10.1002/bbb.1727

Tan, T., Lu, J., Nie, K., Deng, L. & Wang, F. 2010a. Biodiesel production with immobilized lipase: a review. *Biotechnology Advances*, 28(5):628-634. doi:10.1016/j.biotechadv.2010.05.012

Toor, S.S., Rosendahl, L. & Rudolf, A. 2011. Hydrothermal liquefaction of biomass: a review of subcritical water technologies. *Energy*, 36(5):2328-2342. doi:10.1016/j.energy.2011.03.013

Tóth, G., Hermann, T., Da Silva, M.R. & Montanarella, L. 2016. Heavy metals in agricultural soils of the European Union with implications for food safety. *Environment International*,

88:299-309. doi:10.1016/j.envint.2015.12.017

Tran, D.-T., Yeh, K.-L., Chen, C.-L. & Chang, J.-S. 2012. Enzymatic transesterification of microalgal oil from Chlorella vulgaris ESP-31 for biodiesel synthesis using immobilized Burkholderia lipase. *Bioresource Technology*, 108:119-127. doi:10.1016/j.biortech.2011.12.145

Vyas, A.P., Verma, J.L. & Subrahmanyam, N. 2010. A review on FAME production processes. *Fuel*, 89(1):1-9. doi:10.1016/j.fuel.2009.08.014

Wang, F., Tian, Y., Zhang, C.C., Xu, Y.P. & Duan, P.G. 2018. Hydrotreatment of bio-oil distillates produced from pyrolysis and hydrothermal liquefaction of duckweed: a comparison study. *The Science of the Total Environment*, 636:953-962. doi:10.1016/j.scitotenv.2018.04.363

Wang, W., Yu, Q., Meng, H., Han, W., Li, J. & Zhang, J. 2018. Catalytic liquefaction of municipal sewage sludge over transition metal catalysts in ethanol-water co-solvent. *Bioresource Technology*, 249:361-367. doi:10.1016/j.biortech.2017.09.205

Weng, H.X., Ma, X.W., Fu, F.X., Zhang, J.J., Liu, Z., Tian, L.X. & Liu, C. 2014. Transformation of heavy metal speciation during sludge drying: mechanistic insights. *Journal of Hazardous Material*, 265:96-103.

Worldometer. 2021. *Population of South Africa (2020 and historical)*. https://www.worldometers.info/world-population/south-africa-population/ Date of access: 26 Fed. 2020

Xiu, S. & Shahbazi, A. 2012. Bio-oil production and upgrading research: a review. *Renewable and Sustainable Energy Review*, 16(7):4406-4414. doi:10.1016/j.rser.2012.04.028

Xu, D., Lin, G., Liu, L., Wang, Y., Jing, Z. & Wang, S. 2018. Comprehensive evaluation on product characteristics of fast hydrothermal liquefaction of sewage sludge at different temperatures. *Energy*, 159:686-695. doi:10.1016/j.energy.2018.06.191

Xue, Y., Chen, H., Zhao, W., Yang, C., Ma, P. & Han, S. 2016. A review on the operating conditions of producing bio-oil from hydrothermal liquefaction of biomass. *International Journal of Energy Research*, 40(7):865-877. doi:10.1002/er.3473

Yadav, G.D. & Devi, K.M. 2004. Immobilized lipase-catalysed esterification and transesterification reactions in non-aqueous media for the synthesis of tetrahydrofurfuryl

butyrate: comparison and kinetic modeling. *Chemical Engineering Science*, 59:373-383. doi:10.1016/J.CES.2003.09.034

Yan, Y., Li, X., Wang, G., Gui, X., Li, G., Su, F., Wang, X., & Liu, T. 2014. Biotechnological preparation of biodiesel and its high-valued derivatives: a review. *Applied Energy*, 113:1614-1631. doi:10.1016/j.apenergy.2013.09.029

Yuliansyah, A.T., Kumagai, S., Hirajima, T. & Sasaki, K. 2019. Hydrothermal treatment of oil palm biomass in batch and semi-flow reactors. *Energy Procedia*, 158:675-580.

Zastrow, D.J. & Jennings, P.A. 2013. Hydrothermal liquefaction of food waste and model food waste compounds. *2013 American Institute of Chemical Engineers (AIChE) Annual Meeting Online Proceedings*, (336978):1-9.

CHAPTER 3: MATERIALS AND METHODS

This chapter provides details of the experimental procedures, analytical techniques, and reagents used in this study. Sections 3.1 and 3.2 discuss the materials and chemicals used in this study. The experimental procedures of HTL and enzymatic esterification are discussed in Section 3.3, while Section 3.4 describes the analytic techniques used in this study.

3.1 Materials

3.1.1 Feedstock

Primary sewage sludge was sampled at Potchefstroom sewage works (26°45'10.7''S 27°05'17.5''E) and prepared as feedstock together with MSW, as described in Section 3.2.1. The organic fraction of the MSW was prepared based on the quantities of food waste present in the MSW reported in the 2017 South Africa State of Waste Report (Ayeleru *et al.*, 2016; Department of Environmental Affairs, 2018). The food components used in the preparation of the MSW were chopped and placed inside a convection oven at 60 °C until a constant weight was obtained, whereas garden refuse, consisting of grass and small quantities of leaves, was dried in the sun for 7 days. After drying, the dried fruits, vegetables, and garden refuse together with newspaper, corrugated paper and printing paper were milled with a hammer mill to a particle size of 7 mm. The protein and fat content of the MSW consisted of soy protein, milk powder and pig fat. Table 3.1 gives the final composition of the simulated MSW sample used as feedstock to produce biocrude oil through HTL. The MW feedstock that consisted of MSW and sewage sludge were analysed according to the procedures described in Section 3.3.

Table 3.1: MSW composition as prepared for HTL reaction

Component	Dry weight (g)	Moisture (mass %)
Green apples	2.1	84
Bananas	1.2	83
Berries (black)	0.1	85
Red apples	1.3	85
Oranges	1.6	85
Carrots	1.1	85
Cauliflower	0.5	94
Lettuce	0.1	97
Red peppers	0.7	92
Tomatoes	0.3	95
Fruit & vegetables	9.0	88
Soy protein	3.4	-
Pig fat	1.5	-
Meat	4.9	74

Milk powder	1.4	93
Sorghum	42.3	-
Oil	4.9	-
Roots and tubers (potatoes)	3.0	82
Garden waste	8.9	42
News paper	0.46	-
Printing paper	9.0	-
Corrugated paper	2.9	-
Total	86.8	55

3.1.2 Chemicals

Table 3.2 contains a list of the chemicals and materials used in this study.

Table 3.2: List of chemicals and materials

Component	Purity (%)	Supplier	Purpose
Novozym 435	-	Sigma-Aldrich	Catalyst
Acetone	99.99	Glass World	Solvent used in product separation
Methanol	99.99	Sigma-Aldrich	Reagent
Diethyl ether	99	ACE*	Solvent used in product separation
Dichloromethane	99	ACE	Biodiesel drying solvent
Tetrahydrofuran	98	Merck	Lipase regeneration solvent
Deuterated chloroform ($CDCl_3$)	99	Sigma-Aldrich	Solvent for ^1H NMR analysis
Acetonitrile	99.9	Sigma-Aldrich	Lipase regeneration solvent
Isopropanol	99.7	Rochelle chemicals	Lipase regeneration solvent
Dimethyl sulfoxide	99.9	Sigma-Aldrich	Lipase regeneration solvent
Hexane	99	Sigma-Aldrich	Lipase regeneration solvent
Tert-butanol	99.7	Sigma-Aldrich	Lipase regeneration solvent

2,3,4,5,6-pentafluorobenz-aldehyde	98	Sigma-Aldrich	Internal standard for ^{1}H NMR

*Associated Chemical Enterprise (ACE)

3.2 Experimental procedures

3.2.1 HTL experimental setup (Figure 3.1)

A 945 mL SS316 stainless steel batch type autoclave reactor (1) was used to conduct the HTL experiments as shown in Figure 3.1. The MW feedstock was introduced into the reactor via an SS316 stainless reactor sleeve (2) with a working volume of 750 mL. The reactor sleeve was cleaned with acetone and weighed prior to the start-up of the reactor. For all the HTL experiments, a volume loading of 50 % was used meaning that 198.8 g of the dried MSW and 112 g of sewage sludge were placed in the reactor sleeve.

The loaded reactor sleeve (2) was loaded into the reactor and the flange lid was fitted to the bottom, ensuring a tight seal using a copper gasket. The top of the reactor was rotated to align with the alignment markings on the top and bottom of the reactor to ensure that the bolt holes were aligned. The bolts (carbon steel) were lubricated with an anti-seize and corrosion copper grease and inserted into the bolt holes. The bolts were fastened with a torque wrench to 40, 60 and 70 Nm, after which the gas line to the reactor was connected. The extractor unit (to divert all evolved gases to the outside of the laboratory space) was switched on and the gas inlet valve (3) closed. All the connections were leak-checked to ensure that there were no gas leaks present, and that the reactor outlet valve (4) was closed.

The gas inlet valve (3) was slowly opened to pressurise the reactor (1) with nitrogen gas (5) while the reactor pressure was monitored. The gas inlet valve (3) was closed when the desired reactor pressure was obtained. The pressure gauge (6) was monitored, and a liquid leak detector was applied to ensure that no gas leaks were present. The reactor (1) was depressurised by opening the outlet valve (4) to purge the reactor to atmospheric pressure to remove oxygen inside the reactor after which the outlet valve (4) was closed again. The inlet valve (3) was opened slowly again to pressurise the reactor to 10 bar with N_2 gas. The inlet valve was closed, and the two heating jackets (7) were attached to the reactor, while ensuring that all electrical wires were isolated away from the heated surface areas. The heating jackets (7) were switched on and the reactor was heated to the desired temperature of 300 °C at a heating rate of 2.76 K/min.

After the desired temperature was reached, the reactor temperature was kept constant at 300 °C by controlling the temperature of the heating jackets (7) for the entire duration of the residence

time of 20 minutes. At the end of the residence time, the heating jackets (7) were switched off and carefully removed to allow the reactor (1) to cool down to 30 °C with the assistance of a fan. The gas product in the reactor was slowly vented by the extraction fan by carefully opening the reactor outlet valve (4). The gas line was disconnected from the reactor and the bolts were loosened. The top of the reactor and the sleeve (2) were removed. The reactor sleeve was weighed, together with the products and the mass was recorded. The reactor products were separated following the separation procedure described in Section 3.2.2.

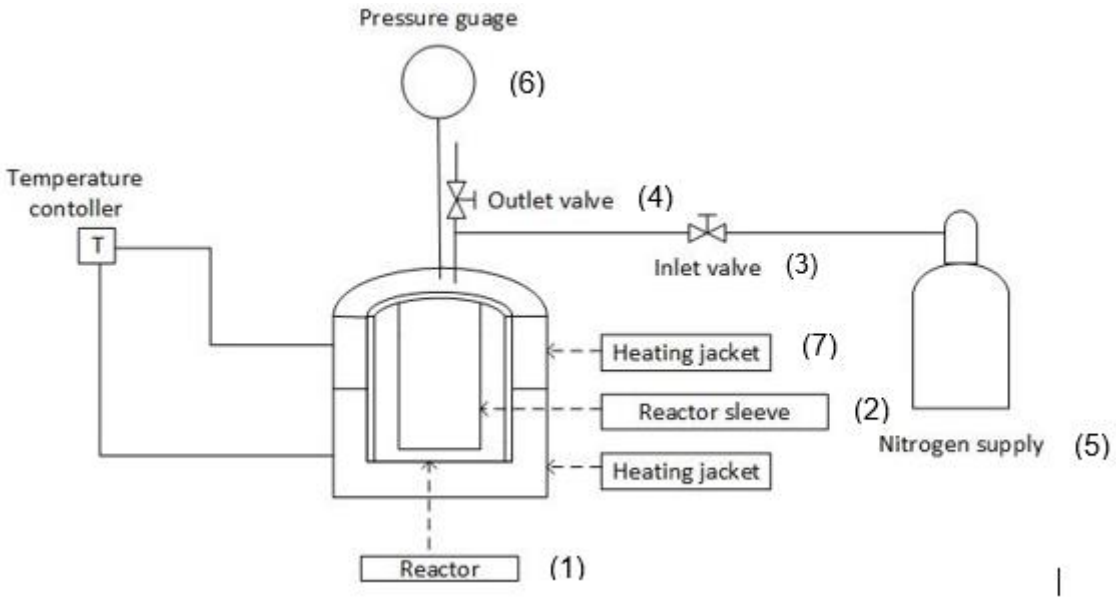

Figure 3.1: Schematic diagram of the batch reactor experimental setup

Figure 3.2:Batch reactor experimental setup

3.2.2 HTL batch reactor product separation and extraction procedure

Two Büchner flasks, a filter paper, and Büchner funnel were weighed, and the weights were recorded. The Büchner funnel containing the filter paper was inserted into the first Büchner flask which was marked as the aqueous flask. The products were quantitatively transferred from the reactor sleeve to the filter paper using 100 mL of acetone. The liquid phase was separated by vacuum filtration and its mass was recorded. A second Büchner flask replaced the first after which the biochar was washed under vacuum with 400 mL acetone. The acetone-washed biochar was dried in a convection oven at 60 °C for 24 hours. A rotary evaporator was used to separate the biocrude oil in the liquid phase from the acetone solvent. The recovered biocrude oil was dried in a convection oven at 60 °C for 2 hours to facilitate the removal of small quantities of acetone still present in the biocrude oil. The biocrude oil and biochar were analysed according to the procedures described in Section 3.3.

3.2.3 Lipase catalysis

Figure 3.3 shows a representation of the experimental procedure followed for the lipase-catalysed esterification of the biocrude oil. For each experiment, a 50 mL pear-shaped reaction flask was used in which 0.1 g of lipase (N435) and 1 g of biocrude oil (2.63 mmol) were weighed to obtain a 10 mass % enzyme loading. A magnet for stirring and an appropriate amount of methanol was added to the reaction flask to obtain the desired methanol to oil molar ratio. The reaction flask was capped, clamped, and immersed into a preheated oil bath. Methanolysis continued for 6 hours under constant stirring at 12.5 Hz. The operating conditions that were investigated in this study were reaction time, reaction temperature, oil to methanol molar ratios, lipase reusability and regeneration.

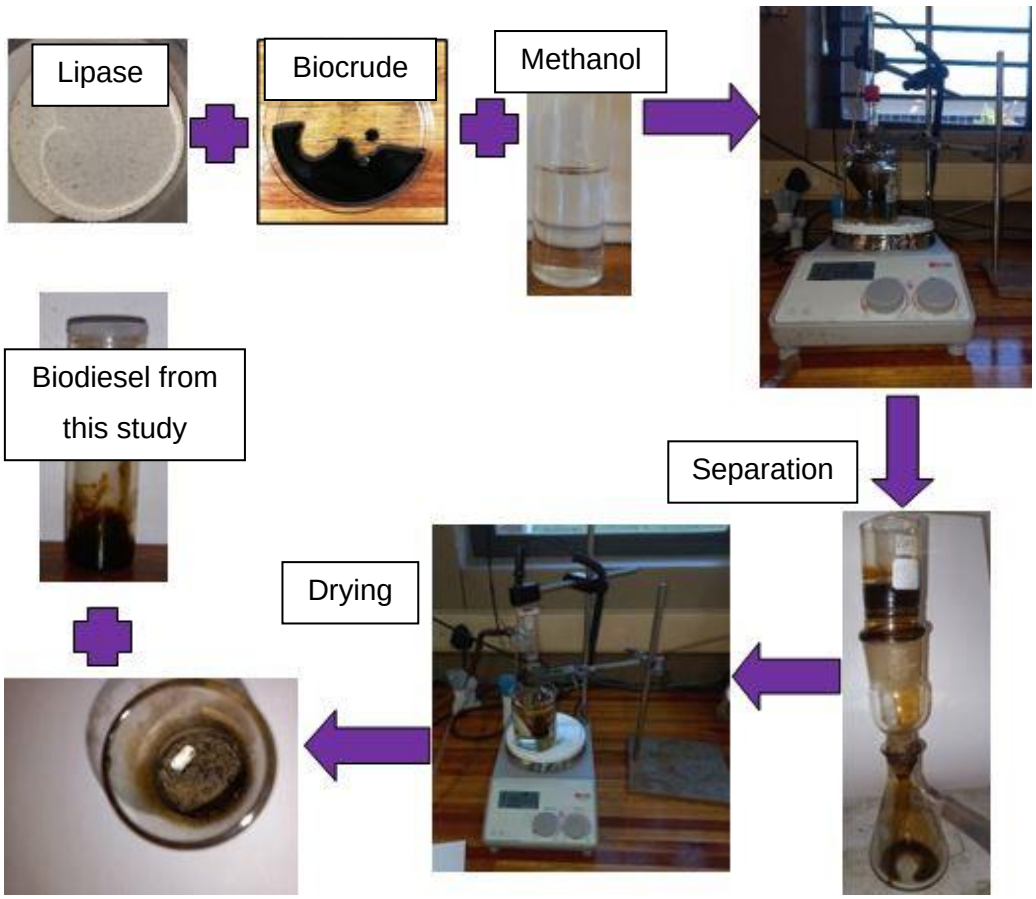

Figure 3.3: Flow diagram representation of experimental procedure of lipase catalysis

3.2.4 Effect of reaction time

The effect of reaction time on the biodiesel yield and quality was determined by keeping all other reaction conditions constant and conducting methanolysis of biocrude oil of 6, 10, 12 and 24 hours. For these reactions, 0.1 g lipase (N435) and 1 g biocrude oil (2.63 mmol) were used to ensure a 10 mass % enzyme loading. Methanol (320 µl) was added to achieve a methanol to oil molar ratio of 3:1. The reactions were carried out at 30°C while stirring constantly at 12.5 Hz.

3.2.5 Effect of temperature

The effect of esterification temperature on biodiesel yield and quality was determined by keeping all other reaction conditions constant and conducting methanolysis of biocrude oil at 27, 30, 35, 40, 45, 50 and 60 °C. For these reactions, 0.1 g lipase (N435) and 1 g biocrude oil (2.63 mmol) were used to ensure a 10 mass % enzyme loading. Methanol (320 µl) was added to achieve a methanol to oil molar ratio of 3:1. The reactions were carried out for 6 hours while stirring constantly at 12.5 Hz.

3.2.6 Effect of oil to methanol molar ratio

The oil to methanol molar ratio was varied by 1:2, 1:3, 1:4, 1:5, 1:6, 1:12 and 1:18 to determine the effect of molar ratio on biodiesel yield and quality. For these reactions 0.1 g N435 (10 mass % enzyme loading) and 1 g biocrude oil (2.63 mmol) were used with oil to methanol ratios of 1:2 (213 µl, 5.26 mmol methanol), 1:3 (320 µl, 7.89 mmol methanol), 1:4 (426 µl, 1.05 mmol methanol), 1:5 (533 µl, 1.32 mmol methanol), 1:6 (640 µl, 1.58 mmol methanol), 1:12 (1279 µl, 3.16 mmol methanol) and 1:18 (1919 µl, 4.74 mmol methanol). The reactions were carried out at 30 °C for 6 hours while stirring constantly at 12.5 Hz.

3.2.7 Biodiesel separation and drying

After a reaction time of 6 hours, the reaction mixture was diluted with 2 mL of diethyl ether to assist in the removal of the lipase, N435, from the reaction mixture and stop the reaction. N435 was filtered off and the mixture was heated under vacuum at 80 °C for 30 minutes to evaporate the diethyl ether from the biodiesel. The method used for product recovery and the lipase-catalysis experimental setup were adopted from Karmee (2016) and Chilabade (2018), respectively. The recovered and dried biodiesel were analysed according to the procedures described in Section 3.3.

3.2.8 N435 regeneration

One of the obstacles associated with enzymatic biodiesel production is the high costs of lipase enzymes (Ghaly *et al.*, 2010) which can be mitigated by the reusability and operational stability of the immobilised lipase, N435 (Gog *et al.*, 2012; Leung *et al.*, 2010). However, N435 is immobilised through adsorption on a microporous acrylic resin that can absorb polar compounds which leads to enzyme deactivation (Amini *et al.*, 2017; Chen & Wu, 2003; Gog *et al.*, 2012). According to Laszlo *et al.* (2011), immobilised lipases like N435 may be reused and has a tolerance for polar and non-polar solvents. Therefore, different solvents were chosen to investigate enzyme regeneration and the effect on FAME conversion.

The N435 lipases used for the temperature and oil to methanol molar ratio experiments were added together and regenerated to determine the reusability of the enzyme. The solvents used to regenerate the enzyme were chosen according to their polarity as indicated by the polarity index of the solvent. The polarity index of the solvents tested for regeneration of the enzyme catalyst is given in Table 3.3.

Table 3.3: List of solvents and their respective polarity indices

Solvent	Polarity	Reference
Acetone	5.1	(Kleiman *et al.*, 2016)
Tetrahydrofuran	4	(Kleiman *et al.*, 2016)
Acetonitrile	5.8	(Snyder *et al.*, 2012)
Isopropanol	3.9	(Ramluckan *et al.*, 2014)
Dimethyl sulfoxide	7.2	(Kleiman *et al.*, 2016)
Hexane	0.1	(Ramluckan *et al.*, 2014)
Tert-butanol	0.39	(Snyder *et al.*, 2012)

The regeneration procedure involved 1 g of used N435 magnetically stirred for 5 minutes in 20 mL solvent at 12.5 Hz. After the regeneration step the mixture was vacuum filtered and the enzyme was left to air dry. For the evaluation of the regenerated enzyme, 0.1 g lipase (N435) and 1 g biocrude oil (2.63 mmol) were used to ensure a 10 mass % enzyme loading with a methanol to oil molar ratio of 3:1 at 30 °C. The reactions were carried out for 6 hours while stirring constantly at 12.5 Hz.

3.3 Analyses and characterisation

3.3.1 Ash content

The ash content of the feedstock mixture and the biocrude oil were determined according to the NREL/TP-510-42622 standard method. Specifically, porcelain crucibles were weighed to the nearest 0.1 mg and the mass was recorded before the crucibles were loaded with approximately 0.5 g of the sample. The samples were ashed using a muffle furnace with temperature control by means of a ramping programme. The furnace was heated from room temperature to 105 °C and held for 12 minutes, then further heated to 250 °C and held for 30 minutes and finally heated to 575 °C and held for 180 minutes after which the crucibles were removed from the furnace and placed in a desiccator to cool. The mass of the crucibles and ash was recorded to the nearest 0.1 mg. The ash content of the samples was calculated using Equations 3.1 and 3.2, respectively.

$$Oven\ Dry\ Weight\ (ODW), (g) = \frac{Weight_{air\ dry\ sample} \times Total\ solids, (mass\ \%)}{100} \qquad (3.1)$$

$$Ash, (mass\%) = \frac{Weight_{crucible\ plus\ ash} - Weight_{crucible}}{ODW_{sample}} \times 100 \quad (3.2)$$

3.3.2 Volatile matter and fixed carbon

The volatile matter and fixed carbon content of the MW were determined according to the SANS 50 standard method. Porcelain crucibles were weighed to the nearest 0.1 mg and the mass was recorded before the crucibles were loaded with approximately 0.5 g of the sample. The crucibles with their lids were placed inside a muffle furnace at approximately 900 °C for 7 minutes. The crucibles were removed and allow to cool until room temperature in a desiccator. The crucibles were weighed, and the weight was recorded. The volatile matter and fixed carbon content of the samples were calculated using Equations 3.3 and 3.4, respectively.

$$Fixed\ carbon, (mass\%) = 100 - (Ash + Moisture + Volatile\ matter) \quad (3.3)$$

$$Volatile\ matter, (mass\%) = \frac{\left(Weight_{crucible+\ lid+\ sample} - Weight_{After\ heat}\right) \times 100}{Weight_{crucible+lid+\ sample} - Weight_{crucible+\ lid}} - Moisture \quad (3.4)$$

3.3.3 Elemental analysis

Elemental analysis was done according to standard method SANS 17247 to determine the atomic hydrogen, carbon, and nitrogen content of the MW, biochar, biocrude oil, and biodiesel. The analysis was conducted using a CE-440 elemental analyser, shown in Figure 3.4.

Figure 3.4: The CE-440 elemental analyser

3.3.4 Higher heating value determination

The HHVs of the MW and biocrude were determined using an IKA C5003 calorific value analyser shown in Figure 3.5. A sample with a mass of 0.5 g was used for this analysis. Equation 3.5 was used to calculate the HHV of the biodiesel samples from the elemental analysis data (Demirbas, 2016; Vargas-Moreno *et al.*, 2012). The HHV of the biodiesel was calculated due to the small sample sizes.

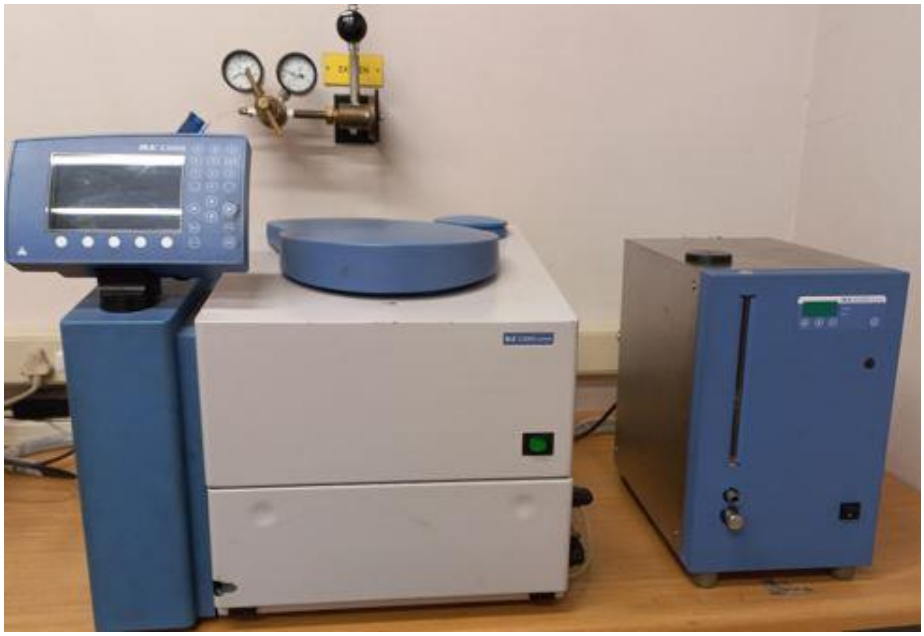

Figure 3.5: The IKA C5003 calorific value analyser

$$HHV\left(\frac{MJ}{Kg}\right) = (33.5C + 142.3H - 15.4O - 14.5N) \times 10^{-2} \quad (3.5)$$

3.3.5 Moisture analysis

A Karl Fischer coulometer shown in Figure 3.6 was used to determine the moisture content of the biocrude oil. A sample with a mass of 0.5 g was weighed and dissolved in 5 mL of ethanol. The solution was analysed by the Karl Fischer coulometer, and the moisture content was calculated using Equations 3.6 and 3.7.

$$Sample\ fraction = \frac{Weight_{sample}}{Weight_{sample} + Weight_{ethanol}} \quad (3.6)$$

$$Moisture\ (mass\%) = \left(\frac{Mixture_{moisture} - \left(1 - Sample_{fraction}\right) \times Moisture_{ethanol}}{Sample_{fraction}}\right)/10000 \quad (3.7)$$

Figure 3.6: Karl Fischer coulometer for moisture analyses

The moisture content of the MW was determined according to the NREL/TP-510-42621 standard method. Porcelain crucibles were weighed to the nearest 0.1 mg and the mass was recorded before the crucibles were loaded with approximately 0.5 g of the sample. The crucibles were placed inside a muffle furnace at approximately 105 °C until a dry constant weight. The crucibles were removed and allow to cool until room temperature in a desiccator. The crucibles were weighed, and the weight was recorded until a ± 0.1 mg change was detected. The moisture content of the samples was calculated using Equation 3.8.

$$Moisture, (mass\%) = 100 - \frac{Weight_{dry\ dish\ plus\ dry\ sample} - Weight_{dry\ dish}}{Weight_{sample\ as\ received}} \quad (3.8)$$

3.3.6 Functional group analysis

An FTIR was used to determine the functional groups present in the biocrude oil. The liquid samples were dissolved in dichloromethane and the spectra were generated using a Shimadzu IRAffinity-1 spectrophotometer shown in Figure 3.7. Three scans were done per sample using a specific range of frequencies (500 cm^{-1} to 4500 cm^{-1}) in the FTIR analysis of the MW and biocrude oil.

Figure 3.7: The Shimadzu IRAffinity-1 spectrophotometer

3.3.7 Molecular weight distribution

The biocrude oil was analysed using a PerkinElmer Flexar GPC system shown in Figure 3.8 to determine its weight average molecular mass (M_w), its number average molecular mass (M_n), and its polydispersity index (PDI). The PerkinElmer Flexar system consists of a degasser, isocratic LC pump, auto-sampler, column oven, two Agilent Polar Gel L columns (7.5 x 300 mm, 8 µm particle size) and a refractive index detector (Muller *et al.*, 2019). Chromatograms were recorded using the TotalChrom version 6.3.2 software. The flowrate was 0.4 mL min^{-1}, oven temperature 55 °C, injection volume 100 µL and sample concentration 8 mg mL^{-1}. The eluant used was DMSO/water (9:1, v/v) and the sample was filtered through a 0.45 µm syringe filter before injection. The same method was used as the one used by Muller *et al.*, (2019).

Figure 3.8: The PerkinElmer Flexar system used for GPC analysis

3.3.8 Biocrude and biodiesel component analyses

Gas chromatography coupled with mass spectrometry (GCMS) was used to analyse the chemical components in the biocrude oil and produced biodiesel. The GCMS system used was an Agilent 7890 GC/MSD gas chromatograph with 5975 Triple Axis MSD detector shown in Figure 3.9. The GCMS was used to determine the fatty acid profile and to quantify phenols and methyl esters in the biocrude oil and biodiesel. The gas chromatograph was fitted with a 30 m VF-5ht Ulti-metal column with a diameter of 0.25 mm and a film thickness of 0.2 µm. The following conditions were used: an inlet temperature of 275 °C, oven programming of 90 °C for 4 minutes, 90 °C to 300 °C at 10 °C.min^{-1}, 300 °C for 20 minutes, injection volume of 0.2 µL (auto-injection), FID detector at 350 °C, H_2 flow rate of 40 mL.min^{-1}, make-up He flow rate of 10 mL.min^{-1} and air flow rate of 400 mL.min^{-1}.

Figure 3.9: The 7890 Agilent GC system used for GCMS analysis

3.3.9 ^{1}H NMR Analysis

The ^{1}H NMR analysis was conducted on the biocrude oil and biodiesel samples to determine the fatty acid profile and FAME conversion by using a Bruker 600 MHz NMR spectrometer. The NMR spectrometer contains a 5 mm PA BBO 1H/DZ-GRD probe and a B-ACS 60 auto-sampler. The ^{1}H NMR analysis was conducted at ambient temperature with a soft pulse set to 30 ° flip angle for proton excitation. The sample was prepared by dissolving 10 mg biodiesel in 750 µL deuterated chloroform and 50 µL internal standard which consisted of 200 mg pentafluoro-benzaldehyde dissolved in 1 mL chloroform. The prepared sample was mixed using a vortex apparatus and then filtered through a 0.45 µm filter into the NMR analysis tube. The processing of the NMR spectrum was done by using Topspin version 4.1 software. The FAME content was calculated by using Equation 3.9. A_1 and A_2 represent the areas of the methoxy and the methylene protons in the NMR spectrum, respectively (Gelbard *et al.*, 1995).

$$FAME\ (\%) = \frac{2}{3}\left(\frac{A_1}{A_2}\right) * 100 \qquad 3.9$$

3.4 Determination of standard deviation in data

Each experiment was carried out in triplicate to determine the variance in the data. The experimental error was determined at a 95 % confidence level using the standard deviation according to Devore *et al.* (2005). Appendix C provides a detailed description of the experimental error calculations for the biocrude oil yield, FAME conversion, bomb calorimeter and elemental analyser.

3.5 References

Ayeleru, O.O., Ntuli, F. & Mbohwa, C. 2016. Of fruits and vegetables wastes in the City of Johannesburg. *Lecture Notes in Computational Science and Engineering*, 2226:659-663.

Chilabade, D. 2018. *Biodiesel production from plant oils of African origin*. Potchefstroom: North-West University. (Dissertation – MChEng).

Demirbas, A. 2016. Calculation of higher heating values of fatty acids. *Energy Sources, Part A: Recovery, Utilization, and Environmental Effects*, 38(18):2693-2697. doi:10.1080/15567036.2015.1115924

Department of Environmental Affairs. 2018. So*uth Africa State of Waste Report: first draft report*. http://sawic.environment.gov.za/documents/8635.pdf Date of access: 16 Jun. 2021.

Gelbard, G., Brès, O., Vargas, R.M., Vielfaure, F. & Schuchardt, U.F. 1995. ^{1}H nuclear magnetic resonance determination of the yield of the transesterification of rapeseed oil with methanol. *Journal of the American Oil Chemists' Society*, 72(10):1239-1241.

Karmee, S.K. 2016. Preparation of biodiesel from nonedible oils using a mixture of used lipases. *Energy Sources, Part A Recover. Util. Environ. Eff. Taylor & Francis*. 38(18):2727–2733.

Muller, L.C., Marx, S., Vosloo, H.C.M. & Chiyanzu, I. 2019. Functionalising lignin in crude glycerol to prepare polyols and polyurethane. *Polymers from Renewable Resources*, 10(1-3):3-18. doi:10.1177%2F2041247919830833

Vargas-Moreno, J.M., Callejón-Ferre, A.J., Pérez-Alonso, J., & Velázquez-Martí, B. 2012. A review of the mathematical models for predicting the heating value of biomass materials. *Renewable and Sustainable Energy Reviews*, 16(5):3065-3083. doi:10.1016/j.rser.2012.02.054

Devore, J., Farnum, N., Doi, J. 2001. Applied statistics for engineers and scientists. *Technometrics*, 43(1):103. doi:10.1198/tech.2001.s554

CHAPTER 4: RESULTS AND DISCUSSION

This chapter provides a detailed description of the results obtained in this study. Sections 4.1 and 4.2 discuss the characterisation of the MW feedstock and HTL-biocrude oil. The results of the effect of the operating conditions on enzymatic esterification are discussed in Section 4.3. Sections 4.4 and 4.5 discuss the characterisation of the biodiesel produced and lipase regenerated using different solvents and the effect on the FAME conversion.

4.1 MW characterisation

Table 4.1 gives some properties and characteristics of the synthetic MSW and sewage sludge used to produce the biocrude oil used in this study.

Table 4.1: Composition analysis (on a dry ash-free basis, daf) and properties of the MW feedstock

Component	Standard	Value (Mass %)
Proximate analysis		
Ash	NREL/TP-510-42622	5.45 ± 0.2
Volatile matter	SANS 50	32.74 ± 2.82
Fixed carbon*	-	2.05 ± 2.14
Moisture	NREL/TP-510-42621	60.93 ± 4.19
Compositional analysis		
Fat (daf)	ASM 044	3.06
Protein (daf)	ASM 078	12.21
Total carbohydrates (daf)	ASM 075	79.88
Neutral detergent fibre (NDF)		46.9 ± 1.5
Acid detergent fibre (ADF)		13.9
Acid detergent lignin (ADL)		4 ± 0.9
Cellulose	Calculated[a]	9.9 ± 1.3

Hemicellulose	Calculated[b]	33.02 ± 1.6
Lignin	Calculated[c]	2.5 ± 0.2
Starch	Calculated[d]	34.5
HHV (MJ/kg)	SANS 1928	18.44 ± 0.6
Elemental analysis		
Carbon	SANS 17247	43.84 ± 0.30
Hydrogen	SANS 17247	6.28 ± 0.32
Nitrogen	SANS 17247	1.88 ± 0.02
Residual*	Calculated	52

a – Cellulose content = ADF-ADL, b – Hemicellulose content = NDF-ADF, c – Lignin = ADL-cutin-ash, d – Starch = Total carbohydrates – cellulose-hemicellulose-lignin, *Calculated by difference

The ash and moisture content of the MW are similar to the results obtained by Ayeleru *et al.* (2016), who reported an ash and moisture content of 5.39 mass % and 62.55 mass %, respectively. Aierzhati *et al.* (2019) who investigated HTL-biocrude from different food waste biomass obtained an ash content of 5 mass % for the fruit peel biomass.

The feedstock was mainly composed of protein and carbohydrates that consisted of cellulose, hemicellulose, lignin, and other carbohydrates, such as starch and sugars (referred to as starch in Table 4.1). According to Akhtar & Amin (2011) and De Caprariis *et al.* (2017), the biocrude oil yield is influenced by a variety of factors, including the high hemicellulose, high cellulose, and low lignin content, that increases the biocrude yield. Therefore, high hemicellulose (33.02 mass %) and low lignin (2.5 mass %) content make the MW an excellent feedstock to produce biocrude oil.

The feedstock had a calorific value of 18.44 MJ/kg which was similar to the calorific value of 17.7 MJ/kg obtained by Minowa *et al.* (1995), who also used an artificial MSW. Aierzhati *et al.* (2019) who investigated HTL-biocrude extracted from different food waste biomass obtained a HHV of 17.16 MJ/kg for the vegetable feedstock and a HHV of 17.82 MJ/kg for the fruit peel feedstock.

The results in Table 4.1 show that carbon was the most abundant element due to the organic waste in the feedstock (Baawain *et al.*, 2017). Similar results were obtained by Ayeleru *et al.* (2016), who reported C (44.95 mass %), H (6.17 mass %) and N (1.95 mass %) in their study.

4.2 Biocrude characterisation

The product yields from HTL of the MW feedstock were 6.80 mass %, 14.82 mass %, 9.52 mass % and 57.84 mass % for the biocrude oil, hydrochar, gas, and aqueous product, respectively. The daf yield of the biochar and biocrude was calculated as 40 mass % and 19.4 mass %, respectively. The experimental error was determined for a 95 % confidence interval as discussed in Appendix C, Section C.1. The experimental errors for the biocrude- and biochar yield were calculated as 0.22 % and 0.45 %, respectively. The low experimental errors obtained indicate that the HTL experiments produced consistent yields. The experimental error of the bomb calorimeter was determined by analysing each sample three times. Furthermore, the elemental analyser produced an error of 0.52 % as shown in Appendix C, Section C.1.

Aierzhati *et al.* (2019) who investigated HTL of biocrude from different kinds of food waste biomass obtained a biocrude yield of 7 mass % for the vegetable biomass and a yield of 8 mass % for the fruit peel biomass. Malins *et al.* (2015), who investigated HTL of wet sewage sludge at 300 °C with a reaction time of 40 min, obtained a bio-oil yield of 33.49 mass %. The highest bio-oil yield of 53.9 mass % was obtained at a biomass to water ratio of 1:15 (Malins *et al.*, 2015). The bio-oil yield increased significantly as the water to biomass ratio increased due to hydrolysis reactions of sewage sludge. Moreover, the increase in the biocrude yield at higher water to biomass ratios is also due to the sufficient mixing of the reactants inside the reactor which promotes heat and mass transfer conditions (Cao *et al.*, 2017; Yang *et al.*, 2016). Similar results were obtained by other authors indicating that a higher water to biomass ratio decreases the hydrochar yield and increases the biocrude yield (Cao *et al.*, 2017; Li *et al.*, 2018; Yang *et al.*, 2016). Additionally, beyond the critical point of water the biocrude yield will decrease due to hydrolysis and repolymerisation reactions (Dimitriadis & Bezergianni, 2017; Xue *et al.*, 2016).

Kohansal *et al.* (2021), who investigated the HTL of pre-treated MSW, obtained a biocrude yield of 28.9 mass % at 350 °C without a catalyst. The biocrude yield increased to 36.6 mass % with the addition of an alkali catalyst (K_2CO_3). Similar results were obtained by Minowa *et al.* (1995), who investigated biocrude production from garbage by HTL. The biocrude yield increased from 16 mass % to 25 mass % after the addition of sodium carbonate as catalyst (Minowa *et al.*, 1995). The addition of a catalyst reduces the formation of biochar and improves the yield of the biocrude by inhibiting side reactions, increasing reaction rates, and reducing reaction pressure and temperature (Cao *et al.*, 2017; Dimitriadis & Bezergianni, 2017; Kumar *et al.*, 2018).

The biocrude yield obtained in this study is in agreement with the results obtained by Aierzhati *et al.* (2019) and lower compared to yields reported by other authors. The low biocrude yield reported

in this study is attributed to the biomass to water ratio and can also be due to the different biomass used and reaction conditions.

According to Yang *et al.* (2016) the HHV of HTL-biocrude oils produced from lignocellulosic biomass without using an organic solvent or a catalyst are between 30-36 MJ/kg. The biocrude oil produced in this study had a calorific value of 31.2 ± 0.5 MJ/kg which was expected according to literature. Similar results were reported by Malins *et al.* (2015), who obtained a calorific value of 31.42 MJ/kg for HTL-biocrude oil from sewage sludge. Aierzhati *et al.* (2019), who investigated HTL-biocrude from different kinds of food waste biomass, obtained a HHV of 32.48 MJ/kg for the biocrude of the vegetable biomass and a HHV of 32.71 MJ/kg for the biocrude of the fruit peel biomass.

The calorific value of the biocrude in this study was lower than the calorific value obtained by Xiu & Shahbazi (2012) for petroleum fuel, 40 MJ/kg. Therefore, upgrading is necessary for biocrude to be used as a liquid fuel. The calorific value of the hydrochar was 28.3 ± 0.5 MJ/kg which is analogous to Grade A coal.

4.2.1 Compositional analysis

The results of proximate and elemental analyses of the MW-derived biocrude oil is given in Table 4.2. The experimental error of the elemental analyser was determined by analysing each sample three times. The elemental analyser produced an error of 0.995 % as shown in Appendix C, Section C.1.

Table 4.2: Proximate and elemental analyses of biocrude oil

	Value (mass %)	Values from literature, (mass %)	Petroleum (mass %)
Proximate analysis		(Xu & Shahbazi, 2012)	
Ash	0.19 ± 0.02	0.78	0.1
Moisture	3.98 ± 0.85	2.4	0.1
Elemental analysis		(Vardon *et al.*, 2002)	
C	69.5 ± 1.8	71.2	
H	8.9 ± 0.2	9.5	
N	2 ± 0.04	3.7	
O	19.6	15.6	

The atomic H/C and O/C ratios of the biocrude oil are compared to some of the fossil-based fuels in the Van Krevelen diagram in Figure 4.1. Values were obtained from the elemental analysis of the feedstock, biocrude, and biochar, while values for the fossil fuel components were obtained from literature (Capunitan & Capareda, 2012; Dos Santos *et al.*, 2016; Gamliel *et al.*, 2018; Ramirez *et al.*, 2015). The biochar obtained in this study had a slightly higher O/C ratio than low-temperature tar with the same H/C ratio. The biochar falls into the region between the MW and biocrude on the Van Krevelen diagram. The decrease in the O/C ratio of the biocrude is attributed to deoxygenation through decarboxylation of protein, lignocellulose, and fatty acids during HTL (Chen *et al.*, 2014; Parthasarathy & Narayanan, 2014). The H/C and O/C ratios of the biocrude oil produced in this study are more comparable to that of FAME biodiesel than fossil fuel diesel. Similar results were obtained by Hossain *et al.* (2017), who investigated the properties of microalgae HTL-biocrude. The decrease in the H/C ratio of the biocrude indicates that aromatic compounds and phenolic derivatives were produced during HTL (Parthasarathy & Narayanan, 2014). The H/C- and O/C ratios of the biodiesel produced in this study are higher compared to the H/C- and O/C ratios of the biocrude oil. The H/C- and O/C values of the feedstock, HTL products and the biodiesel produced in this study are shown Table 4.3.

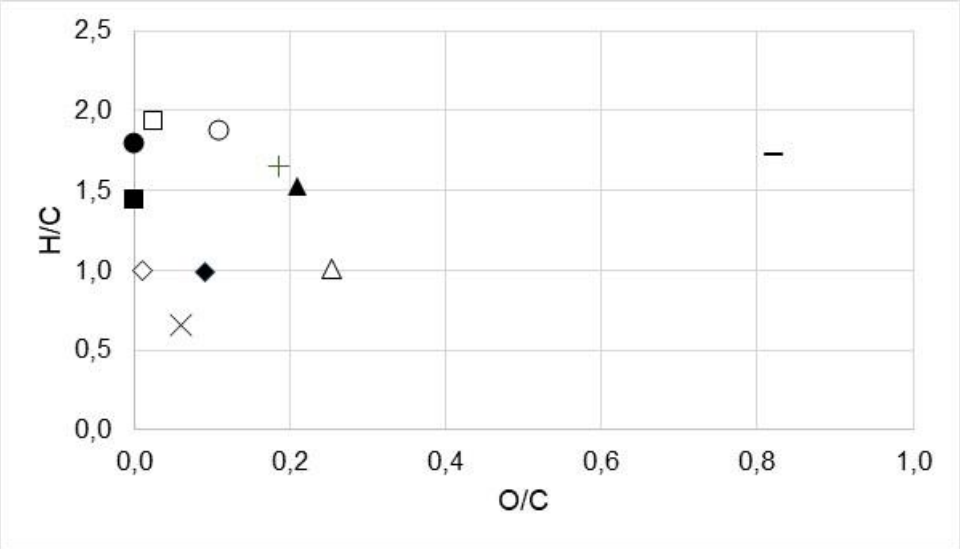

Figure 4.1: Van Krevelen diagram comparing the MW (—), biochar (∆), biocrude (▲), biodiesel in this study (+), diesel (●), biodiesel (o), coke oven tar (◊), coal (x), low-temperature tar (♦), petroleum high value (□), and petroleum low value (■) (Capunitan & Capareda, 2012; Dos Santos *et al.*, 2016; Gamliel *et al.*, 2018; Ramirez *et al.*, 2015)

According to Capunitan and Capareda (2012), petroleum fuel has an H/C ratio that ranges between 1.5 and 2 with an O/C ratio below 0.06. The biocrude obtained in this study had a lower H/C ratio and a higher O/C ratio compared to petroleum fuel. Therefore, further upgrading is necessary to improve the quality of the biocrude for the biocrude to be used as a viable renewable fuel or biodiesel.

Table 4.3:H/C- and O/C values of the feedstock, HTL products and the biodiesel produced in this study

Component	H/C	O/C
MSW	1.72	0.82
Biochar	1.01	0.25
Biocrude oil	1.53	0.21
Biodiesel produced in this study	1.65	0.19

Table 4.4 gives the results of the GPC analysis of the biocrude oil.

Table 4.4: Results of GPC analysis on biocrude oil

Quantity	Standard	Value
M_W (g/mol)	Calculated[a]	380
M_n (g/mol)	Calculated[b]	143
PDI	Calculated[c]	2.7

M_w: Weight average molecular mass, M_n: Number average molecular weight, PDI: Polydispersity index, M_i and N_i are the slice MW and slice signal intensities (Li *et al.*, 2014).

$$a - \mathrm{Mw} = \frac{\sum N_i {M_i}^2}{\sum N_i M_i},\ b - \mathrm{Mn} = \frac{\sum N_i M_i}{\sum N_i},\ c - \mathrm{PDI} = \frac{\mathrm{Mw}}{\mathrm{Mn}}$$

M_n and M_w are determined from the mole fraction distribution and weight fraction distribution of different-sized molecules, respectively (Ishihara *et al.*, 1996; Schulz *et al.*, 2006). The PDI gives an indication of the broadness of the molecular weight distribution that entails the difference between the minimum and maximum molecular weight from the average molecular weight (Hu *et al.*, 2019; Vardon *et al.*, 2011).

The weight average molecular mass (M_w) of the biocrude oil prepared in this study was 380 g/mol, which is within the range of the molecular mass of C_{16} to C_{22} fatty acids. The number average molecular mass is much lower than that of the weight average molecular mass, indicating a large weight dispersion of molecules. A larger weight dispersion is due to more heavy molecules present in the biocrude as compared to low molecular weight molecules (Vardon *et al.*, 2011). A PDI of 2.7 indicates a broad molecular mass distribution and it was thus expected that the GCMS results would show many different fatty acids present in the biocrude oil. This is attributed to a

broad molecular mass distribution that indicates a wide boiling point distribution (Wang *et al.*, 2021).

Similarly, Hu *et al.* (2019), who investigated HTL-biocrude oil derived from microalgae, reported the following values for M_W, 362 g/mol, and M_n, 235 g/mol. A smaller PDI of 1.75 was reported by Hu *et al*. (2019), indicating that their biocrude had a narrower mass distribution compared to the biocrude obtained in this study. The PDI of this study's biocrude is similar to the values obtained by Vardon *et al.* (2011) for digestive sludge-derived biocrude oil (2.59) and swine manure-derived biocrude oil (2.42).

4.2.2 FTIR and NMR

FTIR and NMR spectra were used to obtain and compare the different functional groups of the biocrude, as shown in Figures 4.2 and 4.3. The assigned functional groups were based on standard published FTIR and NMR libraries (Figure 4.2) and compared to results from literature (Figure 4.3) (Bruice, 2011; Coates, 2000; White, 1971).

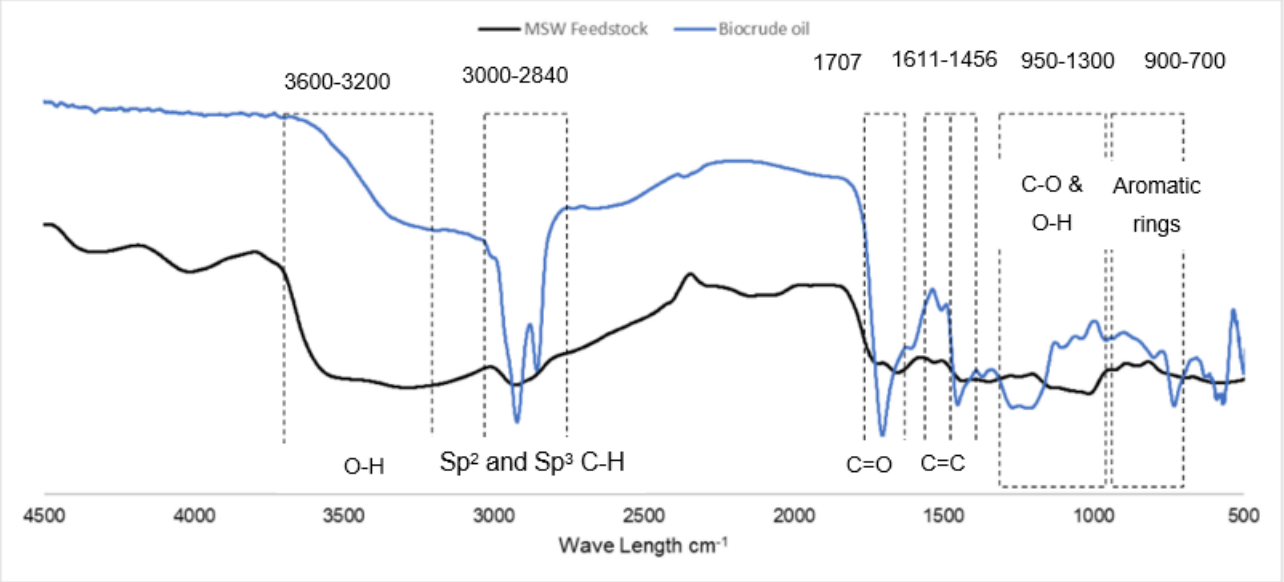

Figure 4.2:FTIR Spectra of biocrude

The O-H stretching vibrations between 3600 cm^{-1} and 3200 cm^{-1} indicates the presence of carboxylic acids, phenols, and alcohols in the biocrude and are smaller compared to those of the MW feedstock. The narrower O-H stretching vibrations of the biocrude oil compared to the MW feedstock is due to the degradation of the cellulose and the conversion of the fatty acids to esters during the HTL reaction (Chen *et al.*, 2019). The GCMS identified the following fatty acid esters in the biocrude oil: dodecanoic acid methyl ester, hexadecenoic acid methyl ester, methyl stearate, and octadecanoic acid methyl ester. According to the GCMS results the following

phenolic derivatives with the largest peak areas were present in the biocrude oil: phenol, p-cresol, 2,4-dimethyl-phenol, 3-methyl-phenol, 4-ethyl-phenol, 2-methoxy-6-methylphenol, 4-ethyl-2-methoxy-phenol and 2,6-dimethoxy-phenol produced by the degradation of lignin in the MW feedstock. The prominent peaks observed for the biocrude oil between 1700 cm^{-1} and 1400 cm^{-1} are not observed for the MW feedstock and indicates the degradation of the lignin, cellulose and hemicellulose content and the formation monomers such as phenolic derivatives. The lignin content of the MW is significantly lower than the hemicellulose and cellulose content of the feedstock, as shown in Table 4.1. The high hemicellulose and cellulose content of the MW feedstock attribute to the phenolic concentration observed in the biocrude oil (Zhu *et al.*, 2015). Zhu *et al.* (2015) and Ohra-Aho *et al.* (2005) confirmed that if the feedstock contains small amounts of lignin, higher concentrations of phenolics can originate from the hydrolysis and dehydration of cellulose and hemicellulose. Sp^3 and Sp^2 C-H stretching vibrations identified between 3000 cm^{-1} and 2840 cm^{-1} of the biocrude oil were stronger than those of the feedstock and indicate an aliphatic chain of fatty acids and hydrocarbons. The major fatty acids identified by the GCMS were n-hexadecanoic acid, oleic acid, dodecanoic acid, tetradecanoic acid, octadecanoic acid and 9,12-octadecadienoic acid (Z,Z)- produced by the decomposition of extractive biomass (Zhu *et al.*, 2015).

The adsorption profile at 1707 cm^{-1} implies the presence of C=O stretching vibrations of ketone, aldehyde groups. Furthermore, the GCMS identified the following ketones and aldehydes with the largest peak areas in the biocrude oil: 2,3-dimethyl-2-cyclopenten-1-one, 3,6-bis(2-methylpropyl)-2,5-piperazinedione, acetaldehyde, and 2-methyl-3methylene-cyclopentane carboxaldehyde. The absorption bands at 1611, 1516, 1456 cm^{-1} (Figure 4.2) were stronger for the biocrude compared to the feedstock and were ascribed to C=C stretching vibrations in aromatic rings and derivatives in the biocrude oil. The absorption between 950 cm^{-1} and 1300 cm^{-1} were attributed to C-O stretch vibrations and O-H bending vibrations in phenols, carboxylic acids, and primary, tertiary alcohols. Additionally, according to the GCMS results the following alcohol derivative with the largest peak area was present in the biocrude oil: (3.beta.,5.alpha.,6.beta.)- Ergost-25-ene-3,5,6-triol.

Absorption between 700 cm^{-1} and 900 cm^{-1} of the biocrude oil is slightly stronger than that of the feedstock and was ascribed to the deformation vibrations in aromatic rings. According to Qiao *et al.* (2018), the presence of carbonyl groups, C-H alkane and alkene groups are the main characteristics of the MSW biocrude which is due to the high organic content of the MSW. The carbonyl groups are present in hemicellulose in the form of fatty acids and methyl esters; however, lignin carbonyl groups are usually detected as ketones and aldehydes (Zhu *et al.*, 2015). The

FTIR spectrum of the MW biocrude obtained similar results than Chen *et al.* (2019) and Qiao *et al.* (2018). The functional groups are listed in Table 4.5.

Table 4.5: Functional groups obtained from the FTIR spectra of the biocrude oil

Wavelength range (cm^{-1})	Fictional group	Mode of vibration	References
3600–3200	O-H	stretching	(Chen *et al.*, 2019)
3000-2840	Sp^3 and Sp^2 C-H	stretching	(Chen *et al.*, 2019); (Wang *et al.*, 2007)
1707	C=O	stretching	(Qiao *et al.*, 2018)
1611, 1516, 1456	C=C	stretching	(Wang *et al.*, 2007)
1300–950	C-O and O-H	stretching and bending	(Chen *et al.*, 2019; Xu *et al.*, 2018)
900–700	Aromatic rings	deforming	(Wang *et al.*, 2007)

Figure 4.3 gives the results of the NMR spectra of the biocrude oil.

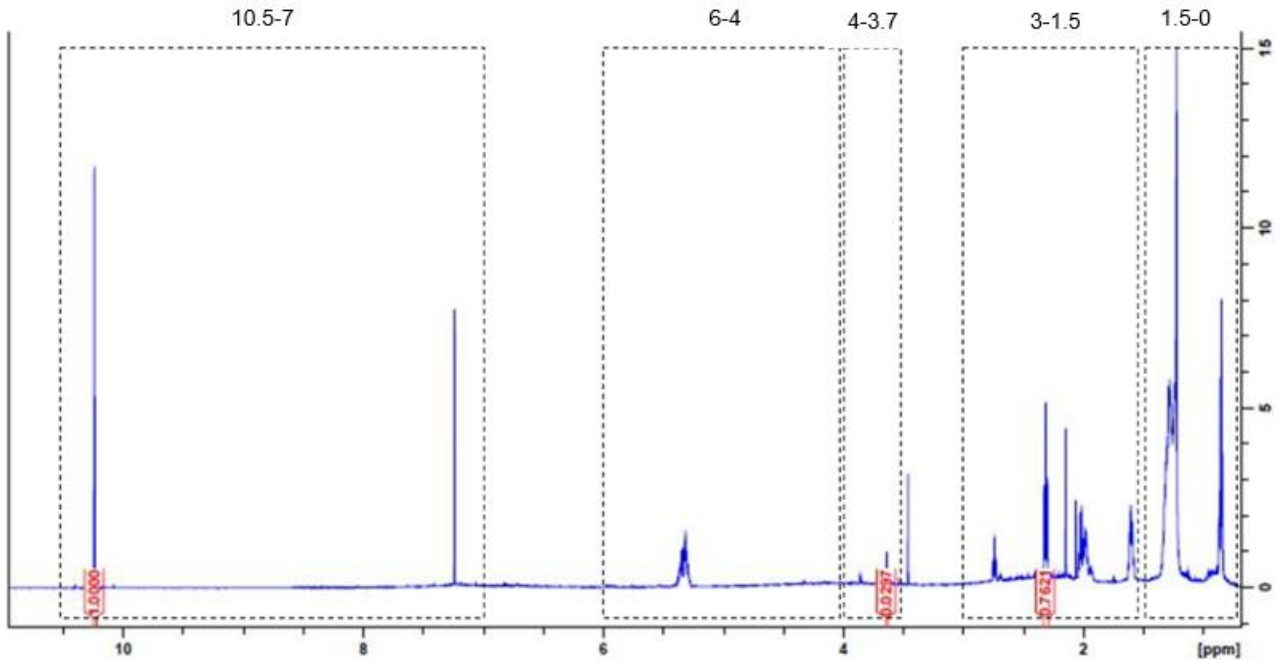

Figure 4.3: NMR Spectra of biocrude oil

The peaks that are present between 7–10.5 ppm were allocated to the chloroform and 2,3,4,5,6-pentafluorobenzaldehyde used for sample preparation. The peak between 4–6 ppm is methoxy or carbohydrate functionalities which are due to the conversion of carbohydrates from the feedstock into the biocrude (Vardon *et al.*, 2011). However, in the FTIR, O-H functional groups are observed indicating that the peaks represent aliphatic alcohols. The region in the spectrum between 3.7–4 ppm either represents aliphatic alcohols and ethers or a methylene group that joins two aromatic rings (Mullen *et al.*, 2009). The small peaks between 1.5–3 ppm were allocated to aliphatics α-to-heteroatom or unsaturated functionalities due to the large amount of oxygen and nitrogen compounds derived from the MSW feedstock (Cheng *et al.*, 2017; Xu *et al.*, 2018). The peaks between 0–1.5 ppm are consistent with aliphatic methyl protons and methylene protons in alkyl chains (Bruice, 2011; Cheng *et al.*, 2017). Furthermore, they are consistent with the aliphatic chain of fatty acids observed in the FTIR. Overall, the NMR results are consistent with the FTIR results.

4.2.3 Fatty acid composition of biocrude

The biocrude was analysed using GCMS and NMR to determine its fatty acid composition and methyl ester content as shown in Table 4.6. The experimental errors of the GCMS and NMR were determined by analysing each sample three times. Furthermore, the elemental analyser produced an error of 0.995 % as shown in Appendix C, Section C.1.

The most common vegetable oils used to produce biodiesel are rapeseed, sunflower and soybean oil (Canakci & Van Gerpen, 2001; Ramos *et al.*, 2009). Animal fats used to produce biodiesel include lard, tallow, and yellow grease. The GCMS detected the following fatty acids $C_{16:0}$ (15.91 mass %), $C_{18:0}$ (6.32 mass %), $C_{18:1}$ (32.82 mass %), $C_{18:2}$ (44 mass %) and $C_{14:0}$ (0.95 mass %) in the biocrude. The fatty acid distribution of soybean oil entails $C_{16:0}$ (10.58 mass %), $C_{18:0}$ (4.76 mass %), $C_{18:1}$ (22.52 mass %), and $C_{18:2}$ (52.34 mass %), whereas the fatty acids of yellow grease include $C_{16:0}$ (23.24 mass %), $C_{18:0}$ (12.96 mass %), $C_{18:1}$ (44.32 mass %), $C_{18:2}$ (6.97 mass %) and $C_{14:0}$ (2.43 mass %) as reported by Canakci and Van Gerpen (2001). There is an insignificant difference in the fatty acid profile between the biocrude used in this study, soyabean oil and yellow grease. Esterification and transesterification do not change the fatty acid composition of the biocrude but affects critical properties of the biodiesel such as the cetane number and cold flow properties (Karmakar *et al.*, 2010; Ramos *et al.*, 2009). However, there will be a significant difference in the properties of the biodiesel produced by biocrude compared to biodiesel produced by soybean oil and yellow grease.

The NMR analyses obtained a methyl ester content of 1.2 % and confirmed the total fatty acid content of 41.5 % as quantified by GCMS. The experimental errors of the GCMS and NMR were

determined by analysing each sample three times. The GCMS and NMR produced errors of 5.40 % and 0.21 %, respectively, as shown in Appendix C, Section C.1.

According to Christopher *et al.* (2014), lipase has great stability, easily produces biodiesel with high FFA feedstocks, and considerably lowers enzymatic biodiesel production costs. Therefore, the high fatty acid content biocrude used in this study is a suitable feedstock for enzymatic esterification.

Table 4.6: Fatty acid composition and methyl ester content of the biocrude

Fatty Acid Composition	Quantity (mass %)
$C_{14:0}$	0.95
$C_{16:0}$	15.91
$C_{18:0}$	6.32
$C_{18:1}$	32.82
$C_{18:2}$	44
FA (%)	41.5 ± 3.38
ME (%)	1.2 ± 0.21

4.3 Enzymatic esterification

4.3.1 Effect of reaction time

According to Freedman *et al.* (1984), the conversion of biocrude to FAME increases as the reaction time increases up to an optimum reaction time, after which the FAME yield starts to decrease. This is due to reversible reactions which result in production costs increasing (Leung *et al.*, 2010; Mathiyazhagan & Ganapathi, 2011). Lipase catalysis was performed at 6, 10, 12 and 24 hours to determine the optimum reaction time while other operating conditions were kept constant at 10 mass % N435 loading, 1:3 biocrude to methanol molar ratio and 30 °C.

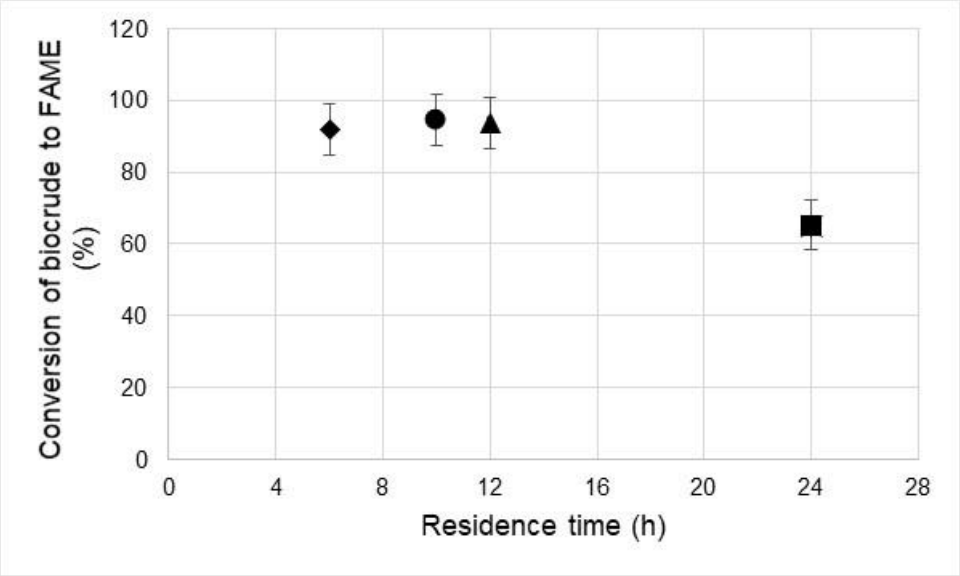

Figure 4.4: The effect of reaction time on FAME conversion

As shown in Figure 4.4, the FAME conversion increased slightly from 91.14 % at 6 hours to 94.60 % at 10 hours and significantly decreased thereafter to 65.27 % at 24 hours. The decrease in FAME conversion observed after 10 hours could be due to alcohol inhibition that is attributed to the denaturation of the enzyme (Guldhe *et al.*, 2015; Mulalee *et al.*, 2015). Based on Figure 4.4, the optimum reaction time for this study appears to have been at 10 hours. However, due to the insignificant increase of FAME conversion between 6 and 10 hours, the reaction time of 6 hours was chosen for further experimental work. Similarly, other authors reported varying optimal reaction times ranging from 7 to 72 hours (Amini *et al.*, 2017; Karmee, 2018; Köse *et al.*, 2002; Kumar *et al.*, 2015; Shimada *et al.*, 1999).

The experimental error of the enzymatic esterification was determined by conducting experiments in triplicate. The enzymatic esterification produced an error of 3.41 %, as shown in Appendix C, Section C.1.

4.3.2 Effect of operating temperature

Various authors have investigated the influence of reaction temperature on FAME conversion and indicated that the optimum temperature was between 30 °C and 50 °C (Ghaly *et al.*, 2010; Karmee *et al.*, 2015; Rodrigues *et al.*, 2008; Shimada *et al*., 1999). Enzymatic esterification was performed at 27, 30, 35, 40, 45, 50 and 60 °C to identify the optimum reaction temperature. Other operating conditions were kept constant at 10 mass % N435 loading, 1:3 biocrude to methanol molar ratio, and a reaction time of 6 hours.

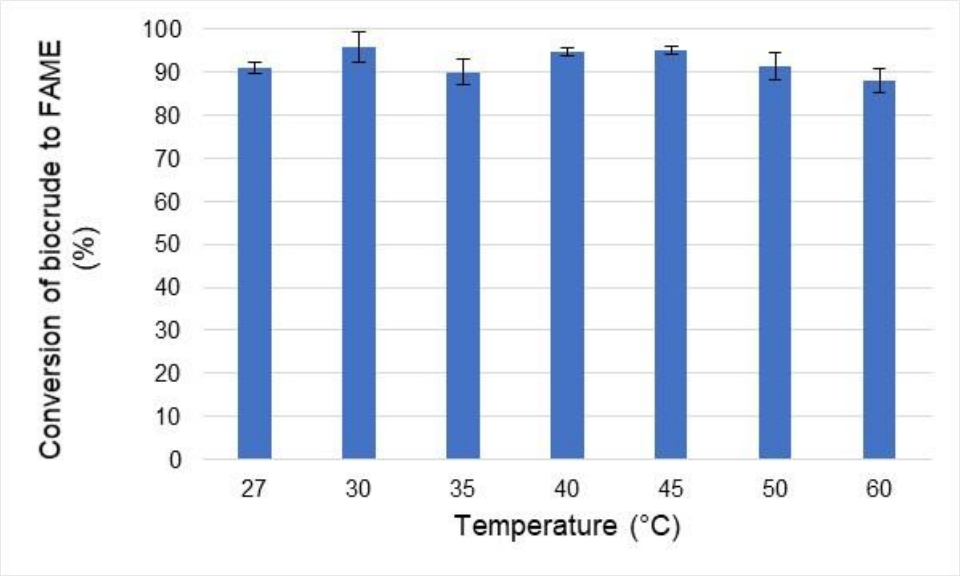

Figure 4.5: The effect of reaction temperature on FAME conversion

The highest FAME conversion of 95.83 % was observed at a reaction temperature of 30 °C, as shown in Figure 4.5. The increase in conversion from 27 °C to 30 °C can be due to the increase in temperature that lowered the viscosity of the reaction mixture and accelerated mass transfer (Guldhe *et al.*, 2015). After the optimum reaction temperature of 30 °C the FAME yield decreased gradually with a more prominent reduction in conversion at 35 °C. This reduction in conversion could be attributed to enzyme activity that gradually decreased due to the occurrence of enzyme denaturation with the increase in temperature beyond the optimum temperature of the reaction (Guldhe *et al.*, 2015). The decrease in FAME conversion beyond 45 °C may be attributed to thermal degradation that decreased the stability of the enzymes (Mulalee *et al.*, 2015; Ribeiro *et al.*, 2011). However, other authors observed a decrease in conversion at 60 °C which they attributed to the evaporation of methanol at the boiling point of methanol at 64.7 °C (Karmee *et al.*, 2015; Mathiyazhagan & Ganapathi, 2011).

From Figure 4.5, it can be observed that there was no significant difference in the FAME conversion between 27 °C and 60 °C since the conversions falls within the experimental error. However, 30 °C was chosen as the optimum reaction temperature to optimize energy consumption and is used in further experimental work. An average enzyme recovery of 48 mass % was obtained for the variation in temperature experiments. Mulalee *et al.* (2013) observed an increase in the FAME conversion between 35 °C and 45 °C and no significant increase in FAME conversion between 45 °C and 60 °C. Rodrigues *et al.* (2008) investigated methanolysis of sunflower- and soybean oil using N435 and obtained an optimum reaction temperature of 30 °C.

4.3.3 Effect of oil to methanol molar ratio

According to Leung *et al.* (2010), an excess of methanol above the stoichiometric ratio of 3 to 1 drives the reaction forward and increases the FAME conversion in a shorter reaction time during enzymatic esterification. Lipase catalysis was performed at 1:2, 1:3, 1:4, 1:5, 1:6, 1:12 and 1:18 oil to methanol molar ratios to investigate the effect on FAME conversion. Furthermore, other operating conditions were kept constant at 10 mass % N435 loading, 30 °C, and a reaction time of 6 hours.

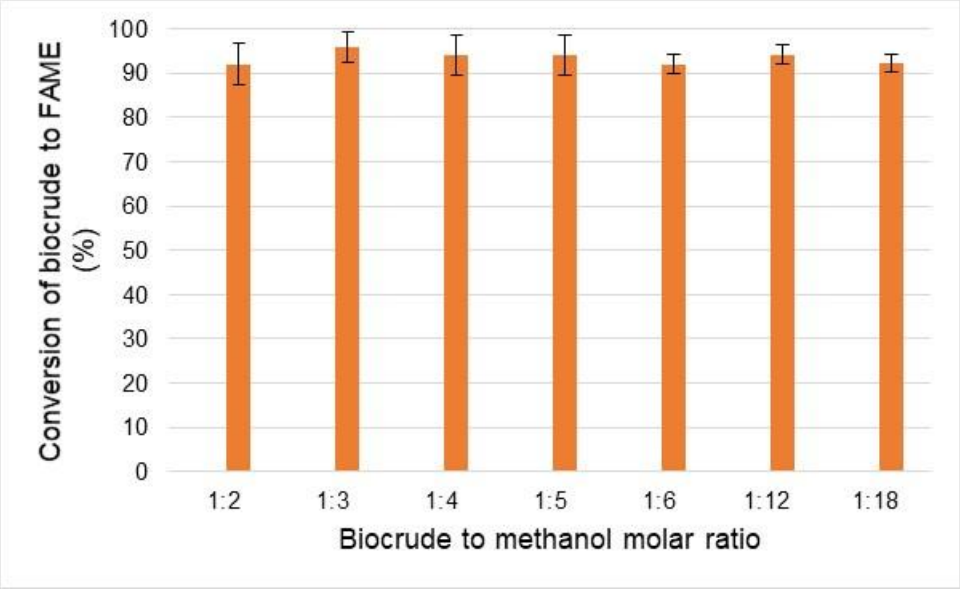

Figure 4.6: The effect of biocrude to methanol molar ratio on FAME conversion

The highest FAME conversion of 95.83 ± 3.41 % was obtained at an oil to methanol molar ratio of 1:3 since it is the stoichiometric ratio for the esterification reaction it was chosen as the optimum oil to methanol molar ratio for this study and used in further experimental work. In Figure 4.6, it is observed that there was no significant difference in the FAME conversion between 1:2 and 1:18 oil to methanol molar ratios since the conversions falls within the experimental error. An average enzyme recovery of 47 mass % was obtained for the variation in oil to methanol molar ratio experiments. According to Lu *et al.* (2007) and other authors, lipase inactivation is avoided by the stepwise addition of methanol during the reaction which assists in lipase stability and therefore results in an increased FAME conversion (Shimada *et al.*, 1999; Soumanou & Bornscheuer, 2003). This phenomenon may be attributed to the insignificant difference observed in the FAME conversion in this study.

The decrease in FAME conversion observed at an oil to methanol molar ratio of 1:18 can be attributed to lipase inactivation due to the presence of excess methanol (Amini *et al.*, 2017b; Gog *et al.*, 2012; Mulalee *et al.*, 2015). Karmee *et al.* (2015) conducted methanolysis of waste food

lipids and observed a FAME conversion of 62 % at a lipid to methanol ratio of 1:5. However, a FAME conversion of 92.54 % was reported by Amini *et al.* (2017b) at an oil to methanol molar ratio of 1:12. According to Amini *et al.* (2017b), the optimum oil to methanol molar ratio could be affected by the properties of the oil and the catalyst used during methanolysis.

The fatty acid to methanol molar ratio is shown in Figure 4.7. It is observed that as in the case of the biocrude to methanol ratio, there was no significant difference in the FAME conversion between 1:3 and 1:28 fatty acid to methanol molar ratios. For the NMR analysis an experimental error of 0.21 % was obtained. The difference in the FAME conversion for the different oil to methanol molar ratios fall within the experimental error of the analysis method and are therefore insignificant.

Figure 4.7: The effect of fatty acid to methanol molar ratio on FAME conversion

4.4 Biodiesel characterisation

The Van Krevelen diagram shown in Figure 4.8, was plotted by using the data obtained from the elemental analyses of the biocrude and biodiesel produced in this study, and fuel components from studies reported in the literature (Capunitan & Capareda, 2012; Dos Santos *et al.*, 2016; Gamliel *et al.*, 2018; Qian *et al.*, 2020; Ramirez *et al.*, 2015). The calorific value of the biodiesel and biocrude produced in this study at optimum conditions are compared with those of fuel components produced in other studies reported in literature in Table 4.7.

Table 4.7: HHVs of the biodiesel, biocrude, and other fuel components (Ramirez *et al.*, 2015)

Component	Calorific value (MJ/kg)
Biodiesel in this study	34.95 ± 1.22
Biocrude in this study	31.20 ± 0.52
Petroleum diesel	45.1
FAME biodiesel	40.5

The HHVs obtained in this study for the biodiesel and the biocrude increased from 31.20 ± 0.5 MJ/kg to 34.95 ± 1.22 MJ/kg, respectively. The biodiesel in this study obtained a lower calorific value than that of the FAME biodiesel and a significantly lower value than that of the petroleum diesel. The lower calorific value compared to that of the biodiesel from literature was expected since biodiesel has a FAME content above 96.5 % that is significantly higher than the FAME content of the biodiesel produced in this study, 48.66 ± 5.40 % (South African National Standards, 2011).

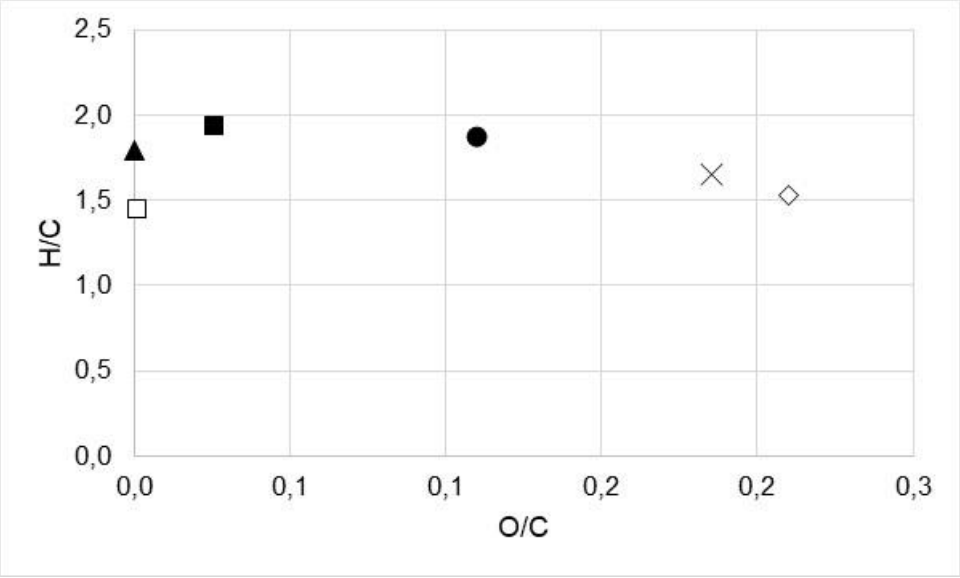

Figure 4.8: Van Krevelen diagram comparing the biocrude (◊), biodiesel in this study (x), biodiesel (●), diesel (▲), petroleum low value (□), and petroleum high value (■) (Capunitan & Capareda, 2012; Dos Santos *et al.*, 2016; Gamliel *et al.*, 2018; Qian *et al.*, 2020; Ramirez *et al.*, 2015)

The atomic H/C and O/C ratios of the biodiesel in this study are compared to some of the fossil-based fuels from other studies in the Van Krevelen diagram as seen in Figure 4.8. Values were

obtained from the elemental analyses of the biocrude and biodiesel produced in this study and values for the fossil fuel components were obtained from the literature (Capunitan & Capareda, 2012; Dos Santos *et al.*, 2016; Gamliel *et al.*, 2018; Qian *et al.*, 2020; Ramirez *et al.*, 2015). The biodiesel in this study obtained higher H/C- and O/C ratios compared to the biocrude oil in this study, as expected. The H/C and O/C ratios of the biodiesel produced in this study are more comparable to that of FAME biodiesel than fossil fuel diesel or petroleum fuel. However, the biodiesel in this study had lower H/C and O/C ratios compared to the H/C and O/C ratios of the FAME biodiesel which was expected due to the significant difference in FAME content.

A fuel must meet the requirements of having an HHV above 40 MJ/kg, an H/C ratio above 1.5 and an O/C value below 0.06 to be classified as a petroleum fuel (Capunitan & Capareda, 2012; Ghaly *et al.*, 2010). The biodiesel produced in this study only met one of the requirements and cannot be used as petroleum fuel without further upgrading or refining. However, the biodiesel in this study could be used for blending with conventional fuels.

The boiling range distribution of the produced biodiesel was evaluated by means of simulated distillation curves compiled from GCMS data. Simulated distillation curves were compiled using a modified method based on the ASTM D7213 Standard Test Method for Boiling Range Distribution of Petroleum Distillates. The biodiesel fractions were quantified based on the boiling ranges for the different fractions shown in Table 4.8.

Table 4.8: Boiling range distribution of petroleum distillates

Fraction	Boiling range (°C)
Naphtha	30–150
Kerosene	150–240
Diesel	240–370

The data obtained from the GCMS analyses was divided into fractions according to their respective boiling point ranges, and the normalised peak area was determined from the area of the internal standard (dodecanoic acid methyl ester) and the area of each component. The kerosene fraction was divided into the following groups: ketones, phenolics, and esters. Furthermore, the components in the diesel fraction were grouped as phenolics, fatty acids, esters, ketones and aldehydes, heterocyclic oxygen, nitrogen, and sulphur compounds. The heavy fraction was grouped as follows: fatty acids, esters, ketones and aldehydes, heterocyclic oxygen,

nitrogen, sulphur compounds, and phytosterols and related compounds. For the fractions their respective components were listed under each group and the group's normalised peak area was determined as can be seen in Appendix D.3. Tables D.21 to D.25 in Appendix D.3 were used to record the investigation of the effect of lipase on the other biocrude components.

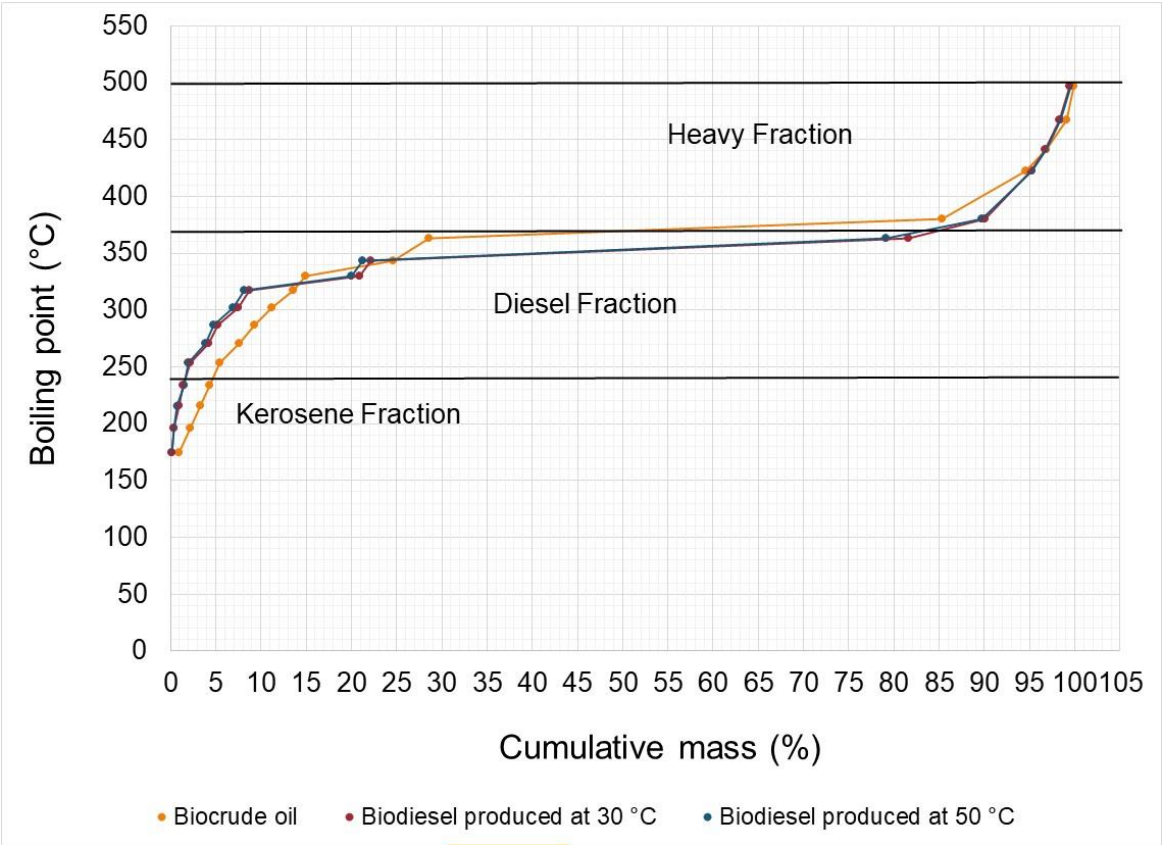

Figure 4.9: SIMDIST curves of the biocrude oil and the biodiesel produced at 30 °C and 50 °C

The simulated distillation (SIMDIST) curve in Figure 4.9 was determined from the GCMS analyses of the biocrude oil and biodiesel produced at 30 °C and 50 °C. Furthermore, the boiling point distribution in Figure 4.10 was determined from the GCMS data by identifying the boiling point range for each fraction and determining the cumulative mass for the respective fractions from the SIMDIST curve as seen in Appendix D.3. The kerosene fraction decreased for both 30 °C and 50 °C to 2.5 mass % and 3 mass %, respectively, compared to that of the biocrude at 4.9 mass %. The diesel fraction significantly increased for both 30 °C and 50 °C to 82 mass % and 80.6 mass %, respectively, compared to that of the biocrude at 38.6 mass %. The heavy fraction significantly decreased for both 30 °C and 50 °C to 14.97 mass % and 15.94 mass %, respectively, compared to that of the biocrude at 56.41 mass %.

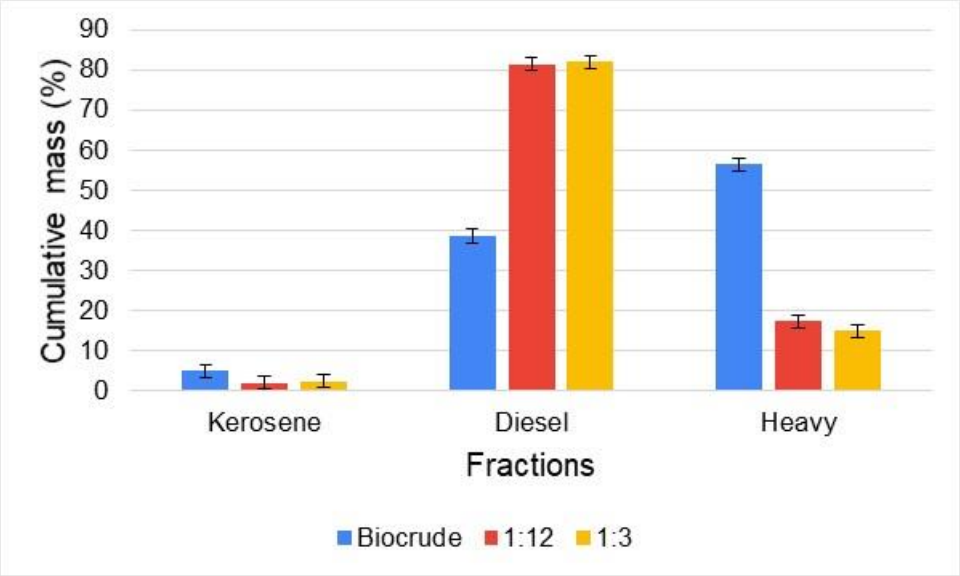

Figure 4.10:The boiling range distribution of the biocrude oil and biodiesel produced at 30 °C and 50 °C

The boiling range distribution of the biocrude oil were compared to that of the biodiesel produced at 30 °C and 50 °C with an oil to methanol ratio of 1:3, as shown in Figure 4.10. The kerosene fraction decreased at both 30 °C and 50 °C, and the GCMS analysis indicated that there was a slight increase in the esters and a decrease in ketones. A possible explanation for this slight decrease could be the formation of acetals which form when ketones react with an alcohol such as methanol. This is shown in Appendix D.3, Table D.21 where the ketones in the biocrude reduced from 0.6 mass % to 0.01 mass % in the biodiesel produced at 30 °C with an oil to methanol molar ratio of 1:3. The diesel fraction significantly increased as expected due to the conversion of fatty acids to FAME.

The GCMS analysis indicated a small difference in the amount of phenolics, aldehydes, heterocyclic oxygen, nitrogen, and sulphur compounds which could probably be attributed to experimental error, indicating that the enzyme reaction is very specific for esterification reactions and does not have much of an effect on the other compounds in the biocrude. The experimental error for the compilation of simulated distillation curves using GCMS data was determined as 1.6 %. The cumulative mass % of the kerosene -, diesel -, and heavy fraction for an oil to methanol molar ratio of 1:12 and 1:3 falls within the experimental error of the analysis method and are therefore insignificant. The only significant increase was observed for the esters which increased from 3.87 % to 73.22 %. The heavy fraction significantly decreased for both 30 °C and 50 °C. This could be explained by the fact that the boiling point of the methyl ester of a fatty acid is lower than that of the boiling point of the fatty acid itself resulting in the fatty acids moving to the diesel boiling range from the heavy fraction's boiling range upon esterification. The GCMS analysis also indicated that there were no fatty acids present at 30 °C in the biodiesel confirming a high

conversion of fatty acids to methyl esters by the lipase catalyst. Furthermore, the highest FAME conversion of 95.83 % was observed at a reaction temperature of 30 °C, as shown in Figure 4.5.

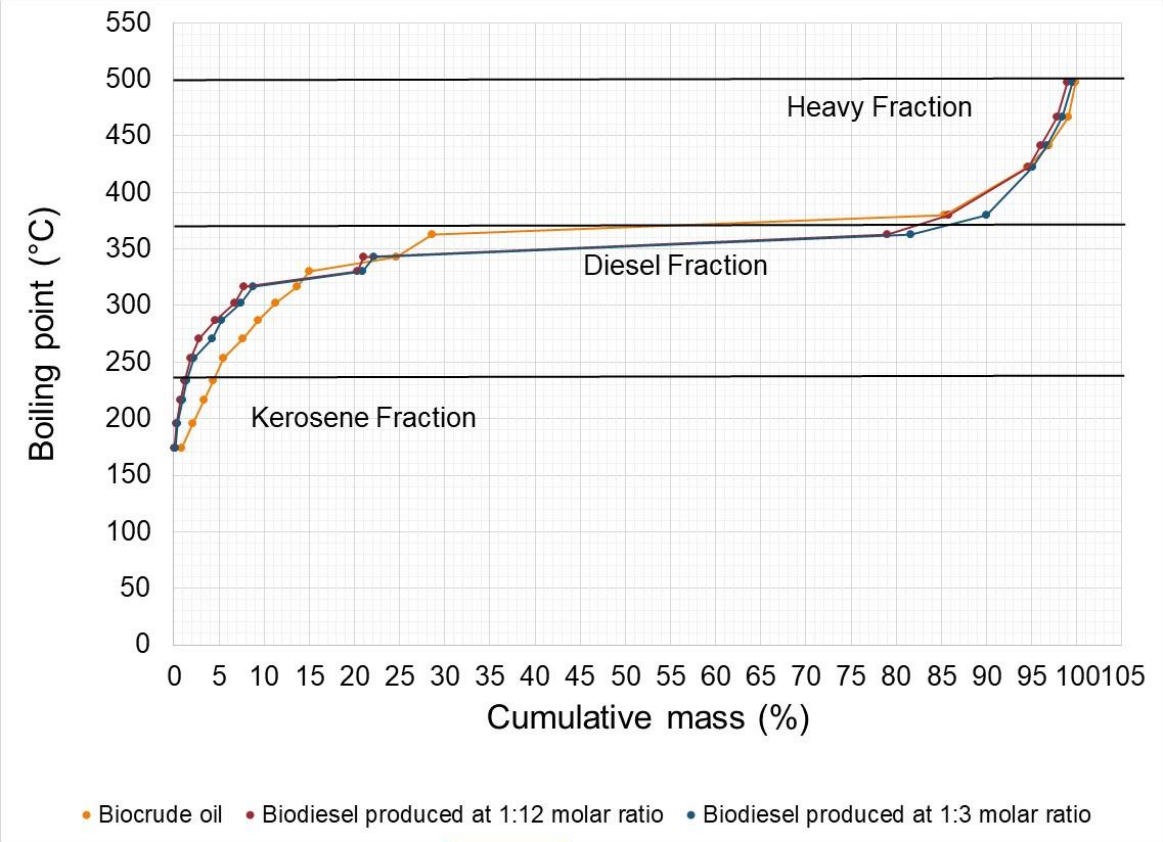

Figure 4.11: SIMDIST curves of the biocrude oil and biodiesel produced oil to methanol molar ratios of 1:3 and 1:12.

The SIMDIST curve in Figure 4.11 was determined from the GCMS analyses on the biocrude oil and biodiesel produced at 30 °C with an oil to methanol molar ratio of 1:3 and 1:12. Furthermore, the boiling point distribution in Figure 4.12 was determined from the GCMS data by identifying the boiling point range for each fraction and determining the cumulative mass for the respective fractions from the SIMDIST curve as shown in Appendix D.3. The kerosene fraction decreased for both molar ratios 1:3 and 1:12 to 2.5 mass % and 2 mass %, respectively, compared to that of the biocrude at 4.9 mass %. The diesel fraction significantly increased for both molar ratios 1:3 and 1:12 to 82 mass % and 81.3 mass %, respectively, compared to that of the biocrude at 38.6 mass %. The heavy fraction significantly decreased for both molar ratios 1:3 and 1:12 to 14.97 mass % and 17.44 mass %, respectively, compared to that of the biocrude at 56.41 mass %.

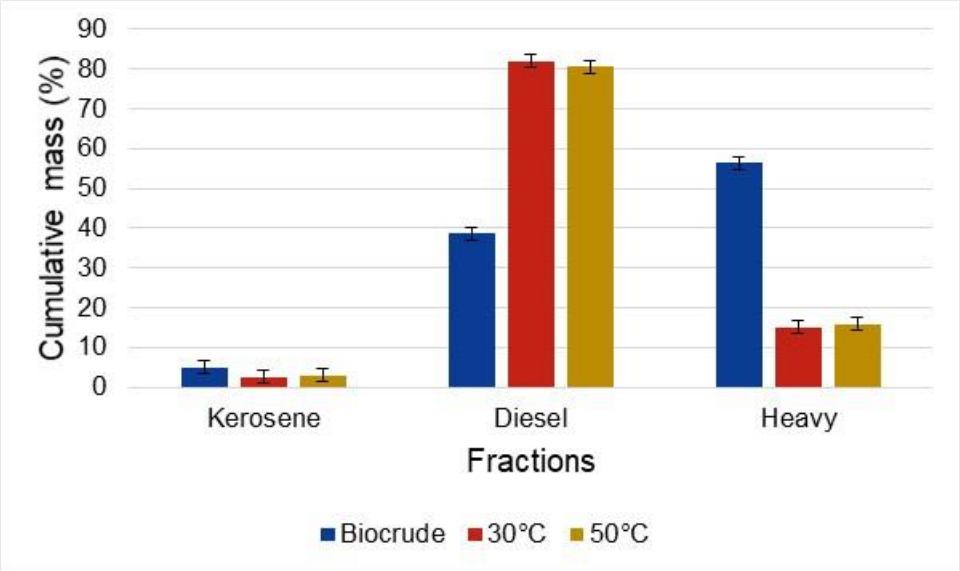

Figure 4.12: The boiling range distribution of the biocrude oil, FAME-produced at oil to methanol ratios of 1:3 and 1:12

The boiling range distribution of the biocrude oil was compared to that of the biodiesel produced with oil to methanol molar ratios of 1:3 and 1:12 at 30 °C, as shown in Figure 4.12. The kerosene fraction decreased for both oil to methanol molar ratios 1:3 and 1:12, and the GCMS analysis indicated that there was a decrease in ketones and phenolics. Again, a possible explanation for this insignificant decrease could be the formation of acetals which form when ketones react with an alcohol such as methanol. This can be seen in Appendix D.3, Table D.21 where the ketones in the biocrude reduced from 0.6 mass % to 0.04 mass % in the biodiesel produced at 30 °C with an oil to methanol molar ratio of 1:12. The esters increased for the oil to methanol ratio of 1:3 and decreased for 1:12. The decrease in FAME conversion observed at an oil to methanol molar ratio of 1:12 can be attributed to lipase inactivation due to the presence of excess methanol.

The diesel fraction also increased significantly due to the conversion of fatty acids to FAME. The GCMS analysis indicated a small difference in the phenolics, ketones, aldehydes and heterocyclic oxygen, nitrogen, and sulphur compounds. As mentioned earlier, the small difference could probably be attributed to experimental error, indicating that the enzyme reaction was very specific for esterification reactions and did not have much of an effect on the other compounds in the biocrude. The experimental error for the compilation of simulated distillation curves using GCMS data was determined as 1.6 %. The cumulative mass % of the kerosene -, diesel -, and heavy fraction for the temperatures 30 °C and 50 °C falls within the experimental error of the analysis method and are therefore insignificant. Furthermore, the fatty acids of the 1:12 molar ratio decreased insignificantly more than that of the 1:3. The only significant increase was observed for the esters where the 1:3 molar ratio produced more esters compared to the 1:12 molar ratio.

The heavy fraction significantly decreased for both oil to molar ratios 1:3 and 1:12. This could be explained by the fact that the boiling point of the methyl ester of a fatty acid is lower than that of the boiling point of the fatty acid itself resulting in the fatty acids moving to the diesel boiling range from the heavy fraction's boiling range upon esterification. The GCMS analysis also indicated that there were no fatty acids present for the oil to methanol molar ratio of 1:3 confirming a high conversion of fatty acids to methyl esters by the lipase catalysis. The tables with the above mentioned GCMS analyses appear as Tables D.21 to D.25 in Appendix D.3.

4.5 Lipase regeneration

One of the obstacles associated with enzymatic biodiesel production is the high costs of lipase enzymes (Ghaly *et al.*, 2010). The latter can be alleviated if the enzyme catalyst can be regenerated and recycled for consecutive reaction cycles. The regeneration and reusability of N435 was investigated by regenerating the supported enzyme with different solvents, as shown in Figure 4.11. Firstly, effectiveness of each chosen solvent was tested through regeneration and reuse of the enzyme after catalysis at an oil to methanol molar ratio of 1:3, a temperature of 30 °C, a reaction time of 6 hours, and a catalyst loading of 10 mass %. Figure 4.12 gives the FAME yields after using the solvent-regenerated enzyme catalyst in a second reaction cycle. The solvents for regeneration were chosen according to polarity based on their polarity indices.

The baseline in Figure 4.13 was chosen as the FAME conversion produced with reused N435 at optimum conditions, 30 °C with an oil to molar ratio of 1:3, and without solvent regeneration. Furthermore, the FAME conversion of the solvent-regenerated N435 was compared to the baseline as reference to investigate the effectiveness of solvent regeneration.

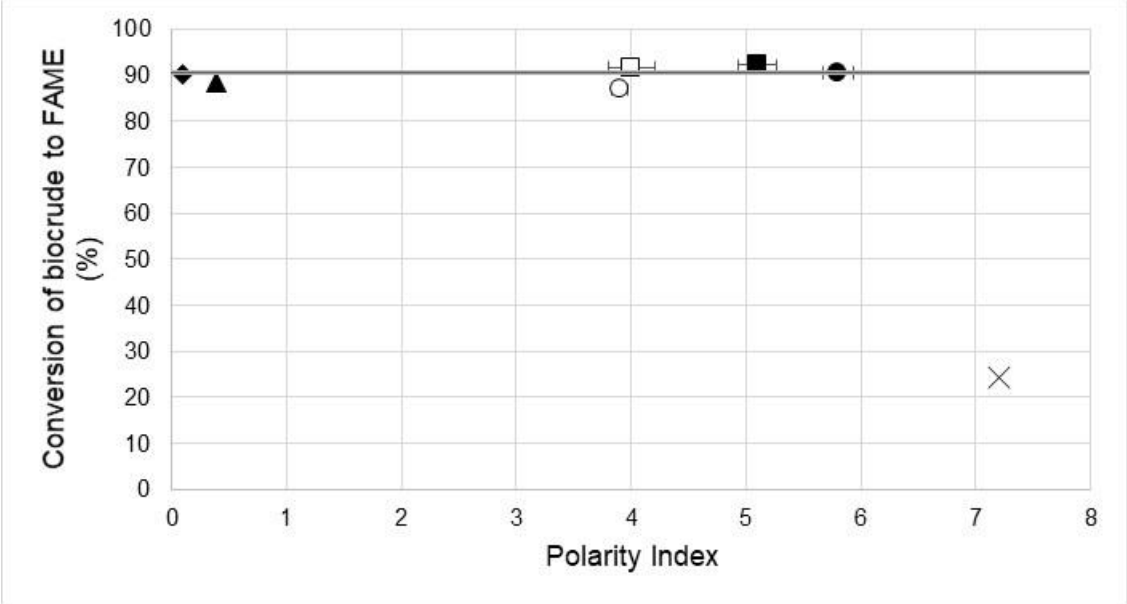

Figure 4.13: The effect of N435 solvent regeneration on FAME conversion, Hexane (♦), THF (□), Acetonitrile (●), Isopropanol (o), Acetone (■), Tert-butanol (▲), DMSO (x)

From Figure 4.13 it can be observed that there was no significant difference in the FAME conversion on the polarity index between 0 and 6. At a higher polarity index, the enzyme was deactivated as shown by the poor performance of DMSO as solvent for regeneration (Reyes-Duarte *et al.*, 2005; Talukder *et al.*, 2010). Similar results were reported by Talukder *et al.* (2010) for the use of hexane, t-butanol and DMSO as solvents for lipase regeneration. The highest FAME conversion of 92.06 ± 3.27 % was observed when N435 was regenerated using acetone compared to the FAME conversion at optimum conditions. Acetone was therefore chosen as the solvent for regeneration to assess the reusability of N435 for consecutive reaction cycles.

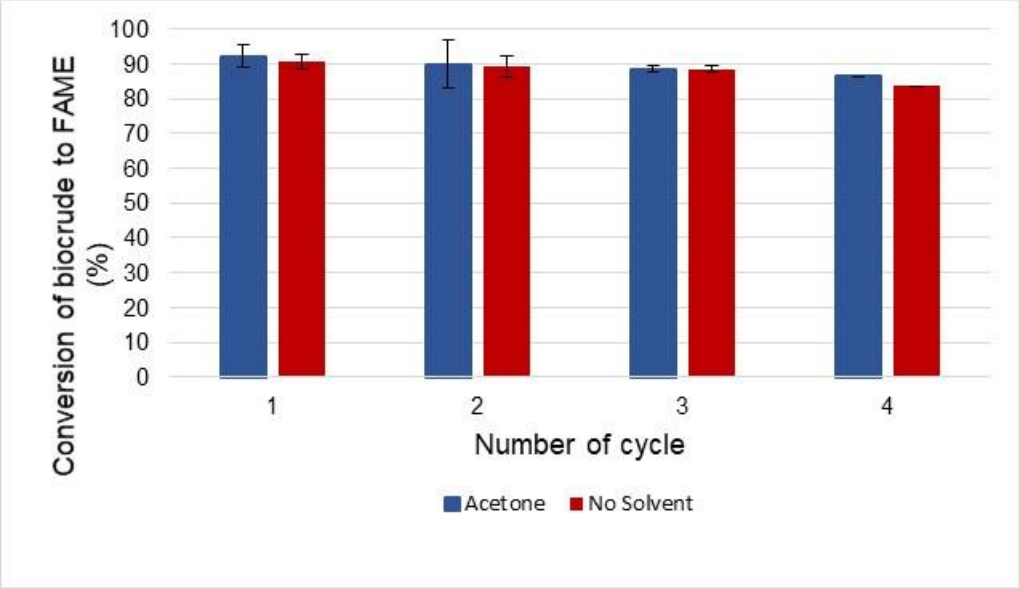

Figure 4.14: The effect of using recycled N435 and acetone-regenerated N435 on FAME conversion

According to Laszlo *et al.* (2011), immobilised lipase, like N435, may be reused and has a tolerance for polar and non-polar solvents. Recovered N435 was successfully reused without solvent regeneration for three cycles and obtained a FAME conversion of 88.52 ± 1.07 % as shown in Figure 4.12. The decrease in FAME conversion between the third and fourth cycle may be attributed to the interaction between methanol and the surface of N435 that resulted in enzyme deactivation (Gog *et al.*, 2012; Mulalee *et al.*, 2015).

According to Nguyen *et al.* (2017), the lipase is provided with a protective shield by the regenerated solvent that minimises methanol deactivation. Acetone-regenerated N435 was successfully reused for four cycles and obtained a FAME conversion of 86.34 %. There was an insignificant difference in the FAME conversion obtained for the acetone-regenerated N435 and recovered N435. However, by comparing the last cycle of the acetone-regenerated N435 with the

recovered 435, it is observed that acetone-regenerated N435 obtained a slightly higher FAME conversion. Similarly, Karmee (2016) investigated the reusability of N435 by using n-pentane as a solvent for regeneration and obtained a FAME conversion of 86 % after the fifth cycle.

The reusability of the enzyme in lipase-catalysed esterification and transesterification together with the low energy requirement of the process make this biocatalytic route attractive.

4.6 References

Aierzhati, A., Stablein, M.J., Wu, N.E., Kuo, C.T., Si, B., Kang, X. & Zhang, Y. 2019. Experimental and model enhancement of food waste hydrothermal liquefaction with combined effects of biochemical composition and reaction conditions. *Bioresource Technology*, 284:139-147. doi:10.1016/j.biortech.2019.03.076

Akhtar, J. & Amin, N.A.S. 2011. A review on process conditions for optimum bio-oil yield in hydrothermal liquefaction of biomass. *Renewable and Sustainable Energy Reviews*, 15(3):1615-1624. doi:10.1016/j.rser.2010.11.054

Amini, Z., Ong, H.C., Harrison, M.D., Kusumo, F., Mazaheri, H., & Ilham, Z. 2017. Biodiesel production by lipase-catalyzed transesterification of Ocimum basilicum L. (sweet basil) seed oil. *Energy Conversion and Management*, 132:82-90. doi:10.1016/j.enconman.2016.11.017

Ayeleru, O.O., Ntuli, F., & Mbohwa, C. 2016. Utilization of organic fraction of municipal solid waste (OFMSW) as compost: a case study of Florida, South Africa. *Lecture Notes Engineering and Computational Science*, 2226:580-585.

Ayeleru, O.O., Okonta, F.N., & Ntuli, F. 2018. Municipal solid waste generation and characterization in the City of Johannesburg: a pathway for the implementation of zero waste. *Waste Management*, 79:87-97. doi:10.1016/j.wasman.2018.07.026

Baawain, M., Al-Mamun, A., Omidvarborna, H., & Al-Amri, W. 2017. Ultimate composition analysis of municipal solid waste in Muscat. *Journal of Cleaner Production*, 148:355-362.

Bruice, P.Y. 2011. *Organic Chemistry.* 6th ed. Santa Barbara: Pearson.

Canakci, M. & Van Gerpen, J. 2001. Biodiesel production from oils and fats with high free fatty acids. *Transactions of the American Society of Agricultural Engineers*, 44(6):1429-1436.

Cao, L., Zhang, C., Chen, H., Tsang, D.C.W., Luo, G., Zhang, S. & Chen, J. 2017. Hydrothermal liquefaction of agricultural and forestry wastes: state-of-the-art review and future prospects. *Bioresource Technology*, 245(June):1184-1193. doi:10.1016/j.biortech.2017.08.196

Capunitan, J.A. & Capareda, S.C. 2012. Assessing the potential for biofuel production of corn stover pyrolysis using a pressurized batch reactor. *Fuel*, 95:563-572.

doi:10.1016%2Fj.fuel.2011.12.029

Chen, W.H., Lin, Y.Y., Liu, H.C., Chen, T.C., Hung, C.H., Chen, C.H., & Ong, H.C. 2019. A comprehensive analysis of food waste derived liquefaction bio-oil properties for industrial application. *Applied Energy*, 237:283-291. doi:10.1016/j.apenergy.2018.12.084

Chen, W.T., Zhang, Y., Zhang, J., Schideman, L., Yu, G., Zhang, P. & Minarick, M. 2014. Co-liquefaction of swine manure and mixed-culture algal biomass from a wastewater treatment system to produce bio-crude oil. *Applied Energy*, 128:209-216. doi:10.1016/j.apenergy.2014.04.068

Cheng, F., Cui, Z., Chen, L., Jarvis, J., Paz, N., Schaub, T., … Brewer, C.E. 2017. Hydrothermal liquefaction of high- and low-lipid algae: bio-crude oil chemistry. *Applied Energy*, 206:278-292.

Christopher, L.P., Kumar, H. & Zambare, V.P. 2014. Enzymatic biodiesel: challenges and opportunities. *Applied Energy*, 119:497-520. doi:10.1016/j.apenergy.2014.01.017

Coates, J. 2000. Interpretation of infrared spectra. In: Meyers, R.A., ed. *Encyclopedia of Analytical Chemistry.* Chichester: John Wily & Sons. pp. 10815-10837.

De Caprariis, B., De Filippis, P., Petrullo, A. & Scarsella, M. 2017. Hydrothermal liquefaction of biomass: influence of temperature and biomass composition on the bio-oil production. *Fuel*, 208:618-625. doi:10.1016/j.fuel.2017.07.054

Dimitriadis, A. & Bezergianni, S. 2017. Hydrothermal liquefaction of various biomass and waste feedstocks for biocrude production: a state of the art review. *Renewable & Sustainable Energy Reviews*, 68:113-125. doi:10.1016/J.RSER.2016.09.120

Dos Santos, R.G., Bordado, J.C. & Mateus, M.M. 2016. Potential biofuels from liquefied industrial wastes: preliminary evaluation of heats of combustion and van Krevelen correlations. *Journal of Cleaner Production*, 137:195-199. doi:10.1016/j.jclepro.2016.07.082

Freedman, B., Pryde, E.H. & Mounts, T.L. 1984. Variables affecting the yields of fatty esters from transesterified vegetable oils. *Journal of the American Oil Chemists' Society*, 61(10):1638-1643.

Gamliel, D.P., Bollas, G.M. & Valla, J.A. 2018. Two-stage catalytic fast hydropyrolysis of

biomass for the production of drop-in biofuel. *Fuel*, 216:160-170. doi:10.1016/J.FUEL.2017.12.017

Ghaly, A.E., Dave, D., Brooks, M.S. & Budge, S. 2010. Production of biodiesel by enzymatic transesterification: review. *American Journal of Biochemistry & Biotechnology*, 6(2):54-76. doi:10.3844/ajbbsp.2010.54.76

Gog, A., Roman, M., Toşa, M., Paizs, C. & Irimie, F.D. 2012. Biodiesel production using enzymatic transesterification: current state and perspectives. *Renewable Energy*, 39(1):10-16. doi:10.1016/j.renene.2011.08.007

Guldhe, A., Singh, B., Mutanda, T., Permaul, K. & Bux, F. 2015. Advances in synthesis of biodiesel via enzyme catalysis: novel and sustainable approaches. *Renewable & Sustainable Energy Reviews*, 41:1447-1464.

Hossain, F.M., Kosinkova, J., Brown, R.J., Ristovski, Z., Hankamer, B., Stephens, E. & Rainey, T.J. 2017. Experimental investigations of physical and chemical properties for microalgae HTL bio-crude using a large batch reactor. *Energies*, 10(4):1-16. doi:10.3390/en10040467

Hu, Y., Qi, L., Feng, S., Bassi, A., & Xu, C. 2019. Comparative studies on liquefaction of low-lipid microalgae into bio-crude oil using varying reaction media. *Fuel*, 238:240-247.

Ishihara, Y., Shimizu, H. & Shioya, S. 1996. Mole fraction control of poly(3-hydroxybutyric-co-3-hydroxyvaleric) acid in fed-batch culture of Alcaligenes eutrophus. *Journal of Fermentation and Bioengineering*, 81(5):422-428.

Karmakar, A., Karmakar, S. & Mukherjee, S. 2010. Properties of various plants and animals feedstocks for biodiesel production. *Bioresource Technology*, 101(19):7201-7210. doi:10.1016/j.biortech.2010.04.079

Karmee, S.K. 2016. Preparation of biodiesel from nonedible oils using a mixture of used lipases. *Energy Sources, Part A: Recovery, Utilization, and Environmental Effects*, 38(18):2727-2733.

Karmee, S.K. 2018. Enzymatic biodiesel production from Manilkara zapota (L.) seed oil. *Waste and Biomass Valorization*, 9(5):725-730. doi:10.1007/s12649-017-9854-8

Karmee, S.K., Linardi, D., Lee, J. & Lin, C.S.K. 2015. Conversion of lipid from food waste to

biodiesel. *Waste Management*, 41:169-173. doi:10.1016/j.wasman.2015.03.025

Kohansal, K., Toor, S., Sharma, K., Chand, R., Rosendahl, L. & Pedersen, T.H. 2021. Hydrothermal liquefaction of pre-treated municipal solid waste (biopulp) with recirculation of concentrated aqueous phase. *Biomass and Bioenergy*, 148. doi:10.1016/j.biombioe.2021.106032

Köse, O., Tüter, M. & Aksoy, H.A. 2002. Immobilized Candida antarctica lipase-catalyzed alcoholysis of cotton seed oil in a solvent-free medium. *Bioresource Technology*, 83(2):125–129. doi:10.1016/s0960-8524(01)00203-6

Kumar, M., Olajire Oyedun, A. & Kumar, A. 2018. A review on the current status of various hydrothermal technologies on biomass feedstock. *Renewable and Sustainable Energy Reviews*, 81:1742-1770. doi:10.1016/j.rser.2017.05.270

Laszlo, J.A., Jackson, M. & Blanco, R.M. 2011. Active-site titration analysis of surface influences on immobilized Candida antarctica lipase B activity. *Journal of Molecular Catalysis. B, Enzymatic*, 69(1-2):60-65.

Leung, D.Y.C., Wu, X. & Leung, M.K.H. 2010. A review on biodiesel production using catalyzed transesterification. *Applied Energy*, 87(4):1083-1095.

Li, H.Y., Hu, J., Zhang, Z.J., Wang, H., Ping, F., Zheng, C.F., Zhang, H.L. & He, Q. 2014. Insight into the effect of hydrogenation on efficiency of hydrothermal liquefaction and physico-chemical properties of biocrude oil. *Bioresource Technology*, 163:143-151. doi:10.1016/j.biortech.2014.04.015

Li, R.D., Ma, Z.M, Yang, T.H., Li, B.S., Wei, L.H. & Sun, Y. 2018. Sub–supercritical liquefaction of municipal wet sewage sludge to produce bio-oil: effect of different organic–water mixed solvents. *Journal of Supercritical Fluids*, 138:115-123. doi:10.1016/j.supflu.2018.04.011

Lu, J., Nie, K., Xie, F., Wang, F. & Tan, T. 2007. Enzymatic synthesis of fatty acid methyl esters from lard with immobilized Candida sp. 99–125. *Process Biochemistry*, 42(9):1367–1370. doi:10.1016/j.procbio.2007.06.004

Malins, K., Kampars, V., Brinks, J., Neibolte, I., Murnieks, R. & Kampare, R. 2015. Bio-oil from thermo-chemical hydro-liquefaction of wet sewage sludge. *Bioresource Technology*, 187:23-29. doi:10.1016/j.biortech.2015.03.093

Mathiyazhagan, M. & Ganapathi, A. 2011. Factors affecting biodiesel production. *Research in Plant Biolology*, 1(2):1-5.

Minowa, T., Murakami, M., Dote, Y., Ogi, T. & Yokoyama, S. 1995. Oil production from garbage by thermochemical liquefaction. *Biomass and Bioenergy*, 8(2):117-120. doi:10.1016/0961-9534(95)00017-2

Mulalee, S., Chanprasert, J., Kerdpoksup, P., Sawangpanya, N.S., & Phisalaphong, M. 2013. Esterification of oleic acid and bioalcohols using immobilized lipase. *Advanced Materials Research*, 724-725:1154–1157. doi:10.4028/www.scientific.net/AMR.724-725.1154

Mulalee, S., Srisuwan, P., & Phisalaphong, M. 2015. Influences of operating conditions on biocatalytic activity and reusability of Novozym 435 for esterification of free fatty acids with short-chain alcohols: a case study of palm fatty acid distillate. *Chinese Journal of Chemical Engineering*, 23(11):1851-1856. doi:10.1016/j.cjche.2015.08.016

Mullen, C.A., Strahan, G.D. & Boateng, A.A. 2009. Characterization of various fast-pyrolysis bio-oils by NMR spectroscopy. *Energy & Fuels*, 23(5):2707-2718. doi:10.1021/EF801048B

Nguyen, H.C., Liang, S.-H., Doan, T.T., Su, C.-H. & Yang, P.-C. 2017. Lipase-catalyzed synthesis of biodiesel from black soldier fly (Hermetica illucens): optimization by using response surface methodology. *Energy Conversion and Management*, 145:335-342.

Ohra-Aho, T., Tenkanen, M. & Tamminen, T. 2005. Direct analysis of lignin and lignin-like components from softwood kraft pulp by Py-GC/MS techniques. *Journal of Analytical and Applied Pyrolysis*, 74(1-2):123-128. doi:10.1016/j.jaap.2004.11.010

Parthasarathy, P. & Narayanan, S.K. 2014. Effect of hydrothermal carbonization reaction parameters on. *Environmental Progress & Sustainable Energy*, 33(3):676-680.

Qian, L., Wang, S., & Savage, P.E. 2020. Fast and isothermal hydrothermal liquefaction of sludge at different severities: reaction products, pathways, and kinetics. *Applied Energy*, 260:114312.

Qiao, Y., Xu, F., Xu, S., Yang, D., Wang, B., Ming, X., … Tian, Y. 2018. Pyrolysis characteristics and kinetics of typical municipal solid waste components and their mixture: analytical TG-FTIR study. *Energy & Fuels*, 32(10):10801-10812.

doi:10.1021/acs.energyfuels.8b02571

Ramirez, J.A., Brown, R.J. & Rainey, T.J. 2015. A review of hydrothermal liquefaction bio-crude properties and prospects for upgrading to transportation fuels. *Energies*, 8(7):6765-6794. doi:10.3390/en8076765

Ramos, M.J., Fernández, C.M., Casas, A., Rodríguez, L. & Pérez, A. 2009. Influence of fatty acid composition of raw materials on biodiesel properties. *Bioresource Technology*, 100(1):261-268. doi:10.1016/j.biortech.2008.06.039

Reyes-Duarte, D., López-Cortés, N., Ferrer, M., Plou, F.J. & Ballesteros, A.O. 2005. Parameters affecting productivity in the lipase-catalysed synthesis of sucrose palmitate. *Biocatalysis and Biotransformation*, 23(1):19-27. doi:10.1080/10242420500071763

Ribeiro, B.D., De Castro, A.M., Coelho, M.A.Z. & Freire, D.M.G. 2011. Production and use of lipases in bioenergy : a review from the feedstocks to biodiesel production. *Enzyme Research*, 2011:615803. doi:10.4061/2011/615803

Rodrigues, R.C., Volpato, G., Wada, K. & Ayub, M. 2008. Enzymatic synthesis of biodiesel from transesterification reactions of vegetable oils and short chain alcohols. *Journal of the American Oil Chemists' Society*, 85(10):925-930. doi:10.1007/s11746-008-1284-0

Schulz, H., Wissen, M., Bogdanski, N., Scheer, H.-C., Mattes, K. & Friedrich, C. 2006. Impact of molecular weight of polymers and shear rate effects for nanoimprint lithography. *Microelectronic Engineering*, 83(2):259-280. doi:10.1016/j.mee.2005.07.090

Shimada, Y., Watanabe, Y., Samukawa, T., Sugihara, A., Noda, H., Fukuda, H. & Tominaga, Y. 1999. Conversion of vegetable oil to biodiesel using immobilized Candida antarctica lipase. *Journal of the American Oil Chemists' Society*, 76:789-793.

Soumanou, M.M. & Bornscheuer, U.T. 2003. Lipase-catalyzed alcoholysis of vegetable oils. *European Journal of Lipid Science and Technology*, 105(11):656-660. doi:10.1002/ejlt.200300871

South African National Standards. 2011. *SANS 1935 : 2011 SOUTH AFRICAN NATIONAL STANDARD Automotive biodiesel — Fatty Acid Methyl Esters (FAME) for diesel engines — Requirements and test methods*. Pretoria: SABS.

Talukder, M.M.R., Jin, C.-W., Ng, M.-F. & Yeo, L.S.M. 2010. Two-step lipase catalysis for production of biodiesel. *Biochemical Engineering Journal*, 49(2):207-212. doi:10.1016/j.bej.2009.12.015

Vardon, D.R., Sharma, B.K., Scott, J., Yu, G., Wang, Z., Schideman, L., … Strathmann, T.J. 2011. Chemical properties of biocrude oil from the hydrothermal liquefaction of Spirulina algae, swine manure, and digested anaerobic sludge. *Bioresource Technology*, 102(17):8295-8303. doi:10.1016/j.biortech.2011.06.041

Wang, C., Du, Z., Pan, J., Li, J. & Yang, Z. 2007. Direct conversion of biomass to bio-petroleum at low temperature. *Journal of Analytical and Applied Pyrolysis*, 78(2):438-444. doi:10.1016/j.jaap.2006.10.016

Wang, Y., Zhang, Y., Yoshikawa, K., Li, H. & Liu, Z. 2021. Effect of biomass origins and composition on stability of hydrothermal biocrude oil. *Fuel*, 302:121138.

White, J.L. 1971. Interpretation of infrared spectra of soil minerals. *Soil Science*, 112(1):22-31. doi:10.1097/00010694-197107000-00005

Xiu, S. & Shahbazi, A. 2012. Bio-oil production and upgrading research: a review. *Renewable and Sustainable Energy Review*, 16(7):4406-4414. doi:10.1016/j.rser.2012.04.028

Xu, D., Lin, G., Liu, L., Wang, Y., Jing, Z. & Wang, S. 2018. Comprehensive evaluation on product characteristics of fast hydrothermal liquefaction of sewage sludge at different temperatures. *Energy*, 159:686-695. doi:10.1016/j.energy.2018.06.191

Xue, Y., Chen, H., Zhao, W., Yang, C., Ma, P. & Han, S. 2016. A review on the operating conditions of producing bio-oil from hydrothermal liquefaction of biomass. *International Journal of Energy Research*, 40(7):865-877. doi:10.1002/er.3473

Yang, L., Nazari, L., Yuan, Z., Corscadden, K., Xu, C.C. & He, Q.S. 2016. Hydrothermal liquefaction of spent coffee grounds in water medium for bio-oil production. *Biomass and Bioenergy*, 86:191-198. doi:10.1016/j.biombioe.2016.02.005

Zhu, Z., Rosendahl, L., Toor, S.S., Yu, D., & Chen, G. 2015. Hydrothermal liquefaction of barley straw to bio-crude oil: effects of reaction temperature and aqueous phase recirculation. *Applied Energy*, 137:183-192. doi:10.1016/j.apenergy.2014.10.005

CHAPTER 5: CONCLUSION AND RECOMMENDATIONS

This study investigated the effectiveness of upgrading biocrude oil obtained from HTL of MW through esterification in the presence of N435. Enzymatic esterification was studied in detail for the upgrading of biocrude oil to evaluate the effect of lipase catalysis on other biocrude components, not only free fatty acids, and determine the effectiveness of the overall FAME conversion. Operating parameters of enzymatic esterification such as reaction time, reaction temperature, oil to methanol molar ratios, lipase reusability and regeneration were evaluated.

5.1 Conclusion

Various esterification conditions were investigated to observe their effect on the FAME conversion. The FAME conversion increased as the reaction time increased until the optimum reaction time was reached. A decrease in the FAME conversion was observed due to alcohol inhibition that was attributed to the denaturation of the enzyme. No significant difference in the FAME conversion was observed at the different reaction temperatures. The insignificant difference in FAME conversion for the oil to methanol ratios could be attributed to the stepwise addition of methanol during the reaction which assisted in lipase stability. The highest FAME conversion of 95.83 ± 3.41 % was obtained at 30 °C with an oil to methanol molar ratio of 1:3 and a residence time of 6 hours.

Esterification uses an alcohol to convert carboxylic acids to esters using biological, alkali or acid catalysts. Biological catalysts such as lipase has the advantage of operating under moderate conditions, requires low energy input and reduces cost through its reusability compared to the severe operating conditions and high costs associated with thermochemical processes. In this study it was observed that N435 was very specific and had no effect on the other components except for the fatty acids. Furthermore, the other biocrude components such as phenolics, ketones and heterocyclic nitrogen, oxygen and sulphur compounds also had no effect on N435.

The boiling range distribution of the biocrude oil was investigated and compared to the biodiesel for different reaction conditions. There was a slight decrease in the kerosene fraction and a significant increase in the diesel fraction due to the conversion of fatty acids to FAME. There was also a significant decrease in the heavy fraction that can be explained by the fact that the boiling point of the methyl ester of a fatty acid is lower than the boiling point of the fatty acid itself. This decrease resulted in the fatty acids moving to the diesel boiling range away from the heavy fraction boiling range upon esterification. The only significant increase observed for each fraction was for the esters. The results were the same based on the composition and how the biodiesel was formed as indicated by the analysis of the different fractions. In Figures 4.5 and 4.6 it can be

observed that there was no significant difference in the FAME conversion between 27 °C and 60 °C and between 1:2 and 1:18 oil to methanol molar ratios.

The produced biodiesel was characterised, and the calorific value was compared to that of FAME biodiesel. The calorific value of the produced biodiesel was lower than the FAME biodiesel due to the significant difference in FAME content as well as the presence of other oxygenates. The biodiesel produced in this study cannot be used as a high-value petroleum fuel without further upgrading or refining. However, it can be used for blending with conventional fuels. The FAME content of the biodiesel produced in this study should be above 96.5 %, as discussed in Chapter 4, to be used as a high-value petroleum fuel. A further decrease in the oxygen content could be obtained by means of hydrotreatment processes or liquid–liquid extraction using the proper solvents.

5.2 Recommendations

It is recommended that different conditions for HTL should be investigated and that optimum conditions that may be obtained should be used to produce biocrude oil. Furthermore, methanol should be used as solvent in the HTL process to determine the effectiveness of converting fatty acids to methyl esters during HTL which could reduce the need for further upgrading.

The enzyme loading and the effect thereof on the FAME conversion should be evaluated. It is also recommended that the yield of the biodiesel produced in this study is quantified and further investigated to compare its fuel properties against the SANS biodiesel standard specifications. Upgrading of the biodiesel produced by lipase catalysis through liquid–liquid extraction with a non-polar solvent like hexane to reduce the oxygen content should be further investigated.

APPENDIX A

A.1 HTL product yield calculations

The HTL product yields were calculated by using Equations A.1, A.2, A.3 and A.4. The yields were based on the relationship between the mass of the product and the mass of the MW feedstock. The daf yield was calculated using the same equations, but with the difference that the moisture and ash content of both the feedstock and product were subtracted before carrying out the calculations.

$$\text{Biocrude oil yield (mass\%)} = \frac{M_{Biocrude\ oil}}{M_{MW\ feedstock}} \times 100 \quad \text{A.1}$$

$$\text{Char yield (mass\%)} = \frac{M_{Char}}{M_{MW\ feedstock}} \times 100 \quad \text{A.2}$$

$$\text{Aqueous yield (mass\%)} = \frac{M_{Aqueous}}{M_{MW\ feedstock}} \times 100 \quad \text{A.3}$$

$$\text{Biogass yield (mass\%)} = \frac{M_{Biogass}}{M_{MW\ feedstock}} \times 100 \quad \text{A.4}$$

APPENDIX B

B.1 Volume of methanol

Lipase catalysis was performed at 1:2, 1:3, 1:4, 1:5, 1:6, 1:12 and 1:18 oil to methanol molar ratios to investigate the effect of lipase on FAME conversion. Furthermore, the volume of methanol used in each reaction was calculated based on the mass of the biocrude used. For these reactions 1 g biocrude oil (380 g/mol) were used to calculate the mole amount of biocrude using Equation B.1. The molecular weight of the biocrude oil was determined with the GPC analysis.

$$n_{Biocrude\ oil} = \frac{mass_{Biocrude\ oil}}{MW_{Biocrude\ oil}} = \frac{1\ g}{380\ g/mol} = 2.63 \times 10^{-3}\ mol \qquad \text{B.1}$$

Equations B.2, B.3 and B.4 were used to calculate the volume of methanol needed for each reaction. The methanol molecular weight of 32.04 g/mol and density of 0.791 g/ml were used in these calculations. First, the mol amount was calculated using the molar ratio used in each reaction and, secondly, the mass amount needed was calculated with Equation B.3. Lastly, the density, mass, and volume relationship in Equation B.4 were used to determine the volume of methanol needed in each reaction.

$$\frac{n_{Biocrude\ oil}}{n_{Methanol}} = \frac{1}{3} \qquad \text{B.2}$$

$$n_{Methanol} = 3 \times n_{Biocrude\ oil} = 7.89 \times 10^{-1}\ mol$$

$$Mass_{Methanol} = \frac{n_{Methanol}}{MW_{Methanol}} = \frac{7.89 \times 10^{-1}\ mol}{32.04\ g/mol} = 0.253\ g \qquad \text{B.3}$$

$$\rho_{Methanol} = \frac{mass_{methanol}}{v_{methanol}} \qquad \text{B.4}$$

$$v_{methanol} = \frac{mass_{methanol}}{\rho_{Methanol}} = \frac{0.259\ g}{0.791\ g/ml} = 0.320\ mL$$

The volume of methanol used for each biocrude oil to methanol molar ratio experiment in this study is shown in Table B.1.

Table B.1: Volume of methanol used for each biocrude oil to methanol molar ratio reaction

Biocrude: Methanol molar ratio	Methanol mol (mol)	Methanol mass (g)	Methanol volume (mL)	Methanol volume (µL)
1:2	5.26E-03	0.169	0.213	213
1:3	7.89E-03	0.253	0.320	320
1:4	1.05E-02	0.337	0.426	426
1:5	1.32E-02	0.422	0.533	533
1:6	1.58E-02	0.506	0.640	640
1:12	3.16E-02	1.012	1.279	1279
1:18	4.74E-02	1.518	1.919	1919

B.2 FAME conversion calculations

The FAME content was calculated by using Equation B.5. A_1 and A_2 represent the areas of the methoxy and the methylene protons in the NMR spectrum, respectively (Gelbard *et al.*, 1995). The methoxy and methylene proton peaks are observed at 3.6–3.7 ppm and 2.3–2.5 ppm, respectively. The ^{1}H NMR spectra of biodiesel produced at 30 °C, 10 mass % N435 loading, and 1:12 oil to methanol molar ratio are shown in Figure B.1.

$$FAME\ (\%) = \frac{2}{3}\left(\frac{A_1}{A_2}\right) * 100 \qquad \text{B.5}$$

$$FAME\ (\%) = \frac{1.5002}{1.0394} * 100 = 96.22\ \%$$

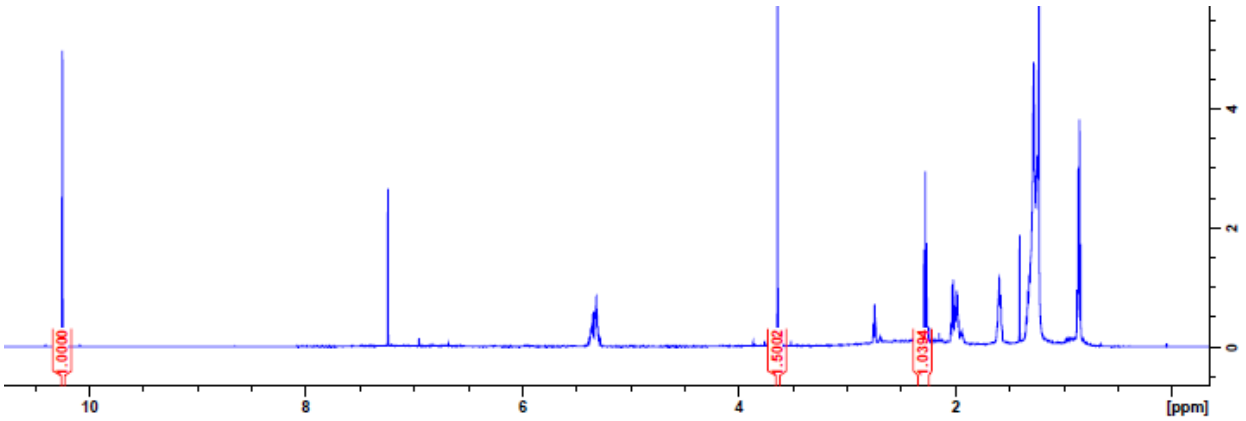

Figure B.1: ^{1}H NMR spectra of biodiesel produced at 30 °C, 10 mass % N435 loading, 1:12 oil to methanol molar ratio and 6 hours reaction time

APPENDIX C

C.1 Experimental error calculations

Each experiment was carried out in triplicate to determine the variance in the data. Experimental errors were determined using t critical values at a 95 % confidence level, average $(\bar{x})$ and standard deviation (s), according to Equations C.1, C.2 and C.3 (Devore *et al.*, 2005).

$$Average, (\bar{x}) = \frac{\sum_{i=1}^{n} x_i}{n} \quad \text{C.1}$$

$$standard\ deviation\ (s) = \sqrt{\frac{\sum_{i=1}^{n} (\bar{x} - \bar{x}_i)^2}{n-1}} \quad \text{C.2}$$

$$Experimental\ error\ \% = \frac{s \times t}{\sqrt{n}} \quad \text{C.3}$$

First, the average was calculated where n is the total number of data points and x_i is an individual data point. Second, the standard deviation was calculated followed by the experimental error.

C.1.1 Experimental error of the biocrude yield

Each experiment was carried out in triplicate to determine the experimental error of the HTL experiments as shown in Table C.1. The experimental error was calculated according to the procedure discussed in Section C.1.

Table C.1: Experimental error of the biocrude yield

Run nr	Biocrude yield (mass %)
5	6.79
15	6.59
23	6.78
Average	6.72
Standard deviation	0.11
Experimental error (%)	0.20

$$Average, (\bar{x}) = \frac{\sum_{i=1}^{3} x_i}{3} = \frac{6.79 + 6.59 + 6.78}{3} = 6.72\ mass\% \quad \text{C.4}$$

$$Standard\ deviation\ (s) = \sqrt{\frac{\sum_{i=1}^{n}(\bar{x} - \bar{x}_i)^2}{n-1}} = \sqrt{\frac{\sum_{i=1}^{3}(\bar{x} - \bar{x}_i)^2}{2}} \quad \text{C.5}$$

$$= \sqrt{\frac{(6.79 - 6.72)^2 + (6.59 - 6.72)^2 + (6.78 - 6.72)^2}{2}} = 0.11$$

$$Experimental\ error\ \% = \frac{s \times t}{\sqrt{n}} = \frac{0.11 \times 3.182}{\sqrt{3}} = 0.20\ \% \quad \text{C.6}$$

C.1.2 Experimental error of the FAME conversion

Each experiment was carried out in triplicate to determine the experimental error of the HTL experiments as shown in Table C.1. The experimental error was calculated according to the procedure discussed in Section C.1.

Enzymatic esterification was performed at 27, 30, 35, 40, 45, 50 and 60 °C to identify the optimum reaction temperature. Other operating conditions were kept constant at 10 mass % N435 loading, 1:3 biocrude to methanol molar ratio, and a reaction time of 6 hours. The experimental error was calculated and listed in Table C.3.

Table C.2: Experimental error of the FAME yield at 30 °C and an oil to methanol ratio of 1:3

Run nr	FAME conversion (%)
1	95.74
2	97.73
3	94.02
Average	95.83
Standard deviation	1.86
Experimental error (%)	3.41

Lipase catalysis was performed at 1:2, 1:3, 1:4, 1:5, 1:6, 1:12 and 1:18 oil to methanol molar ratios to investigate the effect on FAME conversion. Other operating conditions were kept constant at 10 mass % N435 loading, 30 °C, and a reaction time of 6 hours. The experimental error was calculated and listed in Table C.4.

Table C.3: Experimental error of the FAME yield at 30 °C and an oil to methanol ratio of 1:5

Run nr	FAME conversion (%)
1	92.65
2	96.83
3	92.64
Average	94.04
Standard deviation	2.42
Experimental error (%)	4.44

Acetone regeneration and the reuse of the enzyme after catalysis was conducted at an oil to methanol molar ratio of 1:3, a temperature of 30 °C, a reaction time of 6 hours, and a catalyst loading of 10 mass %. The experimental error was calculated and listed in Tables C.4 and C.5.

Table C.4: Experimental error of the acetone-regenerated N435 FAME yield at 30 °C and an oil to methanol ratio of 1:3

Run nr	FAME conversion (%)
1	88.97
2	91.30
3	92.82
Average	92.06
Standard deviation	1.08
Experimental error (%)	3.27

Table C.5: Experimental error of the no-solvent reused N435 FAME yield at 30 °C and an oil to methanol ratio of 1:3

Run nr	FAME conversion (%)
1	88.97
2	91.30
3	92.82
Average	92.06
Standard deviation	1.08
Experimental error (%)	3.27

C.1.3 Experimental error of the bomb calorimeter

Enzymatic esterification was performed at the following operating conditions: a temperature of 30 °C, 10 mass % N435 loading, 1:3 biocrude to methanol molar ratio, and a reaction time of 6 hours. Each experiment was carried out in triplicate to determine the variance in the data. The experimental error was calculated and listed in Table C.7.

Table C. 6: Experimental error of the biocrude oil HHV

Run nr	HHV (MJ/kg)
1	30.82
2	31.30
3	31.49
Average	31.2
Standard deviation	0.28
Experimental error (%)	0.52

C.1.4 Experimental error of the elemental analyser

Enzymatic esterification was performed at the following operating conditions: a temperature of 30 °C, 10 mass % N435 loading, 1:3 biocrude to methanol molar ratio, and a reaction time of 6 hours. Each analysis was carried out in triplicate to determine the variance in the data. The experimental error was calculated and listed in Table C.7.

Table C.7: Experimental error of the elemental analyser

Run nr	C (mass %)	H (mass %)	N (mass %)	R (mass %)
1	71.4	9.95	1.41	17.24
2	70.06	9.72	1.13	19.08
3	72.34	9.8	1.44	16.43
Average	71.27	9.82	1.33	17.58
Standard deviation	1.15	0.12	0.17	1.36
Experimental error (%)	2.11	0.21	0.31	2.49

C.1.5 Experimental error of the GCMS

Enzymatic esterification was performed at the following operating conditions: a temperature of 30 °C. 10. mass % N435 loading. 1:3 biocrude to methanol molar ratio. and a reaction time of 6 hours. Each analysis was carried out in triplicate to determine the variance in the data. The experimental error was calculated and listed in Table C.8.

Table C. 8: Experimental error of the GCMS

Run nr	Methyl ester yield (mass %)
1	37.41
2	49.91
3	47.40
Average	48.66
Standard deviation	1.77
Experimental error (%)	5.40

C.1.6 Experimental error of the NMR

The experimental error was calculated and listed in Table C.9.

Table C.9: Experimental error of the NMR

Run nr	Methyl ester content (mass %)
1	1.1
2	1.3
3	1.1
Average	1.2
Standard deviation	0.12
Experimental error (%)	0.21

APPENDIX D

D.1 MW feedstock experimental data

Table D.1: Feedstock characterisation

Analysis	Method number	MW (%)
Dry matter	ASM013	99.33
Moisture	ASM014	0.67
Ash	ASM048	4.18
Protein	ASM078	12.21
Fat	ASM044	3.06
Carbohydrates	ASM075	79.88

Table D.2: Proximate analysis of the MW feedstock

Sample	Moisture (mass %)	Volatiles (mass %)	Ash (mass %)	Fixed carbon (mass %)
1	62.89	30.55	5.55	1.01
2	58.43	34.40	5.34	1.84
3	53.87	32.46	5.45	8.22
Average	60.93	32.74	5.45	2.05
Standard deviation	2.28	1.53	0.11	1.2
Error (%)	4.19	2.82	0.20	2.14

Table D.3: Elemental analysis of the MW feedstock

Sample	C (mass %)	H (mass %)	N (mass %)	R (mass %)
1	43.9	6.22	1.87	48.01
2	43.96	6.48	1.89	47.67
3	43.65	6.15	1.88	48.33
Average	43.84	6.28	1.88	48.00
Standard deviation	0.16	0.17	0.01	0.33
Error (%)	0.30	0.32	0.02	0.61

Table D.4: Calorific value of the MW feedstock

Sample	Calorific value. (MJ/kg)
1	18.43
2	18.48
3	18.41
Average	18.44
Standard deviation	0.03
Error (%)	0.06

D.2 HTL experimental data

Table D.5 contains the experimental yields obtained for the biocrude oil. aqueous phase. biochar. and biogas. HTL was performed at 300 °C with a residence time of 20 minutes.

Table D.5: HTL product yield

Run	Biocrude oil	Aqueous	Biochar	Biogas

1	6.59	54.12	14.69	10.87
2	6.79	55.73	14.74	10.01
3	6.54	49.45	14.29	8.10
4	6.79	42.76	13.08	8.80
5	7.04	62.02	13.33	9.66
6	7.80	59.86	13.73	10.21
7	6.74	62.02	14.64	7.55
8	7.40	62.63	13.98	9.66
9	7.83	63.74	13.43	12.89
10	6.35	52.01	14.79	12.45
11	6.44	63.35	13.93	7.49
12	6.59	58.90	15.34	11.87
13	6.49	63.54	17.56	6.94
14	6.59	57.13	14.08	9.21
15	7.27	56.32	15.74	8.00
16	6.75	57.68	15.74	10.01
17	7.65	61.60	14.49	8.35
18	6.73	61.09	15.04	9.81
19	6.17	57.53	15.79	8.25
20	6.71	57.86	15.79	8.75
21	6.11	59.32	15.44	9.61
22	6.78	52.53	16.03	11.40

23	6.20	59.19	15.21	9.05
Average	6.80	57.84	14.82	9.52
Standard deviation	0.49	5.09	1.05	1.59
Error	0.22	2.2	0.45	0.683

Table D.6: Calorific value of the biochar

Sample	Calorific value. (MJ/kg)
1	28.04
2	28.10
3	28.61
Average	28.25
Standard deviation	0.25
Error (%)	0.47

Table D.7: Elemental analyses of the biochar

Sample number	C (mass %)	H (mass %)	N (mass %)	R (mass %)
1	68.14	5.71	3.01	23.14
2	68.19	5.73	2.97	23.11
Average	68.17	5.72	2.99	23.13
Standard deviation	0.04	0.01	0.03	0.02
Error (%)	0.11	0.04	0.09	0.06

Table D.8: Moisture. ash. volatile matter. and fixed carbon content of the biochar

Sample	Moisture (mass %)	Volatile matter (mass %)	Ash (mass %)	Fixed carbon (mass %)
1	1.96	49.03	7.61	41.40
2	1.74	47.44	7.17	43.64
3	2.08	49.75	7.01	41.16
4	1.83	47.96	7.32	42.89
Average	1.90	48.54	7.28	42.27
Standard deviation	0.15	1.04	0.26	1.19
Error (%)	0.20	1.45	0.35	1.65

Table D.9: Moisture. ash. and fixed carbon content of the biocrude oil

Sample	Moisture (mass %)	Ash (mass %)	Fixed carbon (mass %)
1	3.75	0.19	96.07
2	3.57	0.20	96.23
3	4.63	0.18	95.19
Average	3.98	0.19	95.83
Standard deviation	0.57	0.01	0.56
Error (%)	1.04	0.02	1.03

Table D.10: Calorific value of the biocrude oil

Sample	Calorific value. (MJ/kg)

1	30.82
2	31.30
3	31.49
Average	31.2
Standard deviation	0.28
Error (%)	0.52

Table D.11: Elemental analyses of the biocrude oil

Sample number	C (mass %)	H (mass %)	N (mass %)	R (mass %)
1	69.09	8.84	2.03	20.03
2	69.93	8.91	2.05	19.11
Average	69.51	8.88	2.04	19.57
Standard deviation	0.59	0.05	0.01	0.65
Error (%)	1.81	0.15	0.04	1.98
Average weighted error (%)	0.995			

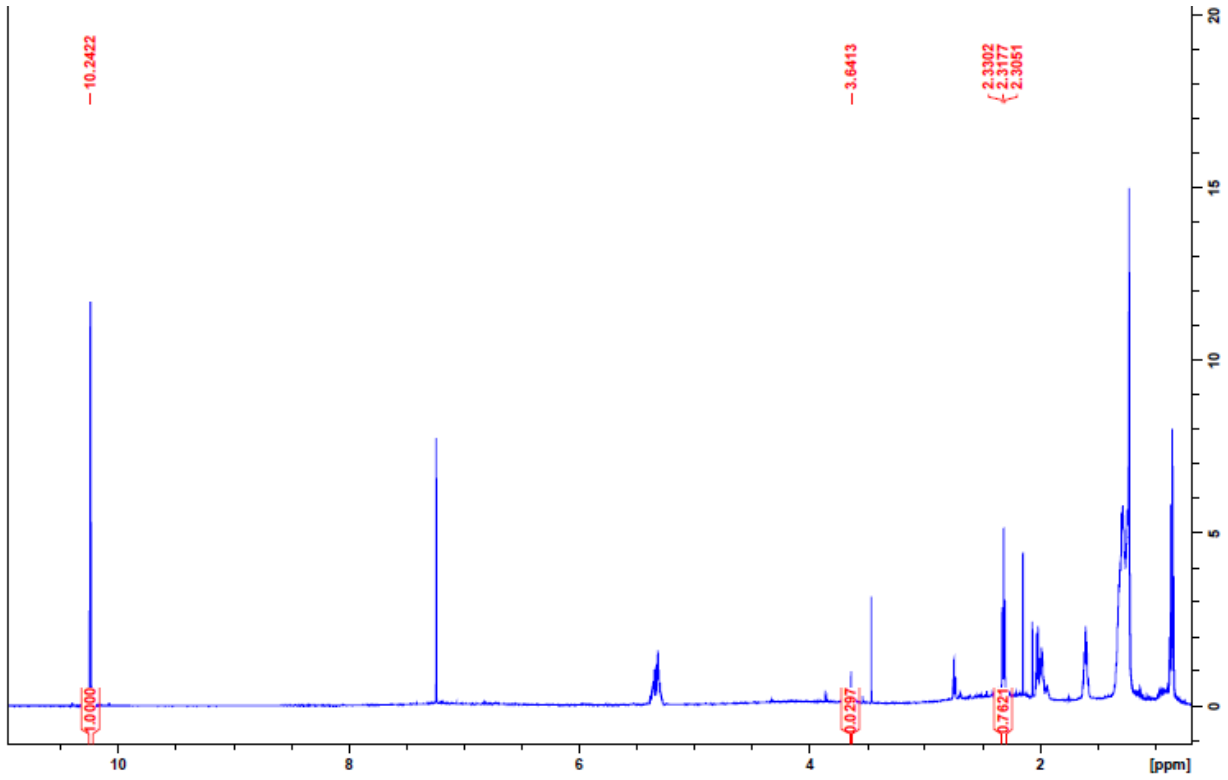

Figure D.1: NMR spectrum of the biocrude oil

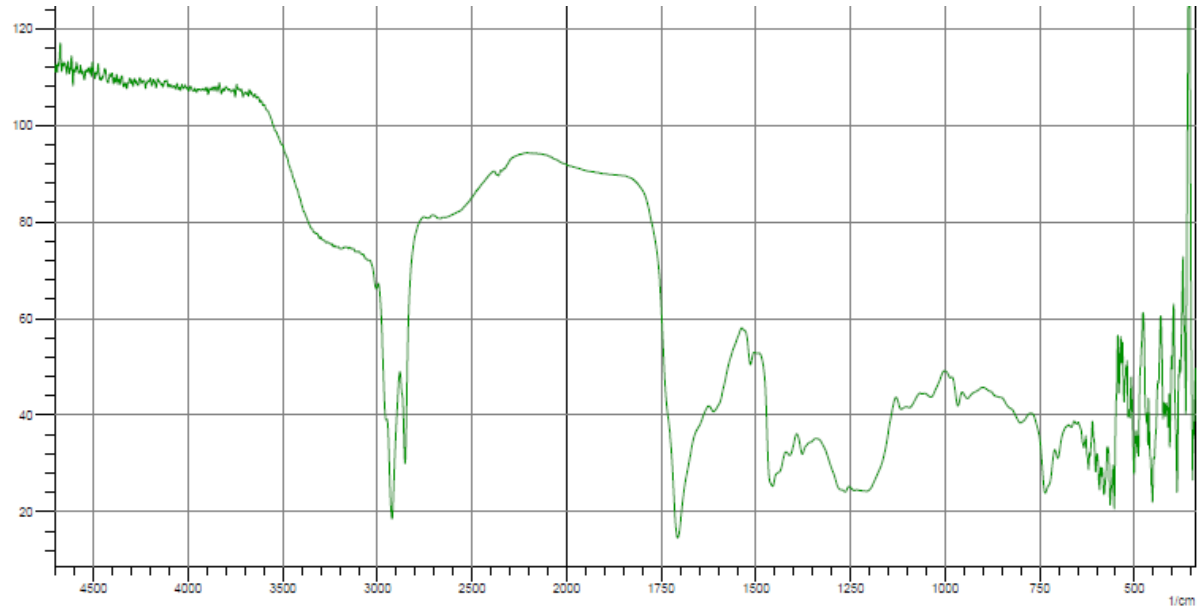

Figure D.2: FTIR spectrum of the biocrude oil

Table D.12: Fatty acid composition of the biocrude oil

Fatty acid	Fatty Acid Composition (mass %)
C16:0	15.91
C18:0	6.32
C18:1	32.82
C18:2	44
C14:0	0.95

Table D.13: GCMS results of the biocrude oil fatty acids

		C16:0	C18:0	C18:1	C18:2	C14:0
mass monster	0.016					
area		4.56E+08	1.89E+08	9.83E+08	1.33E+09	2.41E+07
area std		1.73E+08	1.73E+08	1.73E+08	1.73E+08	1.73E+08
IS concentration	343					
Y		2.63	1.09	5.68	7.66	0.14
intercept		-0.18	-0.33	-0.23	0.09	-0.95
m		1.11	1.32	1.24	1.15	1.63
x		2.55	1.07	4.76	6.59	0.66
X µg per 1.1 mL	1.1	873.87	367.73	1634.08	2258.69	228.25
	1.12	889.46	374.29	1663.24	2298.99	232.33
g per mass oil	0.02	0.09	0.04	0.17	0.23	0.02

Table D.14: Biocrude oil GCMS data divided into boiling rage distributions

RT (min)	area	Name	Normalised peak area %
4.71	1.27E+07	2-Cyclopenten-1-one. 2-methyl-	0.084
7.00	5.89E+06	2-Cyclopenten-1-one. 3-methyl-	0.039
7.21	2.54E+06	2-Cyclopenten-1-one. 3-methyl-	0.017
8.27	9.93E+06	2-Cyclopenten-1-one. 3.4-dimethyl-	0.066
8.45	4.33E+07	Phenol	0.286
10.60	1.89E+06	2.4-Dimethylfuran	0.012
10.73	2.00E+06	1.2-Cyclopentanedione. 3-methyl-	0.013
10.83	1.72E+07	2-Cyclopenten-1-one. 2.3-dimethyl-	0.114
11.16	5.69E+06	6.6-Dimethylhepta-2.4-diene	0.038
11.91	3.51E+06	Bicyclo[2.2.2]octane. 2-methyl-	0.023
12.44	6.70E+06	2-Cyclopenten-1-one. 2.3.4-trimethyl-	0.044
13.09	9.50E+06	p-Cresol	0.063
13.62	1.32E+07	2-Cyclopenten-1-one. 3-ethyl-	0.087
14.16	1.64E+07	1H-Pyrazole. 1-ethyl-3.5-dimethyl-	0.108
14.25	2.10E+07	Phenol. 2-methoxy-	0.139
14.48	7.89E+06	Phenol. 2-methoxy-	0.052
14.68	6.63E+06	p-Cresol	0.044
14.79	1.41E+07	Phenol. 3-methyl-	0.093
14.97	7.33E+06	1-Isopropylcyclohex-1-ene	0.048

15.09	7.23E+06	Cyclopentanecarboxaldehyde. 2-methyl-3-methylene-	0.048
16.95	1.06E+07	1-Isopropylcyclohex-1-ene	0.070
18.22	2.07E+06	Creosol	0.014
19.49	3.58E+06	Phenol. 2.3-dimethyl-	0.024
19.63	3.40E+06	Phenol. 2.3-dimethyl-	0.022
19.77	2.55E+06	Benzene. 1.2-dimethoxy-	0.017
20.13	6.31E+06	Bicyclo[2.2.1]heptane. 2-butyl-	0.042
20.50	4.60E+06	4-Pyridinol	0.030
20.90	1.78E+07	Phenol. 4-ethyl-	0.118
21.47	1.14E+07	2-Methoxy-6-methylphenol	0.076
22.80	5.58E+06	Phenol. 2.4-dimethyl-	0.037
23.25	9.96E+06	Benzoic acid	0.066
25.62	1.07E+07	2-Cyclopenten-1-one. 2-pentyl-	0.071
26.26	1.56E+06	Naphthalen-4a.8a-imine. octahydro-	0.010
26.86	7.67E+06	Benzenethiol. o-isopropyl-.	0.051
26.99	2.99E+07	Phenol. 4-ethyl-2-methoxy-	0.198
29.46	2.99E+06	1-Methylindan-2-one	0.020
30.28	6.95E+06	Dihydrojasmone	0.046
30.65	1.19E+07	Decanoic acid. methyl ester	0.079
31.43	2.89E+06	5H-Benzocycloheptene.6.7.8.9-tetrahydro-	0.019
32.21	1.80E+07	Phenol. 2.6-dimethoxy-	0.119
32.70	5.09E+06	Phenol. 2-methoxy-4-propyl-	0.034

33.17	2.55E+06	Phenol. 5-methoxy-2.3.4-trimethyl-	0.017
35.50	4.81E+06	n-Decanoic acid	0.032
35.61	6.89E+06	n-Decanoic acid	0.046
36.18	3.62E+06	2(3H)-Naphthalenone. 4.4a.5.6.7.8-hexahydro-1-methoxy-	0.024
36.92	8.96E+06	2-Methyl-5-hydroxybenzofuran	0.059
37.18	1.49E+07	Indene-1.7(4H)-dione. 3a.7a-dihydro-5-methyl-	0.098
39.01	1.70E+07	1H-Indole. 2.5-dimethyl-	0.112
39.57	1.58E+07	Benzo[b]thiophene. 2.7-dimethyl-	0.104
40.19	1.49E+08	Dodecanoic acid. methyl ester	0.987
40.87	1.60E+07	1H-Indole. 2.3.5-trimethyl-	0.105
40.98	4.33E+06	2-Propenoic acid. 3-(2-furanyl)-	0.029
41.77	4.55E+07	Dodecanoic acid	0.301
42.54	1.92E+07	1H-Indole. 1.2.3-trimethyl-	0.127
44.19	1.89E+07	2-Benzothiazolamine. 5.6-dimethyl-	0.125
44.39	3.52E+07	Methyl tetradecanoate	0.233
44.73	3.08E+07	2.2.6.6-Tetrachlorocyclohexanol	0.204
45.21	1.85E+07	Carzenide	0.122
45.55	1.29E+08	Tetradecanoic acid	0.853
46.88	1.32E+07	4.5.6.7-Tetrafluoro-2-methyl-1H-benzoimidazole	0.087
46.98	1.11E+07	2-Methyl-5-hydroxybenzofuran	0.073
47.62	2.52E+07	Pentadecanoic acid	0.166
48.08	1.79E+07	(3S.6S)-3-Butyl-6-methylpiperazine-2.5-dione	0.118

49.13	5.07E+07	Hexadecanoic acid. methyl ester	0.335
50.12	7.92E+07	Palmitoleic acid	0.523
51.52	1.27E+09	n-Hexadecanoic acid	8.388
51.75	1.68E+07	n-Hexadecanoic acid	0.111
52.34	2.22E+07	Heptadecanoic acid	0.147
52.61	2.10E+07	Oleic acid	0.139
53.00	2.16E+07	2.5-Piperazinedione. 3.6-bis(2-methylpropyl)-	0.143
53.07	1.61E+07	Heptadecanoic acid	0.107
53.35	1.70E+08	9.12-Octadecadienoic acid (Z.Z)-. methyl ester	1.123
53.51	1.74E+08	9-Octadecenoic acid. methyl ester. (E)-	1.150
53.63	8.58E+07	10.13-Octadecadienoic acid. methyl ester	0.567
54.04	5.29E+07	Methyl stearate	0.349
55.62	7.24E+09	Oleic acid	47.823
55.82	5.30E+08	Octadecanoic acid	3.505
55.97	2.60E+08	9.12-Octadecadienoic acid (Z.Z)-	1.719
56.15	8.33E+07	9.12-Octadecadienoic acid (Z.Z)-	0.550
56.37	2.58E+08	3.4-Octadiene. 7-methyl-	1.706
56.61	3.41E+07	9.12-Octadecadienoic acid (Z.Z)-	0.226
56.70	5.40E+07	E.E-2.13-Octadecadien-1-ol	0.357
56.89	4.83E+07	9.12-Octadecadienoic acid (Z.Z)-	0.319
57.01	8.94E+07	Linoleic acid ethyl ester	0.591
57.30	2.01E+07	Z.Z-10.12-Hexadecadien-1-ol acetate	0.133

57.41	3.89E+07	7.10-Hexadecadienoic acid. methyl ester	0.257
57.80	1.14E+08	Isopropyl linoleate	0.752
57.89	7.47E+07	9-Octadecenamide. (Z)-	0.494
58.25	4.53E+07	Nonadecanamide	0.299
58.37	2.01E+07	Linoleic acid ethyl ester	0.133
58.52	6.36E+07	N.N'-Tetramethylenebis[2-(4-methylphenoxy)acetamide]	0.420
58.74	2.77E+07	9-Octadecenamide. N.N-dimethyl-	0.183
59.12	1.40E+07	7.10-Hexadecadienoic acid. methyl ester	0.092
60.04	2.69E+07	Mercury. chloroethyl-	0.178
60.43	8.18E+07	10-Methyl-dodecanoic acid. pyrrolidide	0.541
62.32	2.88E+07	Pyrrolidine. 1-(1-oxo-9.12-octadecadienyl)-	0.190
62.39	2.87E+07	Pyrrolidine. 1-(1-oxo-9-octadecenyl)-. (Z)-	0.190
62.63	2.72E+07	2H.8H-Benzo[1.2-b:5.4-b']dipyran-10-propanoic acid. 5-methoxy-2.2.8.8-tetramethyl-	0.180
62.71	3.58E+07	Decanoic acid. pyrrolidide	0.237
62.92	2.24E+07	9.11-Octadecadienoic acid. methyl ester. (E.E)-	0.148
63.11	1.69E+07	2H-Pyrrol-2-one. 4-acetyl-1-(2-bromoethyl)-1.5-dihydro-3-hydroxy-5-phenyl-	0.112
63.78	3.11E+07	4-Hydroxy-4-(1-methoxycyclopropyl)-3.3.5.8.10.10-hexamethyltricyclo[6.2.2.0(2.7)]dodeca-5.11-dien-9-one	0.205
64.70	1.19E+07	Tungsten. tris(.pi.-allyl)(.eta.-3-acetato)-	0.079
65.08	1.50E+07	Tungsten. tris(.pi.-allyl)(.eta.-3-acetato)-	0.099
65.18	2.01E+07	.beta.-Tocopherol	0.133

65.41	2.38E+07	Stigmastan-3.5-diene	0.158
65.53	1.60E+07	5-Pyrrol[6-(4-methoxycarbonyl-butylcarbamoyl)-pyridine-2-carbonyl]-aminomorpho-pentanoic acid. methyl ester	0.106
65.89	4.01E+07	(+)-.gamma.-Tocopherol. O-methyl-	0.265
66.72	2.08E+07	Campesterol	0.137
66.89	4.45E+06	Cholesta-5.7.9(11)-trien-3-ol. 4.4-dimethyl-. (3.beta.)-	0.029
66.98	2.20E+07	Stigmasterol	0.145
67.50	3.80E+07	.gamma.-Sitosterol	0.251
67.77	7.17E+06	Ergost-25-ene-3.5.6-triol. (3.beta..5.alpha..6.beta.)-	0.047
68.62	8.57E+06	Stigmast-4-en-3-one	0.057
68.91	3.11E+06	Molybdenum. tetrakis[.mu.-(acetato-O:O')]di-. (Mo-Mo)	0.021
71.24	2.59E+06	Phentolamine	0.017

Table D.15: Groups and components in the kerosene fraction of the biocrude oil

Group and components	Normalised peak area (%)
Ketones	
2-Cyclopenten-1-one. 2-methyl-	0.084
2-Cyclopenten-1-one. 3-methyl-	0.056
2-Cyclopenten-1-one. 3.4-dimethyl-	0.066
1.2-Cyclopentanedione. 3-methyl-	0.013
2-Cyclopenten-1-one. 2.3-dimethyl-	0.114
2-Cyclopenten-1-one. 2.3.4-trimethyl-	0.044
2-Cyclopenten-1-one. 3-ethyl-	0.087

2-Cyclopenten-1-one. 2-pentyl-	0.071
1-Methylindan-2-one	0.020
Dihydrojasmone	0.046
Phenol and derivatives	
Phenol	0.286
p-Cresol	0.107
Phenol. 2-methoxy-	0.191
Phenol. 3-methyl-	0.093
Creosol	0.014
Phenol. 2.3-dimethyl-	0.046
Phenol. 4-ethyl-	0.118
2-Methoxy-6-methylphenol	0.076
Phenol. 2.4-dimethyl-	0.037
Phenol. 4-ethyl-2-methoxy-	0.198
Cyclo alkanes	
Bicyclo[2.2.2]octane. 2-methyl-	0.023
Bicyclo[2.2.1]heptane. 2-butyl-	0.042
Alkenes and Cyclo alkenes	
1-Isopropylcyclohex-1-ene	0.048
6.6-Dimethylhepta-2.4-diene	0.038
Fatty acids / Esters	
Decanoic acid. methyl ester	0.079

Heterocyclic oxygen compounds	
2.4-Dimethylfuran	0.013
Heterocyclic nitrogen compounds	
1H-Pyrazole. 1-ethyl-3.5-dimethyl-	0.108
4-Pyridinol	0.030
Acids	
Benzoic acid	0.066
Sulphur containing aromatics	
Benzenethiol. o-isopropyl-.	0.051

Table D.16: Groups and components in the diesel fraction of the biocrude oil

Group and components	Normalised peak area (%)
Ketones	
2(3H)-Naphthalenone. 4.4a.5.6.7.8-hexahydro-1-methoxy-	0.024
Indene-1.7(4H)-dione. 3a.7a-dihydro-5-methyl-	0.098
2.5-Piperazinedione. 3.6-bis(2-methylpropyl)-	0.143
(3S.6S)-3-Butyl-6-methylpiperazine-2.5-dione	0.118
Phenol and phenol derivatives	
Phenol. 2.6-dimethoxy-	0.119
Phenol. 2-methoxy-4-propyl-	0.034
Phenol. 5-methoxy-2.3.4-trimethyl	0.017

Fatty acids/esters	
n-Decanoic acid	0.077
2-Propenoic acid. 3-(2-furanyl)-	0.029
Dodecanoic acid	0.301
Methyl tetradecanoate	0.233
Tetradecanoic acid	0.853
Pentadecanoic acid	0.166
Hexadecanoic acid. methyl ester	0.335
Palmitoleic acid	0.523
n-Hexadecanoic acid	8.388
n-Hexadecanoic acid	0.111
Heptadecanoic acid	0.107
Oleic acid	0.139
9.12-Octadecadienoic acid (Z.Z)-. methyl ester	1.123
9-Octadecenoic acid. methyl ester. (E)-	1.150
10.13-Octadecadienoic acid. methyl ester	0.567
Methyl stearate	0.349
Oleic acid	47.823
Octadecanoic acid	3.505
Heterocyclic oxygen compounds	
2-Methyl-5-hydroxybenzofuran	0.059

Heterocyclic nitrogen compounds	
4.5.6.7-Tetrafluoro-2-methyl-1H-benzoimidazole	0.087
1H-Indole. 1.2.3-trimethyl-	0.127
1H-Indole. 2.3.5-trimethyl-	0.105
1H-Indole. 2.5-dimethyl-	0.112
Sulphur and nitrogen containing aromatics	
Carzenide	0.122
2-Benzothiazolamine. 5.6-dimethyl-	0.125
Alcohols	
2.2.6.6-Tetrachlorocyclohexanol	0.204
Heterocyclic sulphur compounds	
Benzo[b]thiophene. 2.7-dimethyl-	0.104

Table D.17: Groups and components in the heavy fraction of the biocrude oil

Group and components	Normalised peak area (%)
Ketones	
2H-Pyrrol-2-one. 4-acetyl-1-(2-bromoethyl)-1.5-dihydro-3-hydroxy-5-phenyl-	0.112
Fatty acids / Esters	
9.12-Octadecadienoic acid (Z.Z)-	2.50
Linoleic acid ethyl ester	0.591
Z.Z-10.12-Hexadecadien-1-ol acetate	0.133

7.10-Hexadecadienoic acid. methyl ester	0.257
Isopropyl linoleate	0.752
Linoleic acid ethyl ester	0.591
7.10-Hexadecadienoic acid. methyl ester	0.092
9.11-Octadecadienoic acid. methyl ester. (E.E)-	0.148
5-Pyrrol[6-(4-methoxycarbonyl-butylcarbamoyl)-pyridine-2-carbonyl]-aminomorpho-pentanoic acid. methyl ester	0.106
Sulphur and nitrogen containing compounds	
9-Octadecenamide. (Z)-	0.183
Nonadecanamide	0.299
N.N'-Tetramethylenebis[2-(4-methylphenoxy)acetamide]	0.420
9-Octadecenamide. N.N-dimethyl-	0.183
Heterocyclic nitrogen compounds	
10-Methyl-dodecanoic acid. pyrrolidide	0.541
Pyrrolidine. 1-(1-oxo-9.12-octadecadienyl)-	0.190
Pyrrolidine. 1-(1-oxo-9-octadecenyl)-. (Z)-	0.190
Decanoic acid. pyrrolidide	0.237
Phentolamine	0.017
Phyto sterols and related compounds	
.beta.-Tocopherol	0.133
Stigmastan-3.5-diene	0.158

(+)-.gamma.-Tocopherol. O-methyl-	0.265
Campesterol	0.137
Cholesta-5.7.9(11)-trien-3-ol. 4.4-dimethyl-. (3.beta.)-	0.029
Stigmasterol	0.145
.gamma.-Sitosterol	0.251
Ergost-25-ene-3.5.6-triol. (3.beta..5.alpha..6.beta.)-	0.047
Stigmast-4-en-3-one	0.057
Alcohols	
E.E-2.13-Octadecadien-1-ol	0.357
Z.Z-10.12-Hexadecadien-1-ol acetate	0.133

D.3 Esterification experimental data

Table D.18: Biodiesel produced at 30 °C with an oil to methanol molar ratio of 1:3 GCMS data divided into boiling range distributions

RT (min)	area	Name	Normalised peak area %
8.61	1.38E+07	Phenol	0.077
11.22	1.99E+06	2-Cyclopenten-1-one. 2.3-dimethyl-	0.011
13.18	5.17E+06	Phenol. 2-methyl-	0.029
14.50	6.10E+06	Phenol. 2-methoxy-	0.034
14.82	1.04E+07	p-Cresol	0.058
15.15	2.87E+06	p-Cresol	0.016

17.08	2.17E+06	1-Isopropylcyclohex-1-ene	0.012
17.20	4.58E+06	Octanoic acid. methyl ester	0.026
19.56	2.37E+06	Phenol. 2.4-dimethyl-	0.013
19.69	3.79E+06	Phenol. 2.6-dimethyl-	0.021
20.66	4.02E+06	Benzeneacetic acid. methyl ester	0.022
20.94	7.16E+06	Phenol. 4-ethyl-	0.040
21.09	1.20E+07	Phenol. 2-ethyl-	0.067
21.56	3.35E+06	Creosol	0.019
24.09	2.07E+06	Methyl 7-methylhexadecanoate	0.012
27.03	3.03E+07	Phenol. 4-ethyl-2-methoxy-	0.169
30.62	3.92E+07	Decanoic acid. methyl ester	0.219
32.26	1.21E+07	Phenol. 2.6-dimethoxy-	0.067
32.74	3.78E+06	Phenol. 2-methoxy-4-propyl-	0.021
33.23	2.29E+06	Benzenethiol. 4-(1.1-dimethylethyl)-	0.013
36.36	5.61E+06	17-Octadecynoic acid. methyl ester	0.031
36.57	2.41E+06	Acetaldehyde. (3.3-dimethylcyclohexylidene)-. (E)-	0.013
37.20	1.08E+07	2-Cyclopenten-1-one. 3-methyl-2-(1.3-pentadienyl)-. (E.Z)-	0.060
38.93	7.78E+06	Bicyclo[4.1.0]heptane-7-methanol. 1.5.5-trimethyl-2-methylene-. (1.alpha..6.alpha..7.alpha.)-	0.043
39.03	9.37E+06	1H-Indole. 1.2-dimethyl-	0.052
39.31	2.37E+07	Butylated Hydroxytoluene	0.132
39.59	1.25E+07	Benzo[b]thiophene. 2.7-dimethyl-	0.070

40.20	1.97E+08	Dodecanoic acid. methyl ester	1.101
40.56	1.85E+07	3-Benzofurancarboxaldehyde. 2-methoxy-	0.103
40.87	2.18E+07	Nonanedioic acid. dimethyl ester	0.122
42.09	2.67E+07	4-Propyl-1.1'-diphenyl	0.149
43.26	1.67E+07	4-Pyridinamine. N.N.2.6-tetramethyl-	0.093
44.13	2.20E+07	Methyl myristoleate	0.123
44.41	1.95E+08	Methyl tetradecanoate	1.087
44.60	1.97E+07	4-(1.3.3-Trimethyl-bicyclo[4.1.0]hept-2-yl)-but-3-en-2-one	0.110
45.45	1.85E+07	Tetradecanoic acid	0.103
45.59	1.80E+07	Methyl 9-methyltetradecanoate	0.101
45.74	2.26E+07	Methyl 9-methyltetradecanoate	0.126
46.00	1.40E+07	Furan. 2-(3-imino-3-ethoxyprop-1-enyl)-	0.078
46.24	1.15E+07	1.2.4-Triazolo[4.3-b]pyridazin-8-ol. 7-ethyl-6-methyl-	0.064
46.40	3.06E+07	Pentadecanoic acid. methyl ester	0.171
48.00	9.56E+06	Pentadecanoic acid. 14-methyl-. methyl ester	0.053
48.24	2.00E+07	9-Hexadecenoic acid. methyl ester. (Z)-	0.111
48.41	1.14E+08	9-Hexadecenoic acid. methyl ester. (Z)-	0.635
48.55	1.94E+07	9-Hexadecenoic acid. methyl ester. (Z)-	0.108
48.67	7.32E+06	Methyl 11-hexadecenoate	0.041
49.46	1.96E+09	Hexadecanoic acid. methyl ester	10.957
50.71	7.45E+06	2.5-Piperazinedione. 3.6-bis(2-methylpropyl)-	0.042
51.04	3.87E+07	Octadecanoic acid	0.216

51.17	9.25E+07	n-Hexadecanoic acid	0.517
51.45	9.20E+06	Cyclooctadecane. ethyl-	0.051
51.96	2.07E+07	Hexadecanoic acid. 15-methyl-. methyl ester	0.116
52.70	1.03E+07	Methyl 2-octylcyclopropene-1-heptanoate	0.057
52.94	1.31E+07	Methyl 10-trans.12-cis-octadecadienoate	0.073
53.12	2.32E+07	9.12-Octadecadienoic acid (Z.Z)-. methyl ester	0.129
53.51	1.81E+09	9.12-Octadecadienoic acid (Z.Z)-. methyl ester	10.113
53.70	2.87E+09	9.12-Octadecadienoic acid (Z.Z)-. methyl ester	16.027
53.89	3.73E+09	9-Octadecenoic acid. methyl ester. (E)-	20.820
53.98	1.09E+09	10.13-Octadecadienoic acid. methyl ester	6.110
54.25	7.71E+08	Methyl stearate	4.305
54.52	3.23E+08	9.12-Octadecadienoic acid (Z.Z)-	1.801
54.60	1.53E+08	9.12-Octadecadienoic acid (Z.Z)-	0.856
54.68	1.97E+08	10.13-Octadecadienoic acid. methyl ester	1.098
54.80	1.58E+08	9.12-Octadecadienoic acid (Z.Z)-	0.883
55.06	6.68E+07	Octadecanoic acid	0.373
55.21	3.39E+08	Methyl 10-trans.12-cis-octadecadienoate	1.891
55.92	1.78E+07	9.12-Octadecadienoic acid. methyl ester. (E.E)-	0.100
56.01	2.23E+07	Methyl 9.cis.11.trans.t.13.trans.-octadecatrienoate	0.124
56.21	3.09E+07	Methyl 9.cis.11.trans.t.13.trans.-octadecatrienoate	0.173
56.31	1.94E+07	Octanamide. N.N-dimethyl-	0.109
56.47	1.65E+07	7.10-Hexadecadienoic acid. methyl ester	0.092

56.62	6.01E+07	9.17-Octadecadienal. (Z)-	0.336
56.74	3.77E+07	Oxacyclohexadecan-2-one	0.210
56.86	1.90E+08	cis-11-Eicosenoic acid. methyl ester	1.062
57.28	1.53E+08	Methyl 18-methylnonadecanoate	0.855
57.50	1.27E+07	Methyl 5.12-octadecadienoate	0.071
57.75	3.82E+07	9-Octadecenamide. (Z)-	0.214
58.07	7.29E+07	(R)-(-)-14-Methyl-8-hexadecyn-1-ol	0.407
58.33	1.45E+07	n-Propyl 9.12-octadecadienoate	0.081
58.67	2.01E+07	9-Octadecenamide. N.N-dimethyl-	0.112
59.71	8.17E+06	Palladium. (.eta.-3-allyl)-isopropylcyclopentadienyl-	0.046
59.85	1.04E+08	Docosanoic acid. methyl ester	0.579
60.40	3.71E+07	22-Methyl-tricosanoic acid. pyrrolidide	0.207
60.63	1.25E+07	Nonadecane	0.070
60.99	1.75E+07	Tricosanoic acid. methyl ester	0.098
61.79	2.47E+07	2.5-Furandione. 3-dodecyl-	0.138
61.87	1.92E+07	4-Oxabicyclo[6.1.1]deca-2.6-diene-3-carboxylic acid. 5-oxo-6-phenyl-. methyl ester	0.107
62.09	6.37E+07	Tetracosanoic acid. methyl ester	0.356
62.30	2.53E+07	Pyrrolidine. 1-(1-oxo-9.12-octadecadienyl)-	0.141
62.37	4.71E+07	Pyrrolidine. 1-(1-oxo-9-octadecenyl)-. (Z)-	0.263
62.59	1.85E+07	2H.8H-Benzo[1.2-b:5.4-b']dipyran-10-propanoic acid. 5-methoxy-2.2.8.8-tetramethyl-	0.103
62.70	2.76E+07	10-Methyl-dodecanoic acid. pyrrolidide	0.154

62.88	1.59E+07	Tungsten. tris(.pi.-allyl)(.eta.-3-acetato)-	0.089
63.03	1.50E+07	Tungsten. tris(.pi.-allyl)(.eta.-3-acetato)-	0.084
63.12	1.68E+07	Methyl 22-methyl-tetracosanoate	0.094
63.45	1.99E+07	Isosteviol methyl ester	0.111
63.79	2.49E+07	Cyclopentaneoctanoic acid. 5-(acetyloxy)-.epsilon.3-bis(methoxyimino)-2-(3-methoxy-3-oxopropyl)-. methyl ester. [1R-(1.alpha.2.beta.5.beta.)-	0.139
63.96	1.18E+07	7-Cholesten-3-one	0.066
64.11	1.67E+07	Hexacosanoic acid. methyl ester	0.093
64.25	2.15E+07	Stigmasta-4.22-diene	0.120
64.38	1.02E+07	1.1':3'.1"-Tercyclopentane. 2'-dodecyl-	0.057
64.56	1.62E+07	Tungsten. tris(.pi.-allyl)(.eta.-3-acetato)-	0.090
64.82	2.13E+07	Furo[3'.4':6.7]naphtho[2.3-d]-1.3-dioxol-6(5aH)-one. 5.8.8a.9-tetrahydro-5-(3.4.5-trimethoxyphenyl)-. [5R-(5.alpha.5a.beta.8a.alpha.)]-	0.119
65.18	1.92E+07	.gamma.-Tocopherol	0.107
65.41	2.38E+07	Stigmastan-3.5-diene	0.133
65.74	1.97E+07	Cholesterol	0.110
65.89	3.03E+07	Vitamin E	0.169
66.71	2.53E+07	Campesterol	0.141
66.96	2.57E+07	Stigmasterol	0.144
67.50	7.65E+07	.gamma.-Sitosterol	0.427
67.77	8.21E+06	Olean-12-ene	0.046

67.85	1.74E+07	9.19-Cycloergost-24(28)-en-3-ol. 4.14-dimethyl-. (3.beta.4.alpha.5.alpha.)-	0.097
68.18	1.15E+07	Lupeol	0.064
68.37	4.38E+06	Tungsten. dicarbonylbis(.eta.-4-ethyl methacrylate)	0.024
68.63	1.30E+07	Stigmast-4-en-3-one	0.073
70.34	1.28E+07	1.37-Octatriacontadiene	0.072
71.33	1.95E+07	Pyridine-3-carboxamide. oxime. N-(2-trifluoromethylphenyl)-	0.109

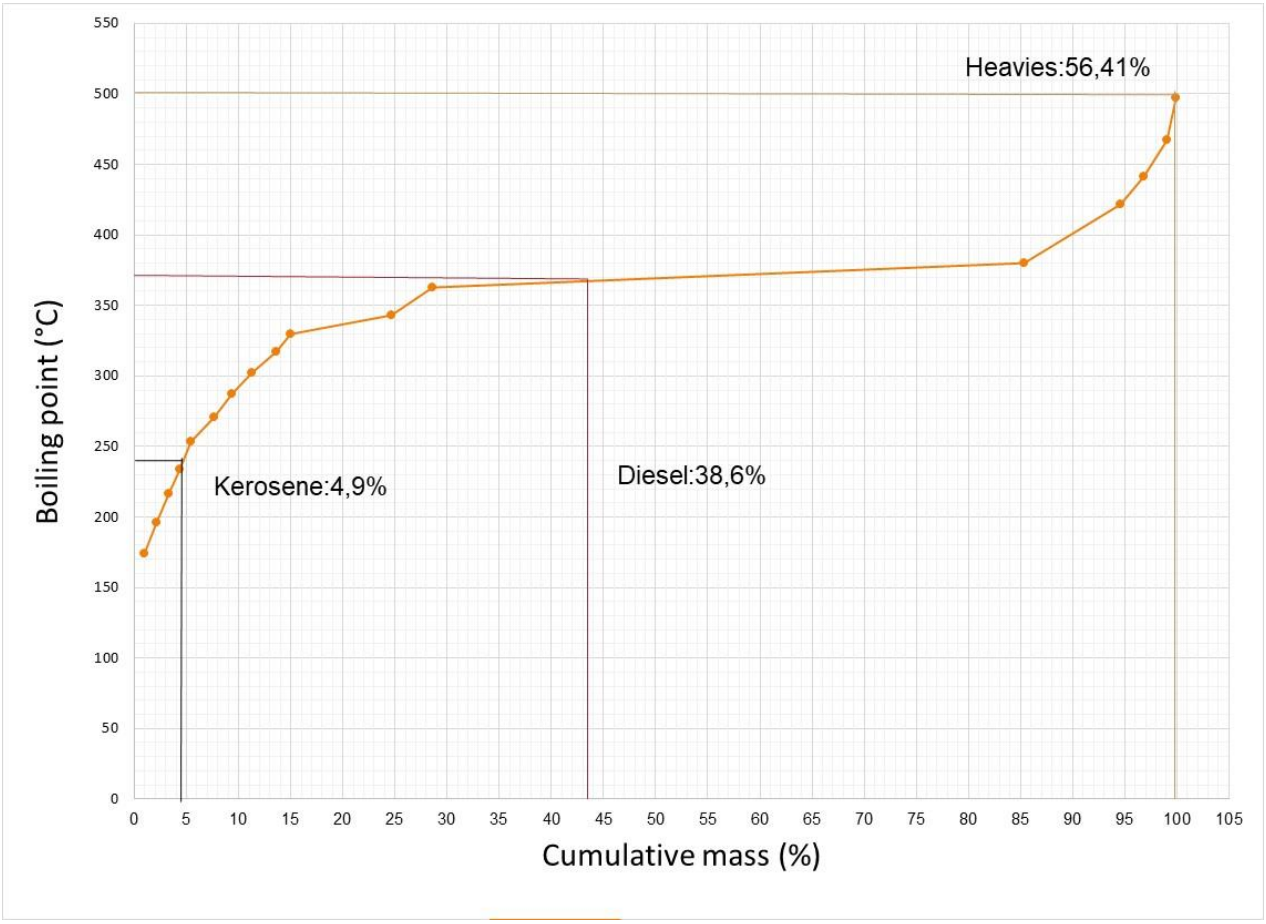

Figure D.3: SIMDIST curve of the biocrude oil

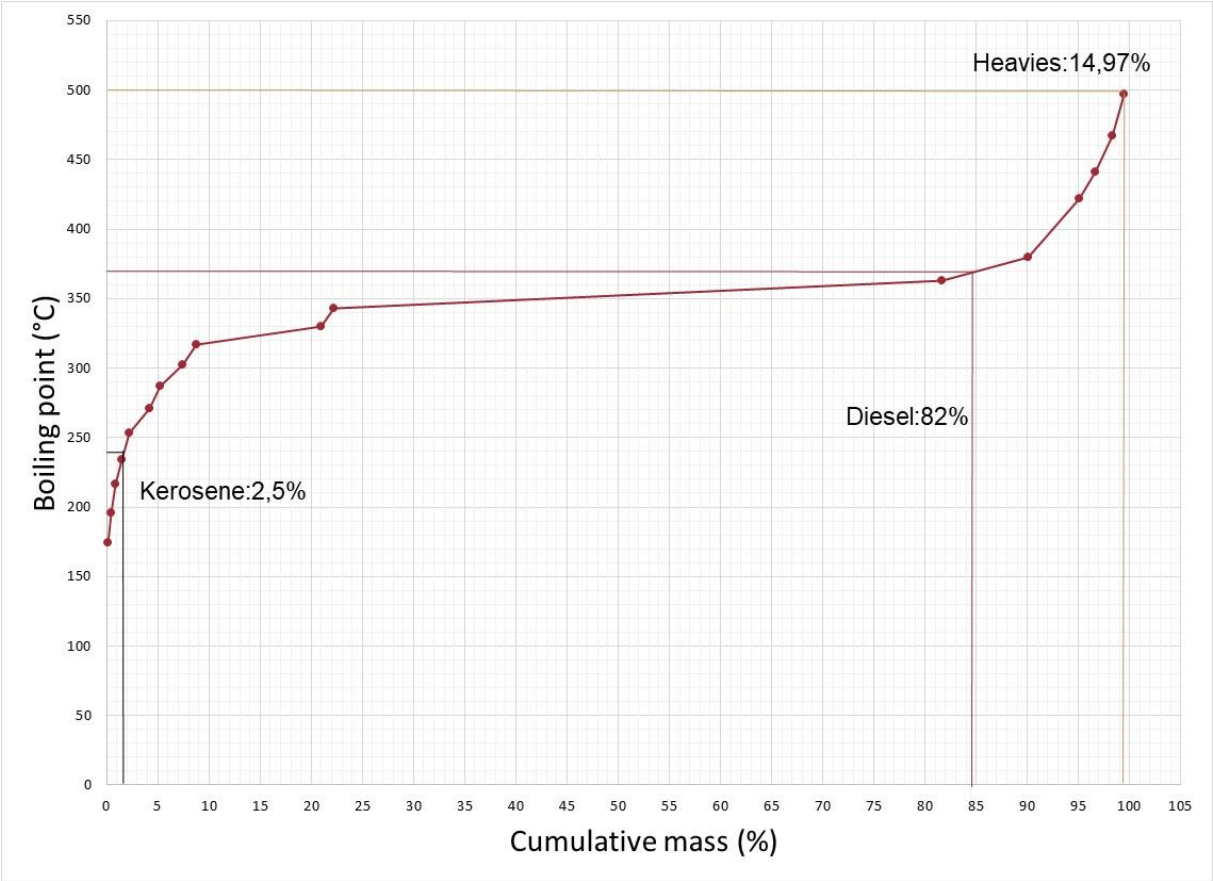

Figure D.4: SIMDIST curve of biodiesel produced at 30 °C with an oil to methanol molar ratio of 1:3

Table D.19: Methyl ester content of the biocrude oil determined by the NMR

Sample	Methyl ester content. (mass %)
1	1.1
2	1.3
3	1.1
Average	1.2
Standard deviation	0.12
Error (%)	0.21

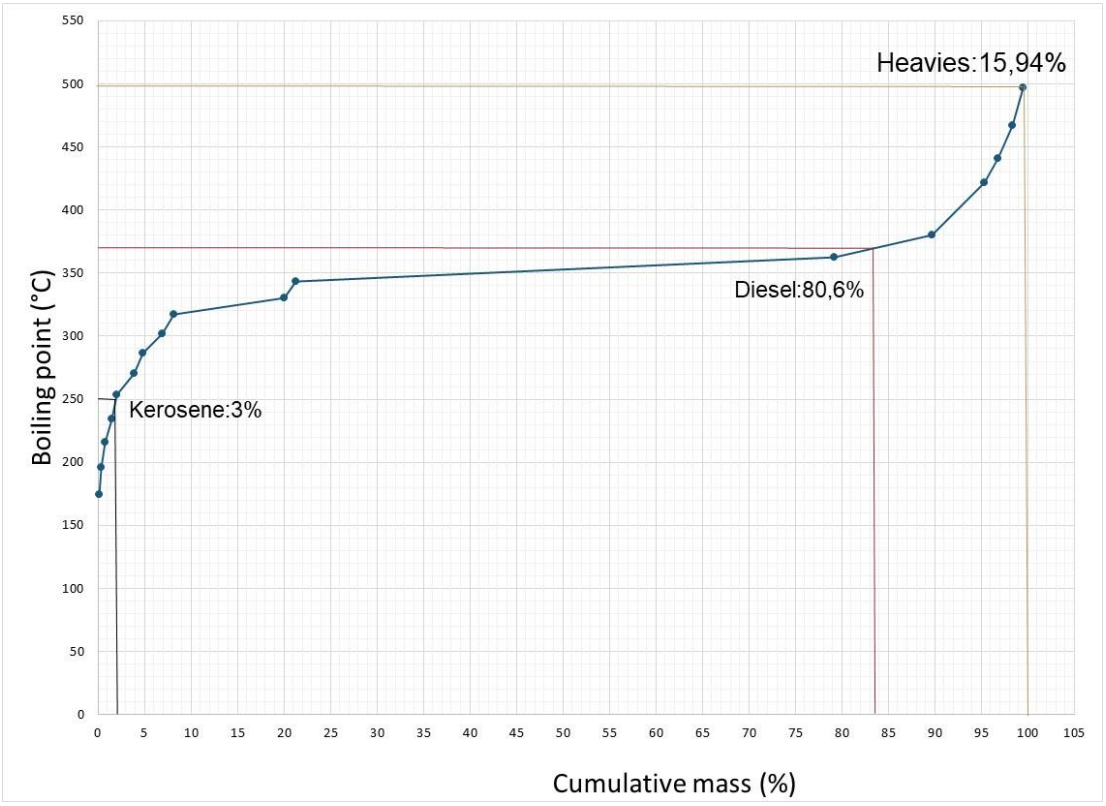

Figure D.5: SIMDIST curve of biodiesel produced at 50 °C with an oil to methanol molar ratio of 1:3

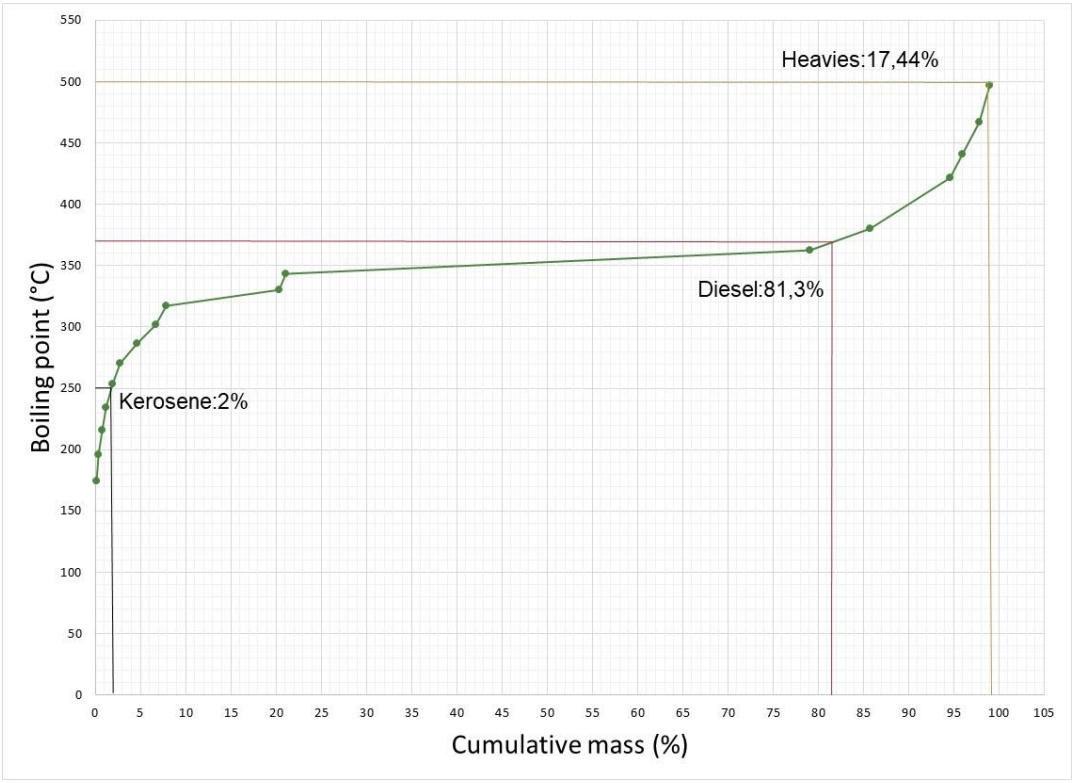

Figure D.6: SIMDIST curve of biodiesel produced at 30 °C with an oil to methanol molar ratio of 1:12

Table D.20: Fatty acid content of the biocrude oil determined by NMR

Sample	Fatty acid content. (mass %)
1	40.8
2	40.1
3	43.6
Average	41.5
Standard deviation	1.84
Error (%)	3.38

Table D.21: Groups identified in the kerosene fraction of the biocrude and biodiesel

Groups	Ketones	Phenolics	Esters	Other
Biocrude oil	0.6	1.16	0.08	0.15
30 °C	0.01	0.54	0.28	0.01
50 °C	0.05	0.48	0.28	0.02
1:12	0.04	0.49	0.06	0.01
1:3	0.01	0.54	0.28	0.01

Table D.22: Groups identified in the diesel fraction of the biocrude and biodiesel

Groups	Ketones/Aldehydes	Phenolics	Fatty acids
Biocrude oil	0.38	0.17	61.17
30 °C	0.23	0.22	4.75
50 °C	0.07	0.23	0.12
1:12	0.23	0.3	0.13
1:3	0.23	0.22	4.75

Table D.23: Groups identified in the diesel fraction of the biocrude and biodiesel

Groups	Esters	Heterocyclic O_2. N and S compounds	Other
Biocrude oil	3.87	0.92	0.45
30 °C	73.22	0.46	0.16

50 °C	71.56	0.25	0.51
1:12	68.08	0.26	0.6
1:3	73.22	0.46	0.16

Table D.24: Groups identified in the heavy fraction of the biocrude and biodiesel

Groups	Ketones/Aldehydes	Fatty acids	Esters
Biocrude oil	0.32	2.49	2.54
30 °C	0.55	-	5.78
50 °C	1.92	1.36	9.54
1:12	0.69	0.63	13.6
1:3	0.55	-	5.78

Table D.25: Groups identified in the heavy fraction of the biocrude and biodiesel

Groups	Heterocyclic O_2. N and S compounds	Phytosterols and related compounds	Other
Biocrude oil	1.17	1.22	1.58
30 °C	1.38	1.77	1.13
50 °C	1.02	2.23	0.95
1:12	1.14	1.66	0.78
1:3	1.38	1.77	1.13

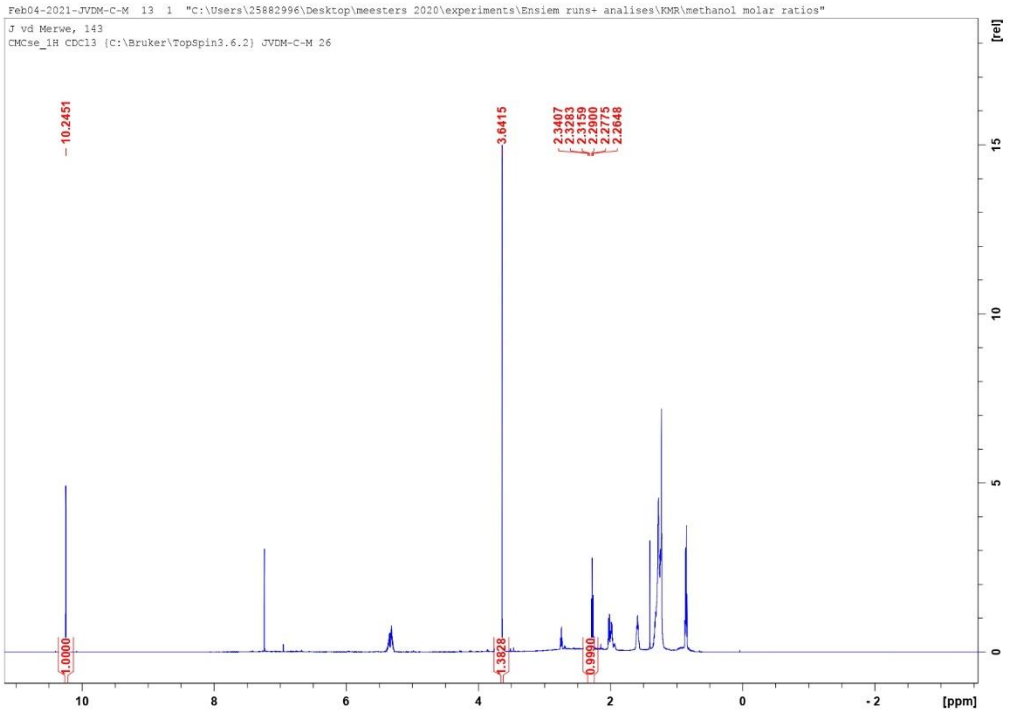

Figure D.7: NMR analysis of the biodiesel produced at 27 °C with an oil to methanol molar ratio of 1:3

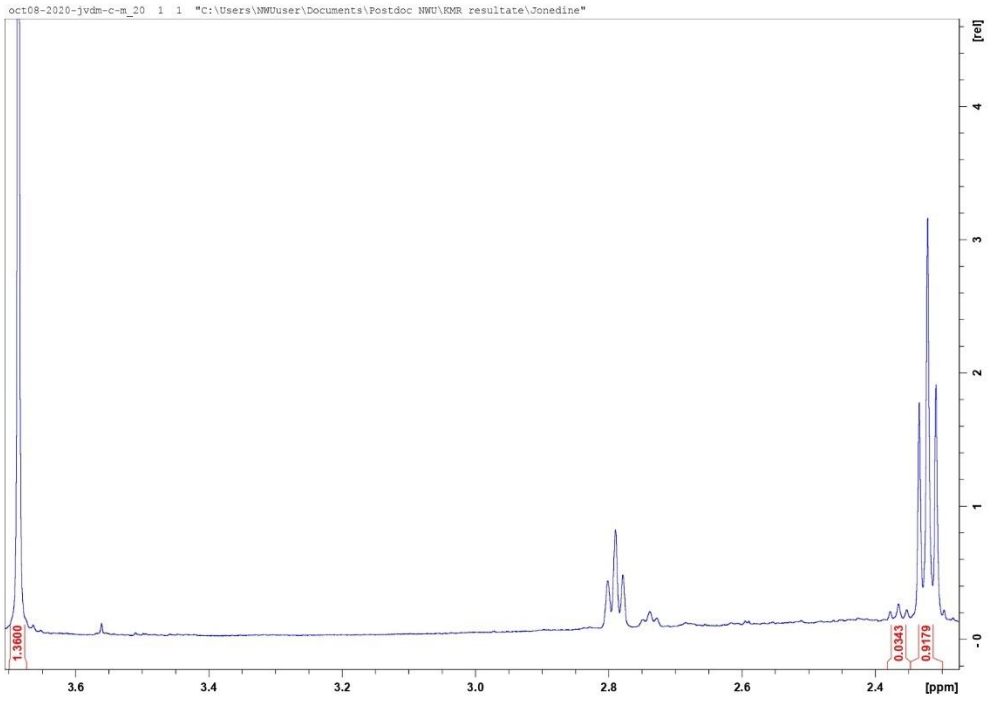

Figure D.8: NMR analysis of the biodiesel produced at 30 °C with an oil to methanol molar ratio of 1:3

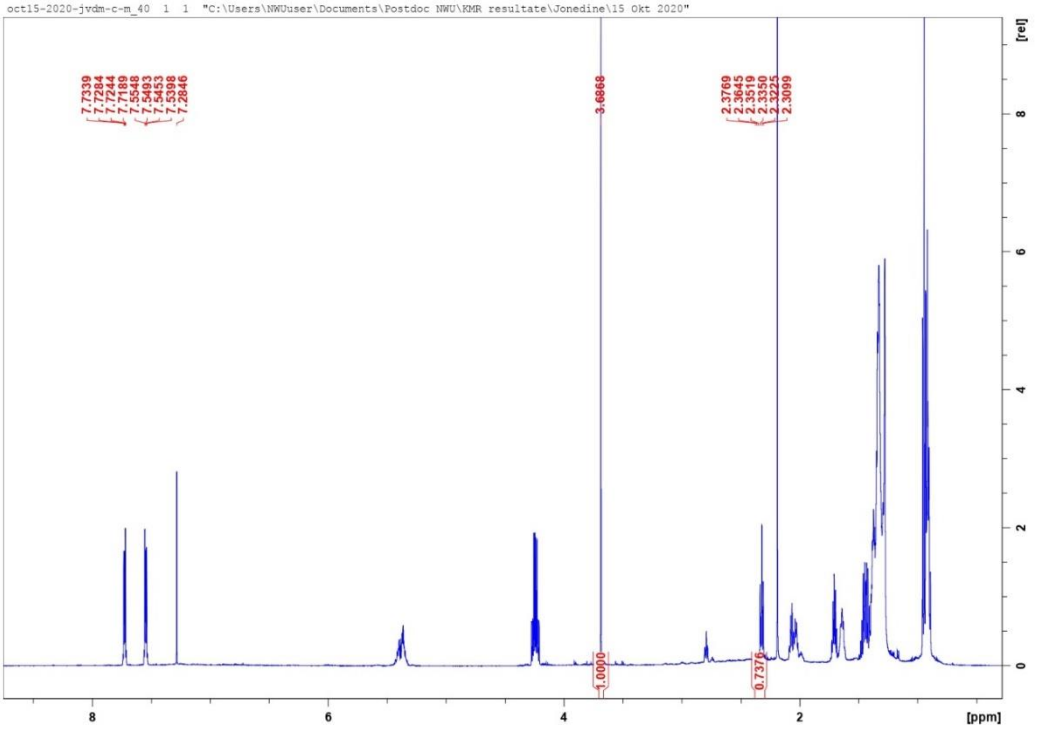

Figure D.9: NMR analysis of the biodiesel produced at 35 °C with an oil to methanol molar ratio of 1:3

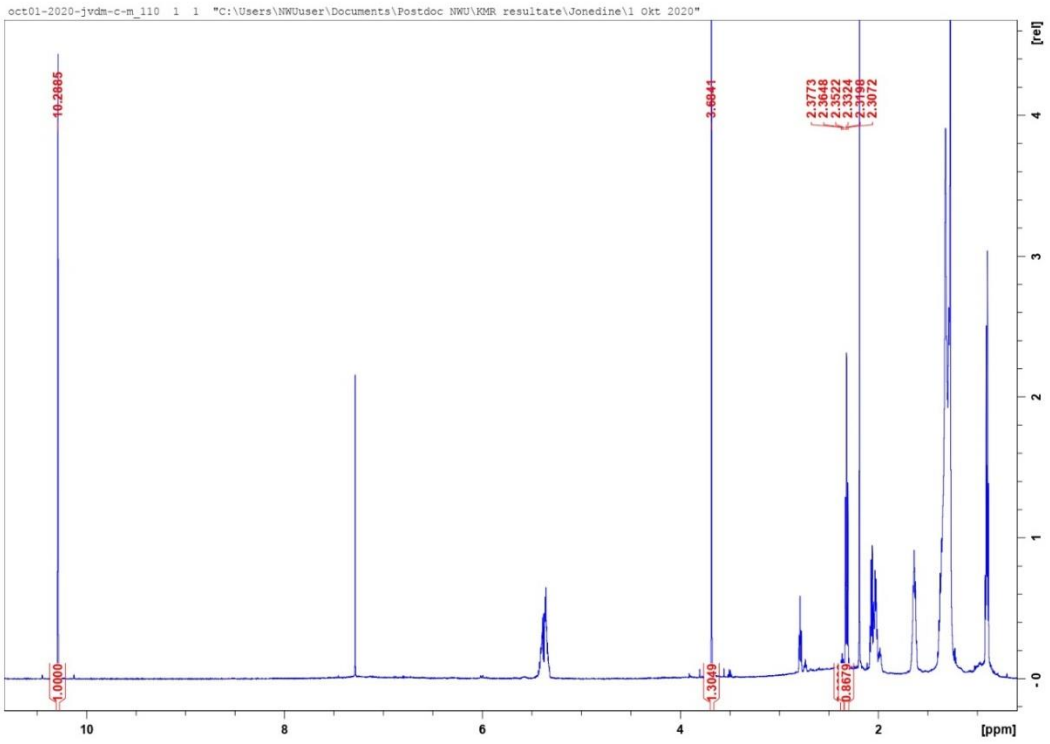

Figure D.10: NMR analysis of the biodiesel produced at 40 °C with an oil to methanol molar ratio of 1:3

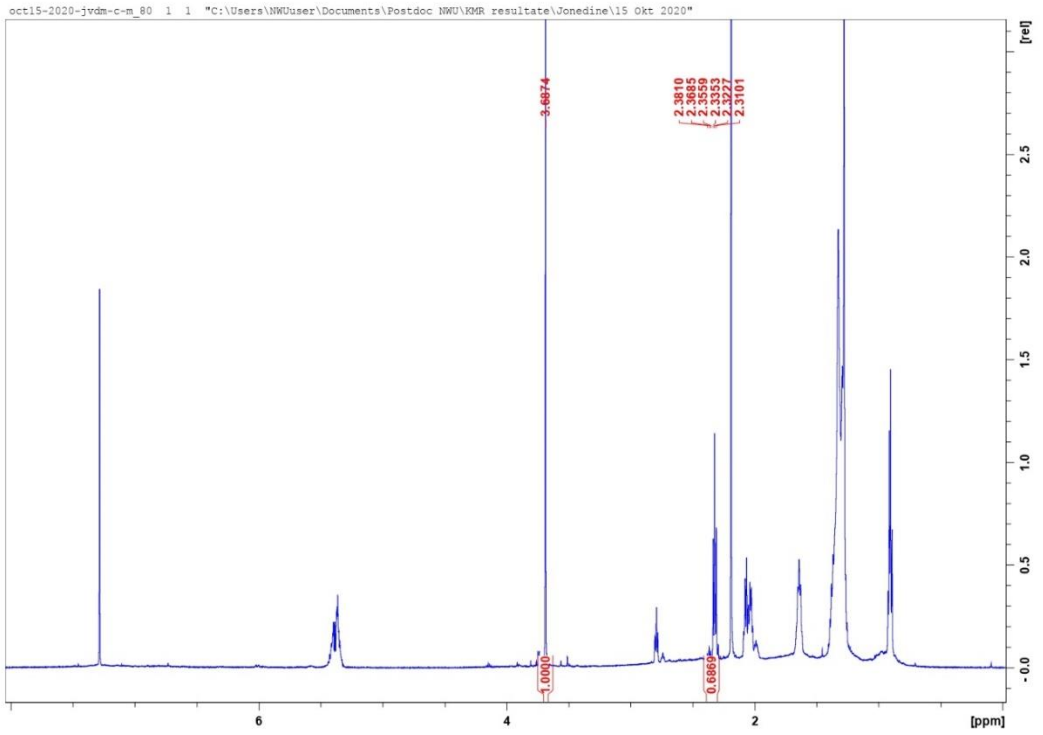

Figure D.11: NMR analysis of the biodiesel produced at 45 °C with an oil to methanol molar ratio of 1:3

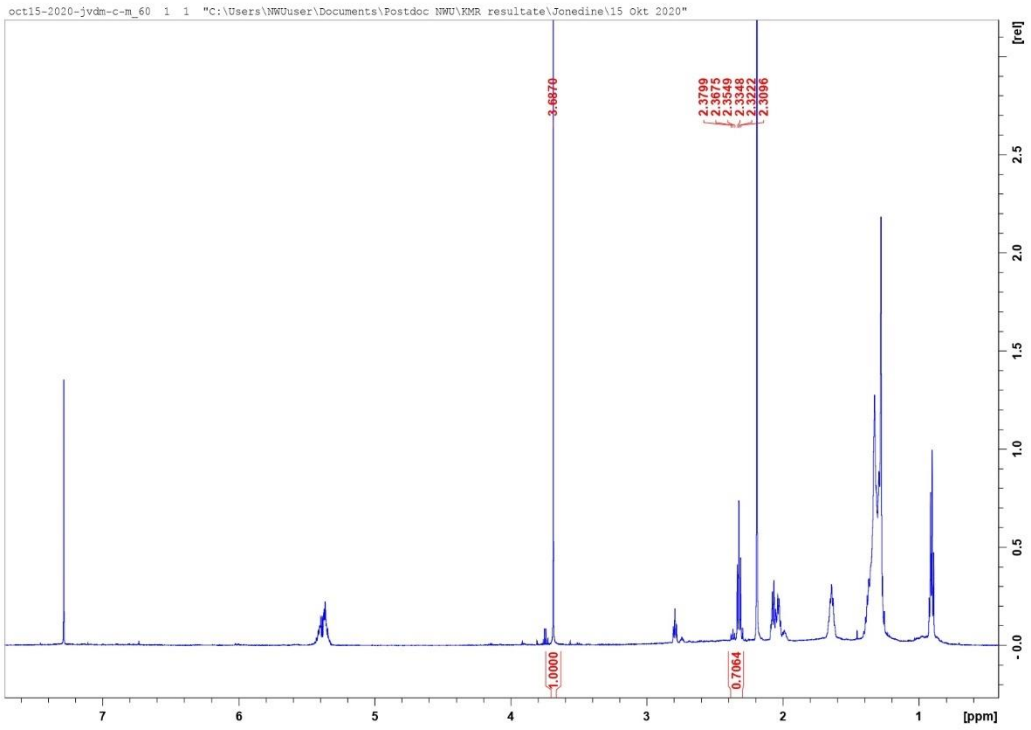

Figure D.12: NMR analysis of the biodiesel produced at 50 °C with an oil to methanol molar ratio of 1:3

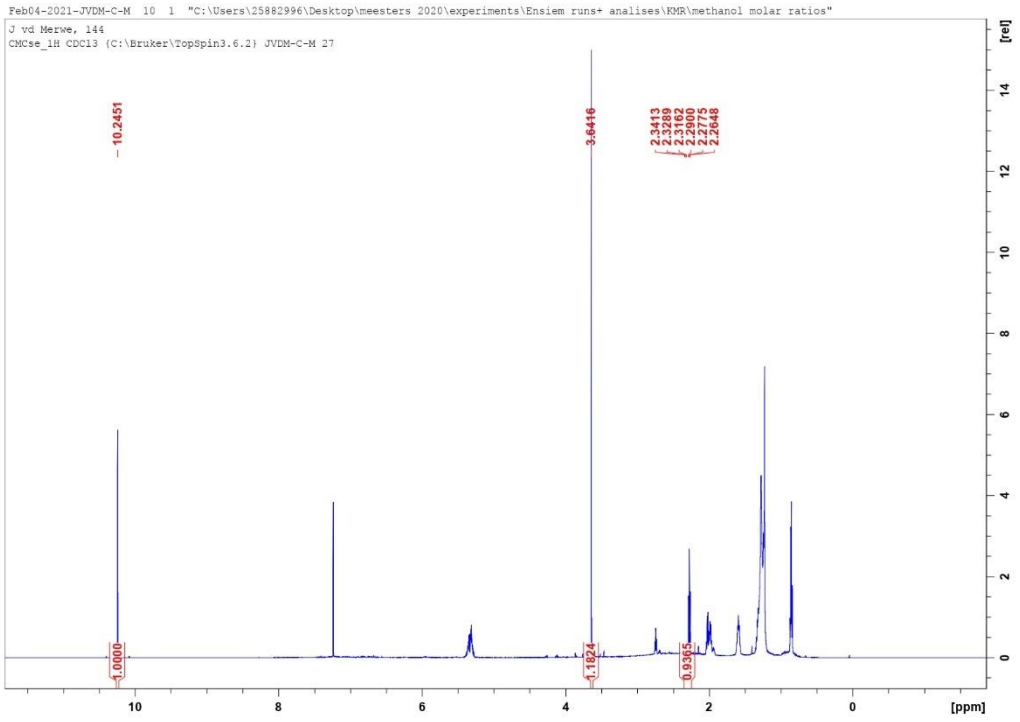

Figure D.13: NMR analysis of the biodiesel produced at 60 °C with an oil to methanol molar ratio of 1:3

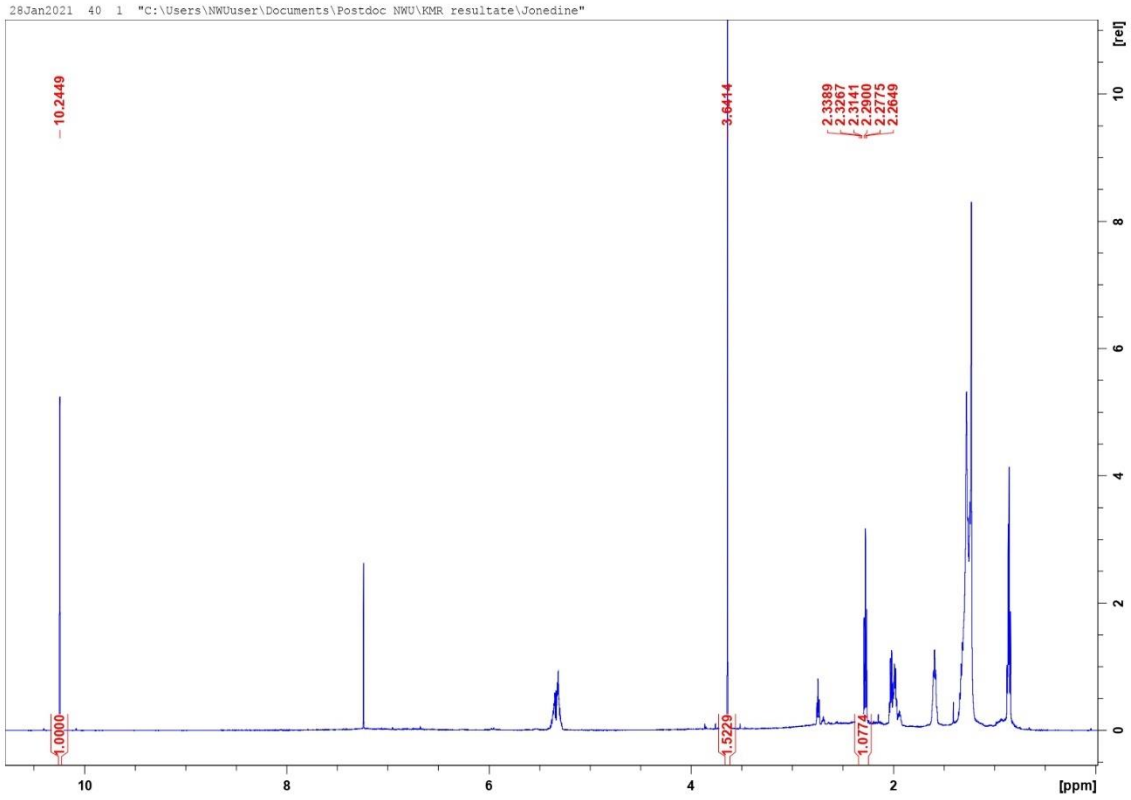

Figure D.14: NMR analysis of the biodiesel produced with an oil to methanol molar ratio of 1:2 at 30 °C

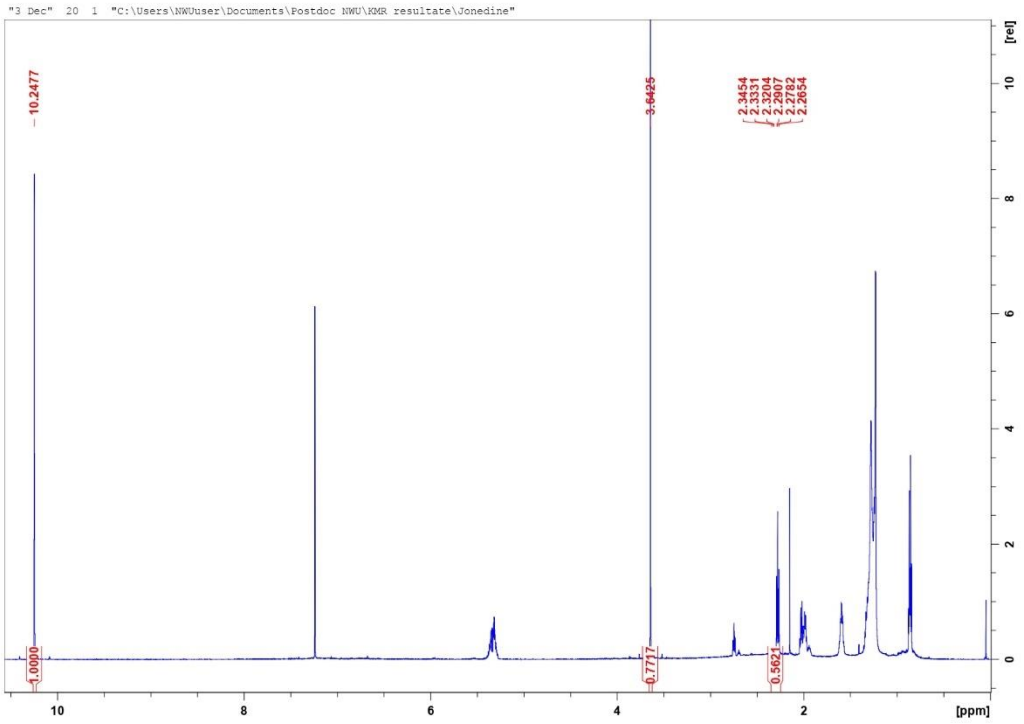

Figure D.15: NMR analysis of the biodiesel produced with an oil to methanol molar ratio of 1:4 at 30 °C

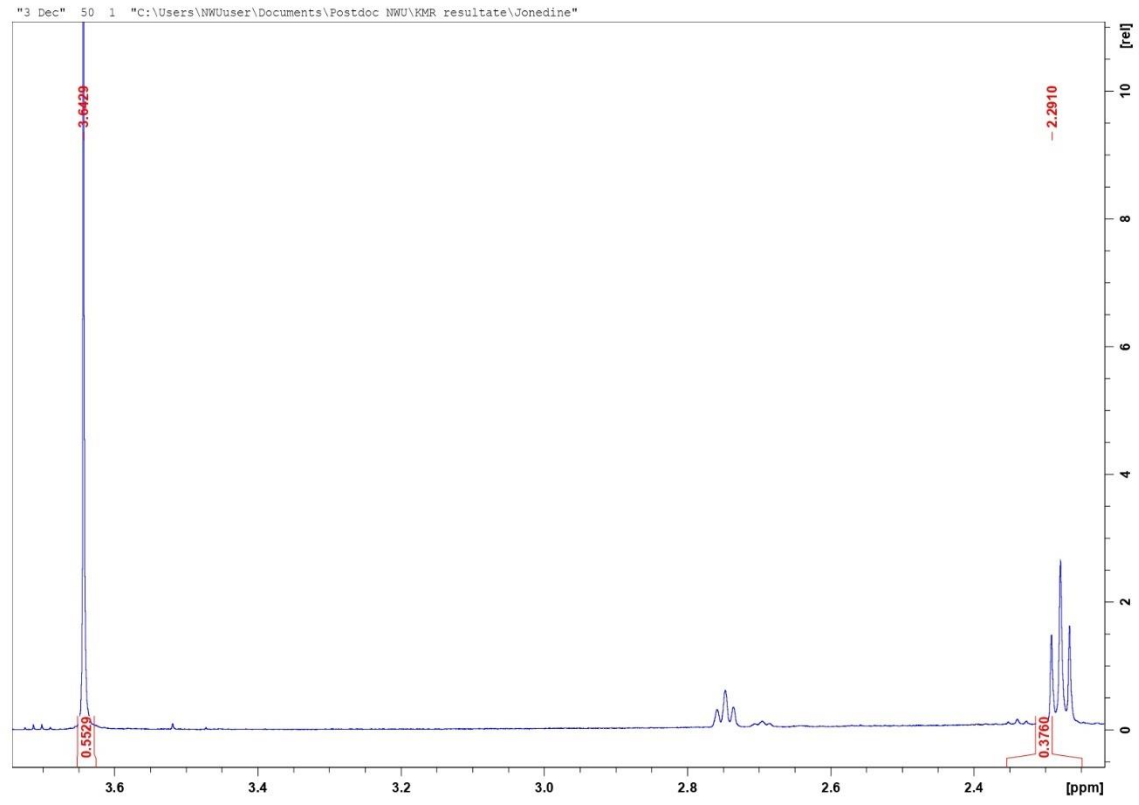

Figure D.16: NMR analysis of the biodiesel produced with an oil to methanol molar ratio of 1:5 at 30 °C

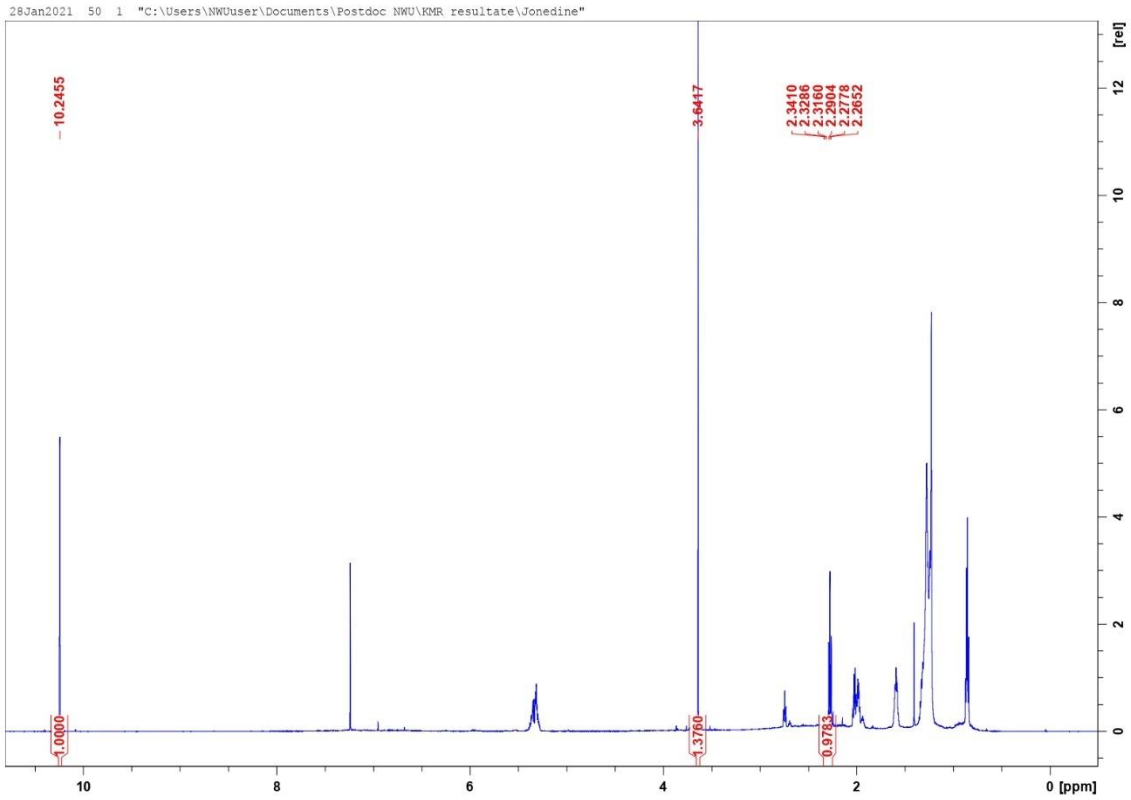

Figure D.17: NMR analysis of the biodiesel produced with an oil to methanol molar ratio of 1:6 at 30 °C

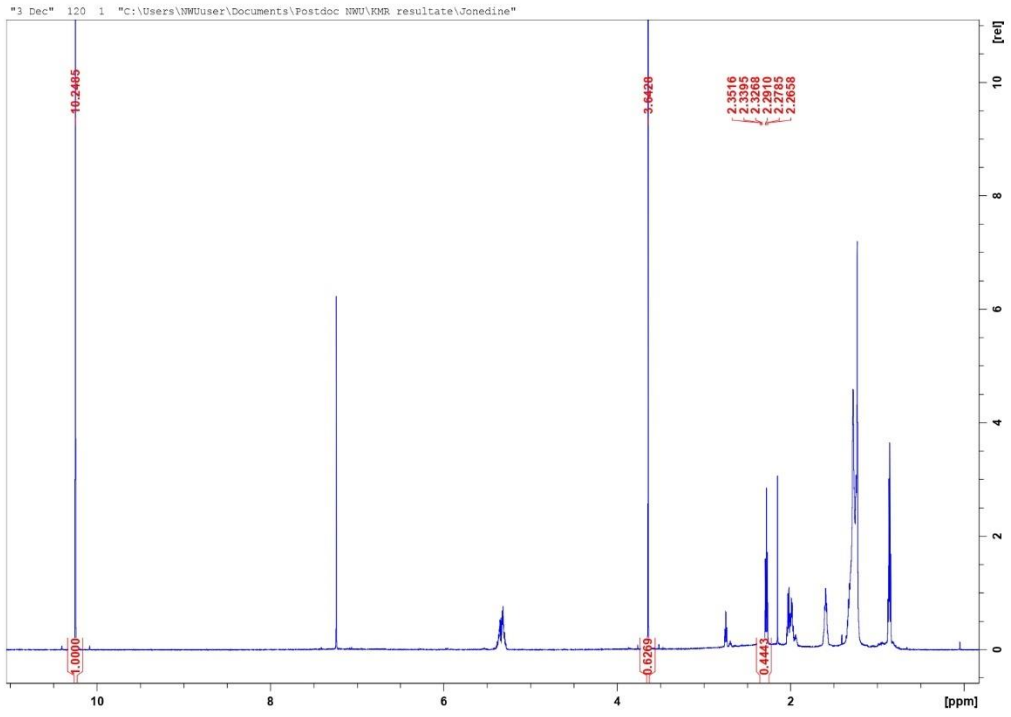

Figure D.18: NMR analysis of the biodiesel produced with an oil to methanol molar ratio of 1:12 at 30 °C

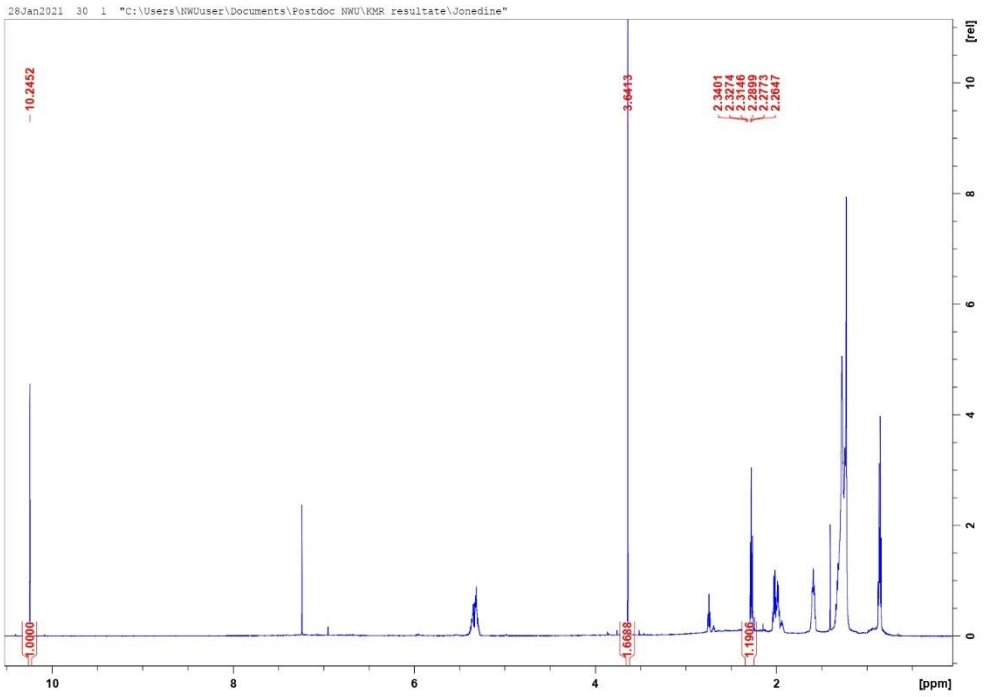

Figure D.19: NMR analysis of the biodiesel produced with an oil to methanol molar ratio of 1:18 at 30 °C

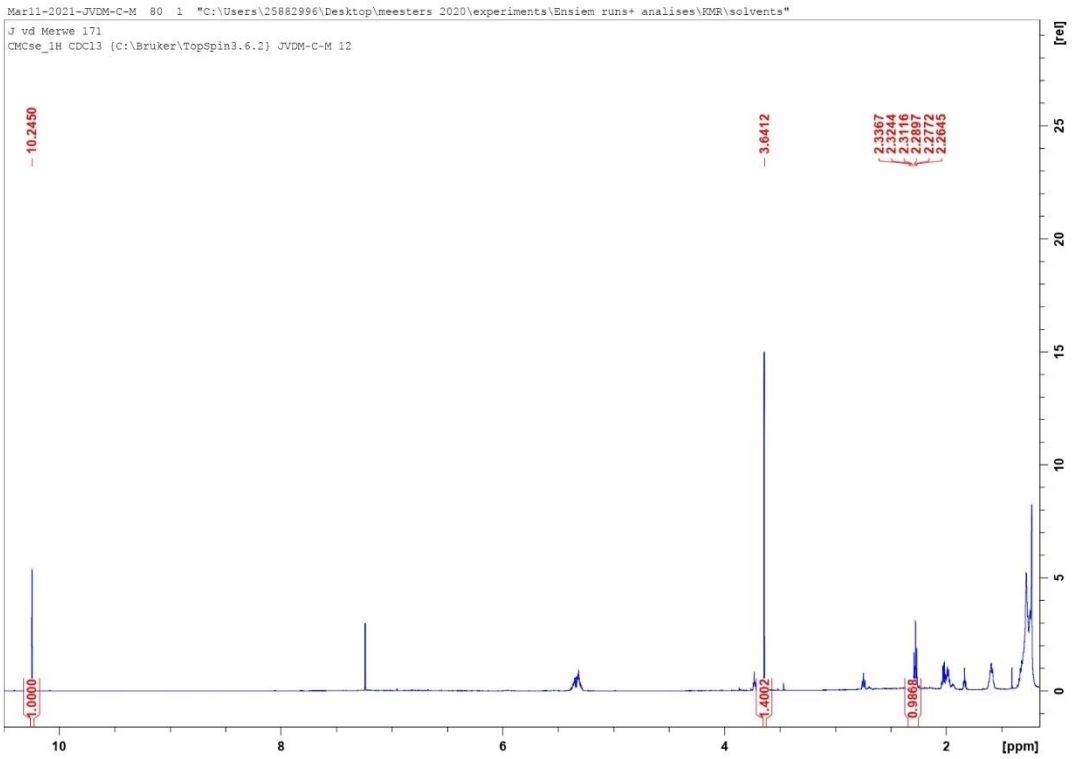

Figure D.20: NMR analysis of the biodiesel produced with an oil to methanol molar ratio of 1:3 at 30 °C with a reaction time of 10 hours

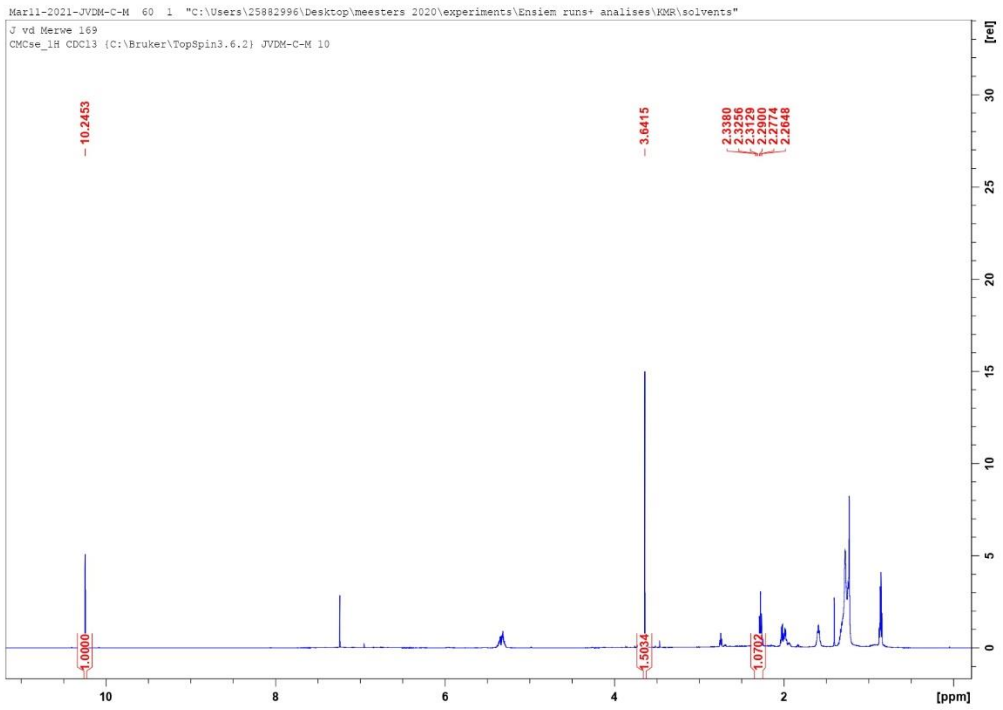

Figure D.21: NMR analysis of the biodiesel produced with an oil to methanol molar ratio of 1:3 at 30 °C with a reaction time of 12 hours

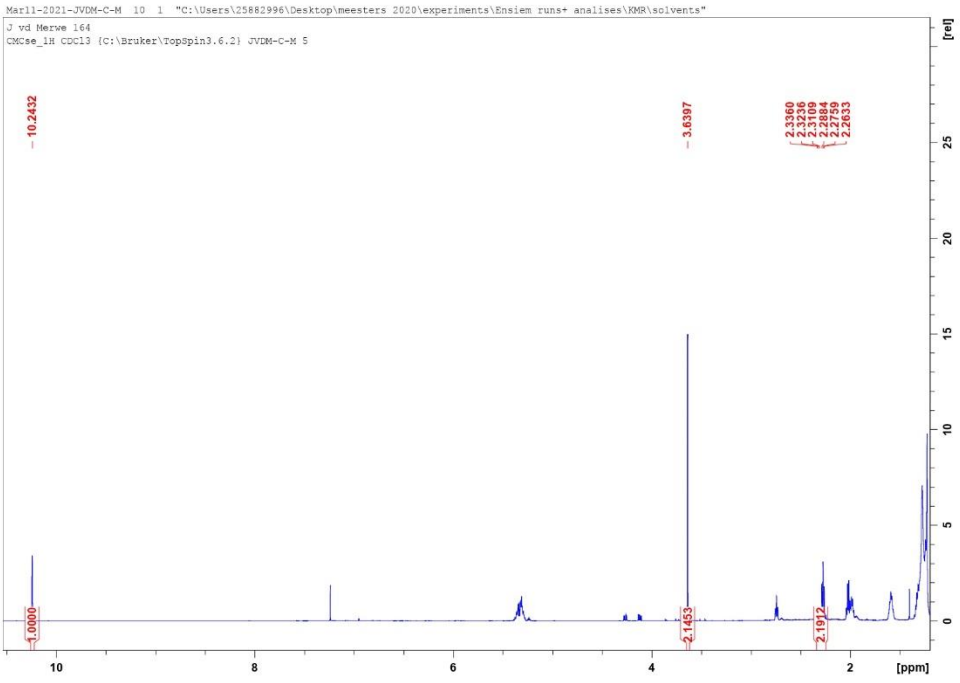

Figure D.22: NMR analysis of the biodiesel produced with an oil to methanol molar ratio of 1:3 at 30 °C with a reaction time of 24 hours

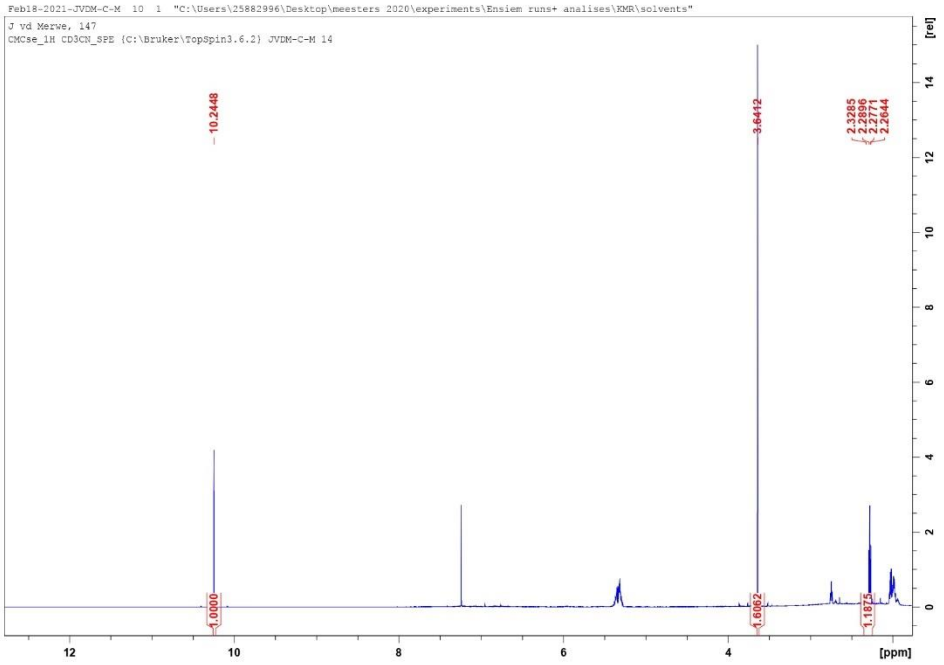

Figure D.23: NMR analysis of the biodiesel produced with acetone-washed lipase, and an oil to methanol molar ratio of 1:3 at 30 °C

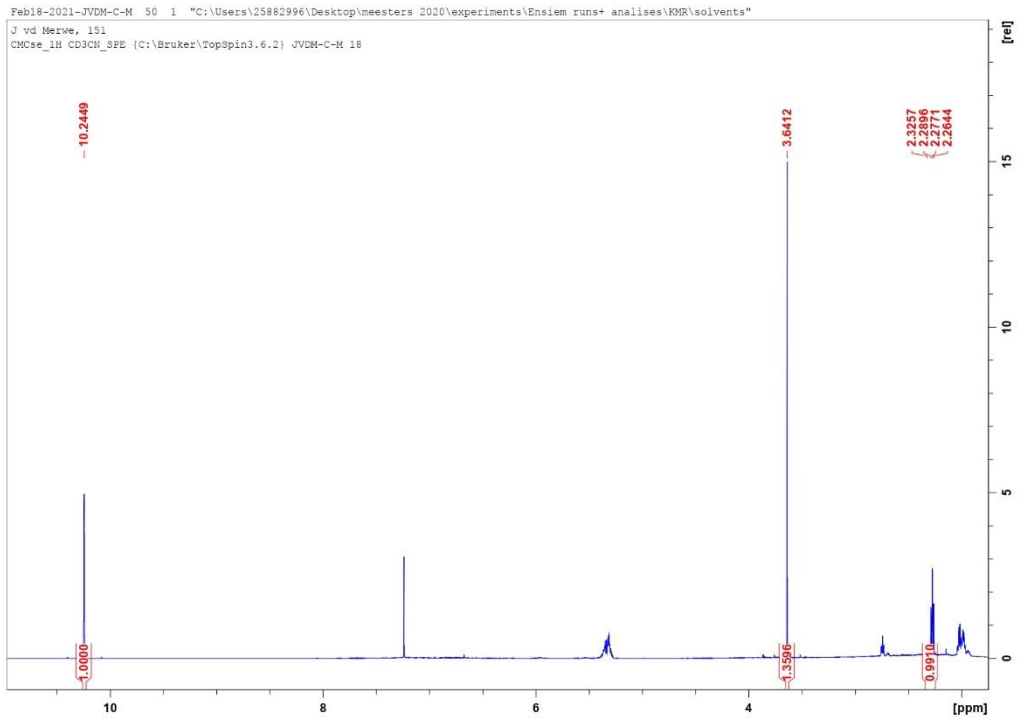

Figure D.24: NMR analysis of the biodiesel produced with acetonitrile-washed lipase, and an oil to methanol molar ratio of 1:3 at 30 °C

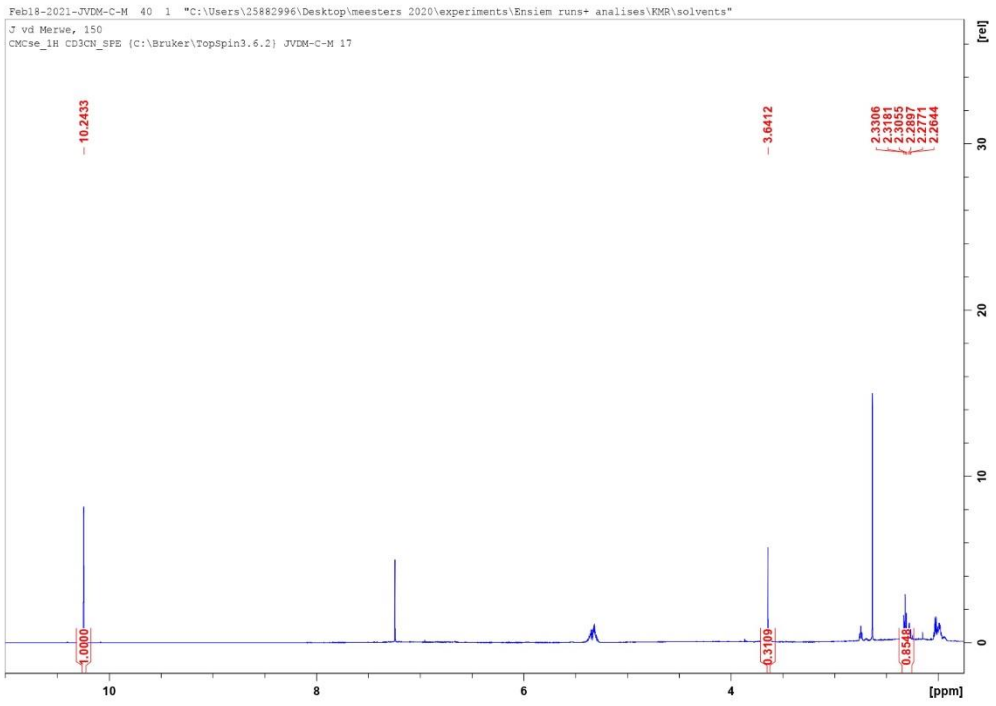

Figure D.25: NMR analysis of the biodiesel produced with DMSO-washed lipase, and an oil to methanol molar ratio of 1:3 at 30 °C

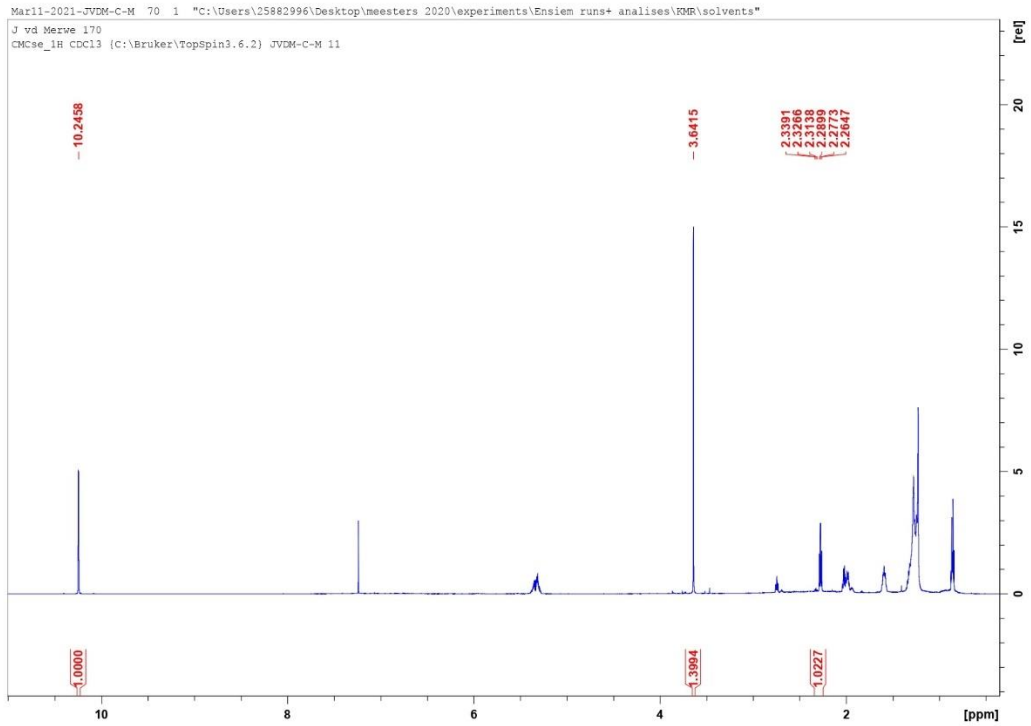

Figure D.26: NMR analysis of the biodiesel produced with hexane-washed lipase, and an oil to methanol molar ratio of 1:3 at 30 °C

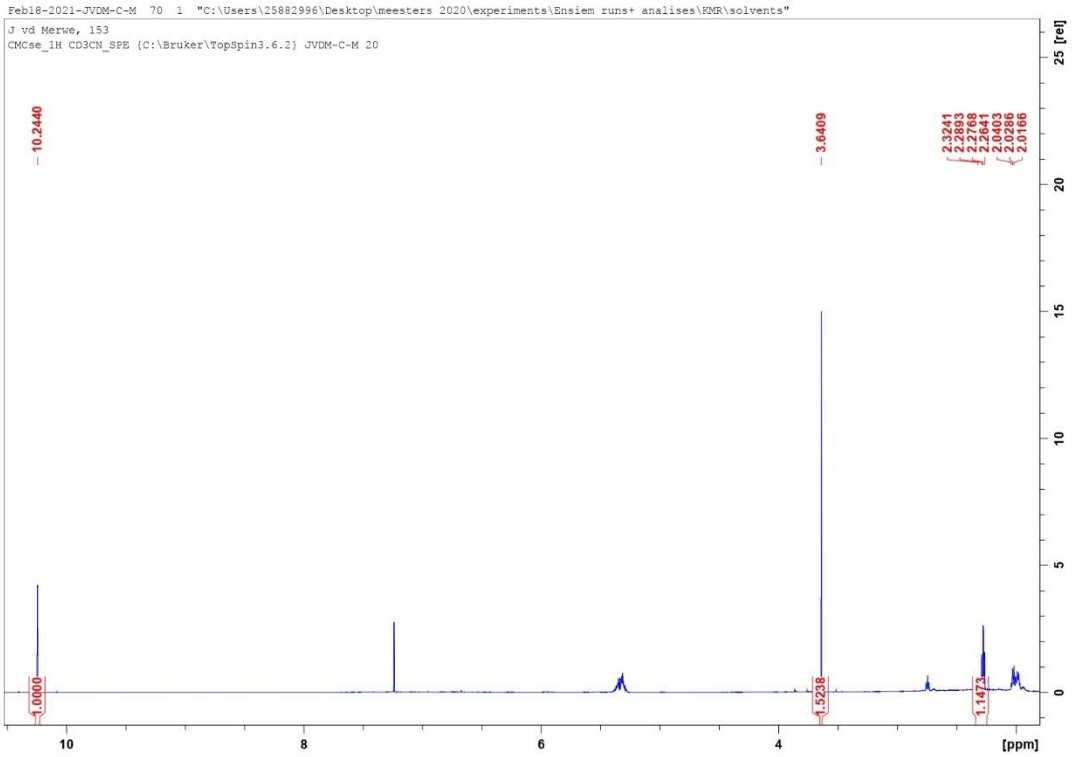

Figure D.27: NMR analysis of the biodiesel produced with isopropanol-washed lipase, and an oil to methanol molar ratio of 1:3 at 30 °C

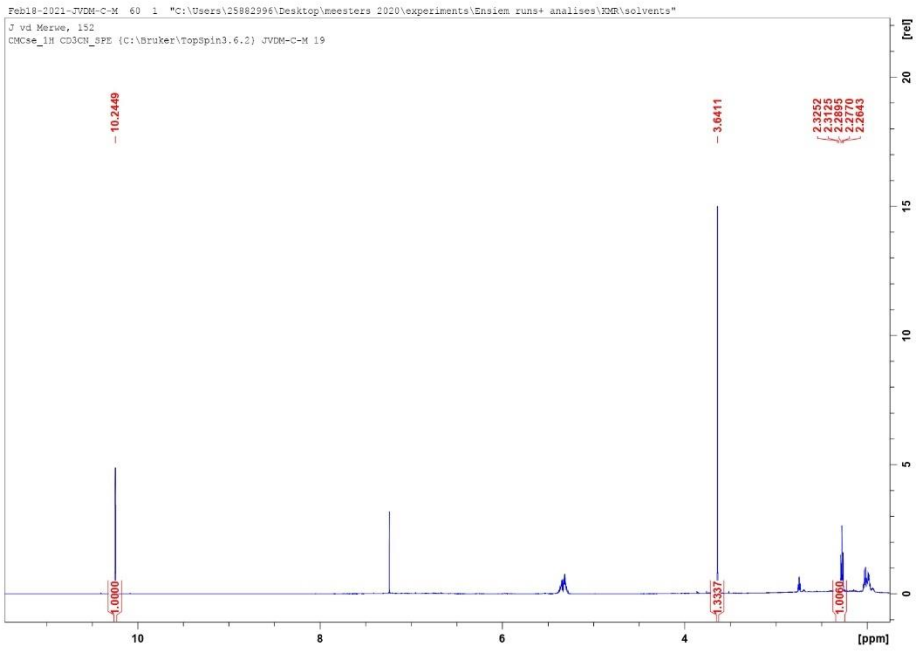

Figure D.28: NMR analysis of the biodiesel produced with tert-butanol-washed lipase, and an oil to methanol molar ratio of 1:3 at 30 °C

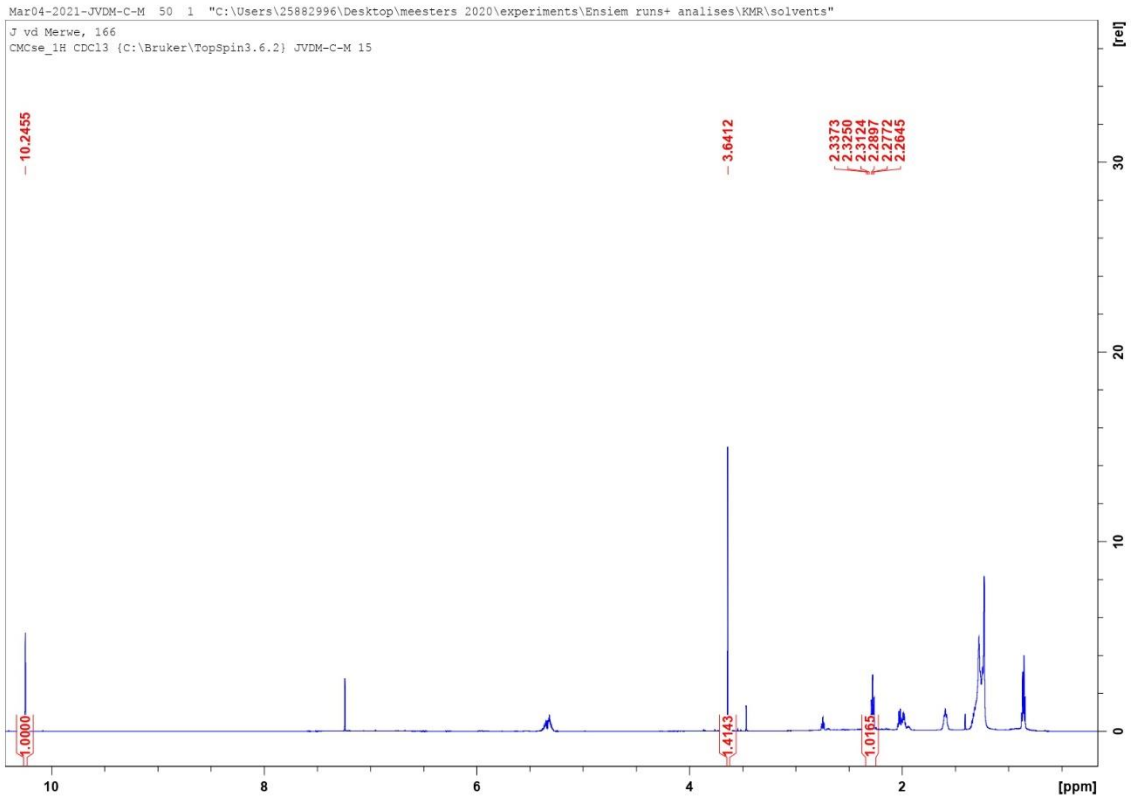

Figure D.29: NMR analysis of the biodiesel produced with THF-washed lipase, and an oil to methanol molar ratio of 1:3 at 30 °C

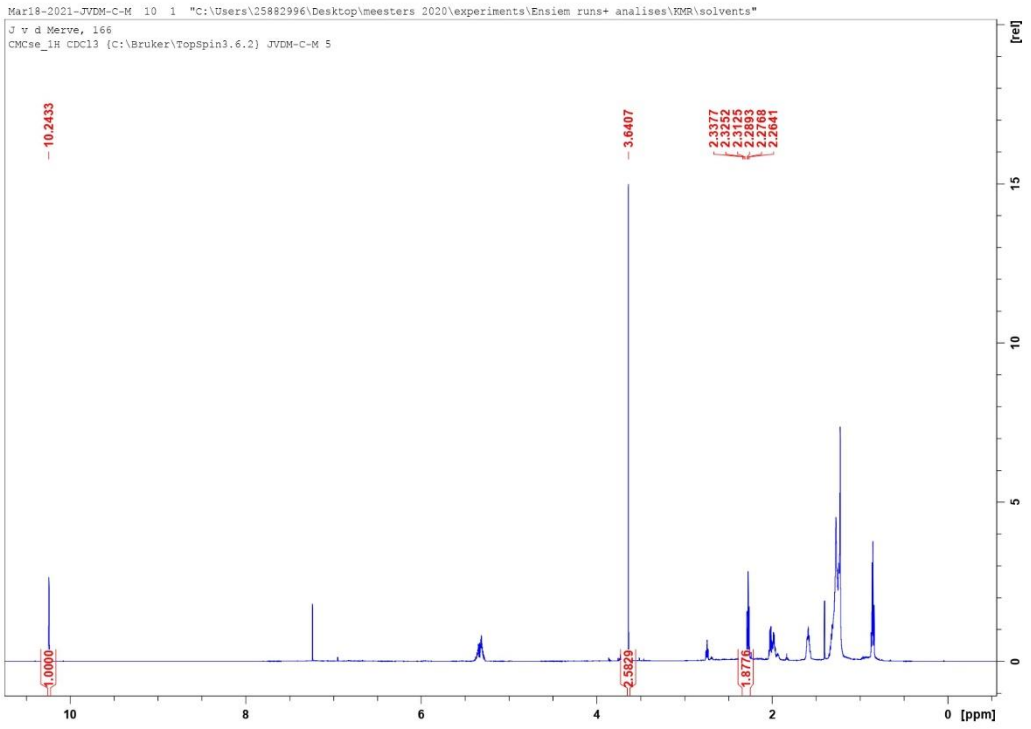

Figure D.30: NMR analysis of the biodiesel produced with recycled lipase (no solvent), and an oil to methanol molar ratio of 1:3 at 30 °C

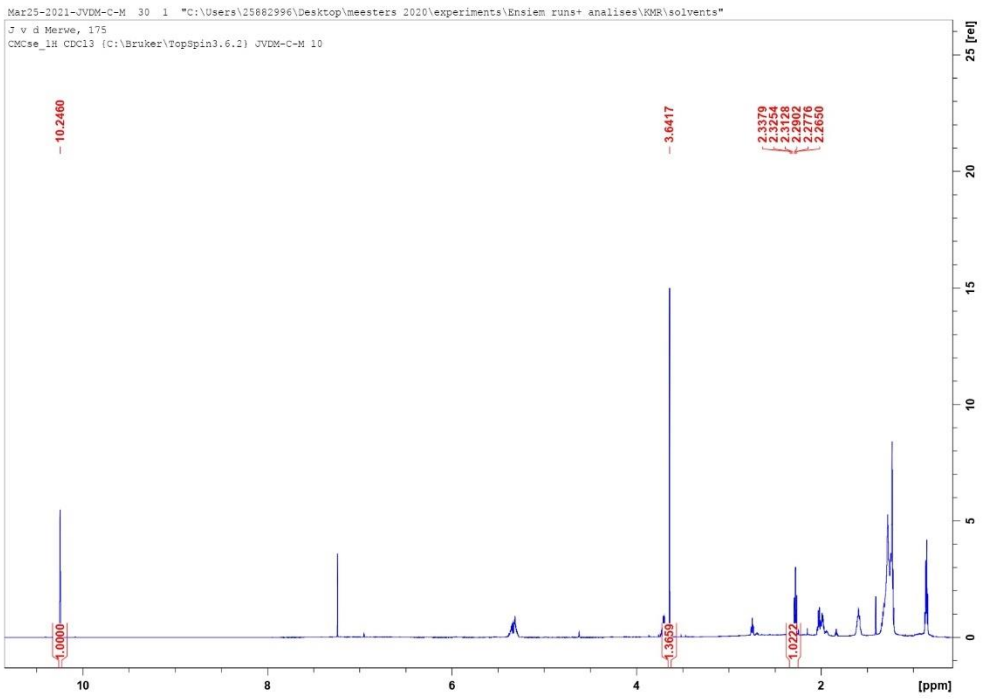

Figure D.31: NMR analysis of the biodiesel produced with recycled lipase (no-solvent second cycle), and an oil to methanol molar ratio of 1:3 at 30 °C

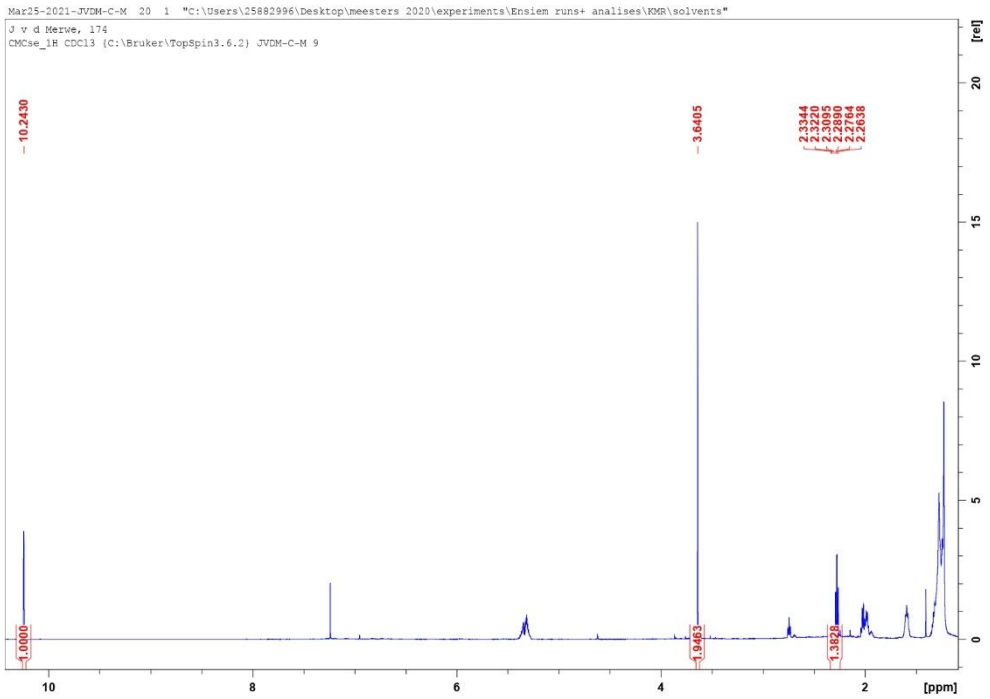

Figure D.32: NMR analysis of the biodiesel produced with recycled lipase (no-solvent third cycle), and an oil to methanol molar ratio of 1:3 at 30 °C

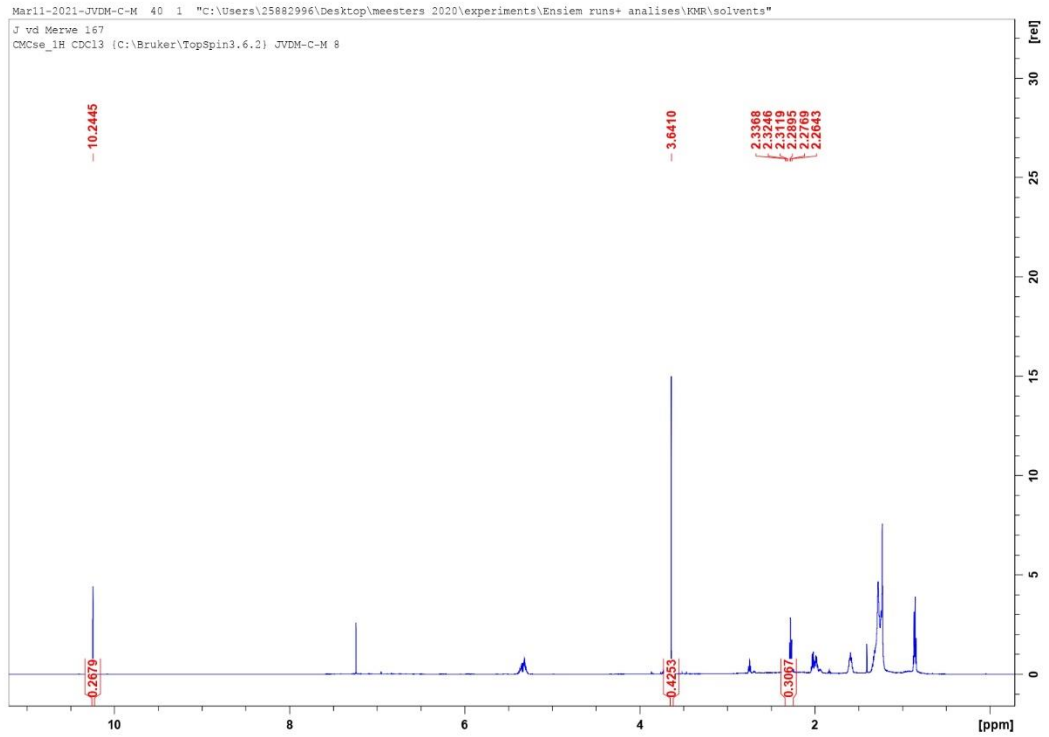

Figure D.33: NMR analysis of the biodiesel produced with acetone-washed lipase (second cycle), and an oil to methanol molar ratio of 1:3 at 30 °C

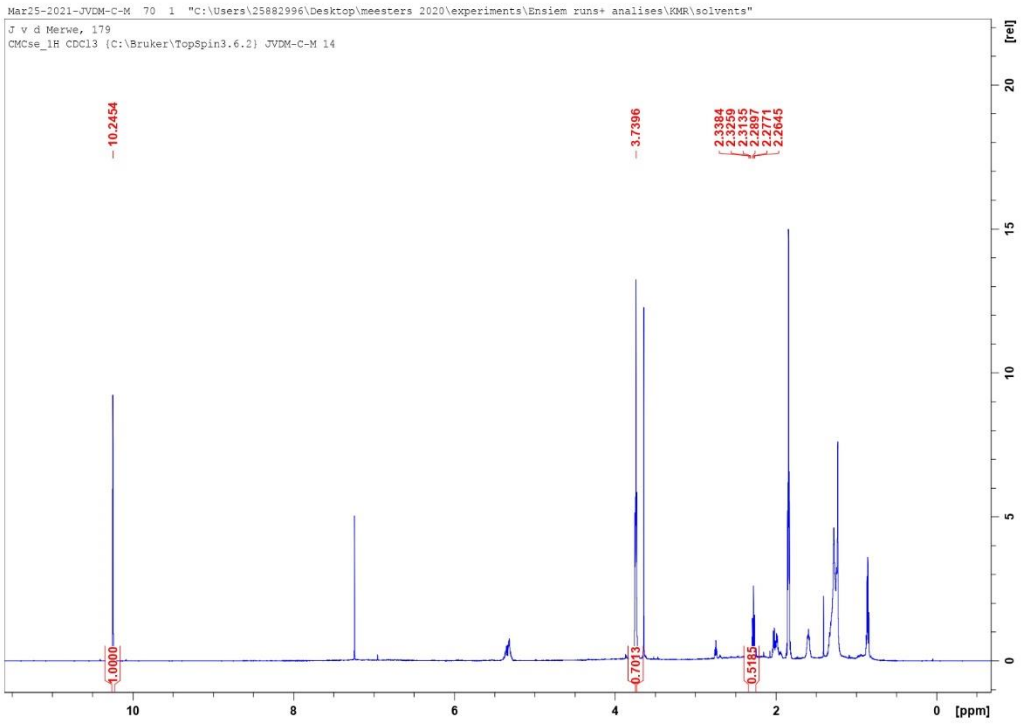

Figure D.34: NMR analysis of the biodiesel produced with acetone-washed lipase (third cycle), and an oil to methanol molar ratio of 1:3 at 30 °C

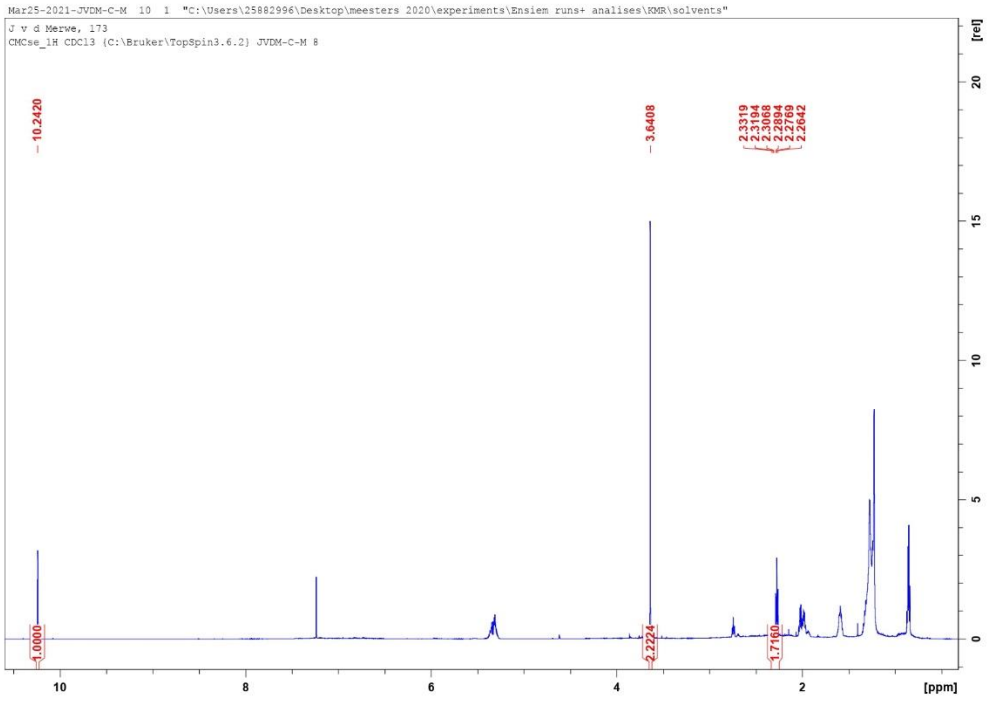

Figure D.35: NMR analysis of the biodiesel produced with acetone-washed lipase (fourth cycle), and an oil to methanol molar ratio of 1:3 at 30 °C

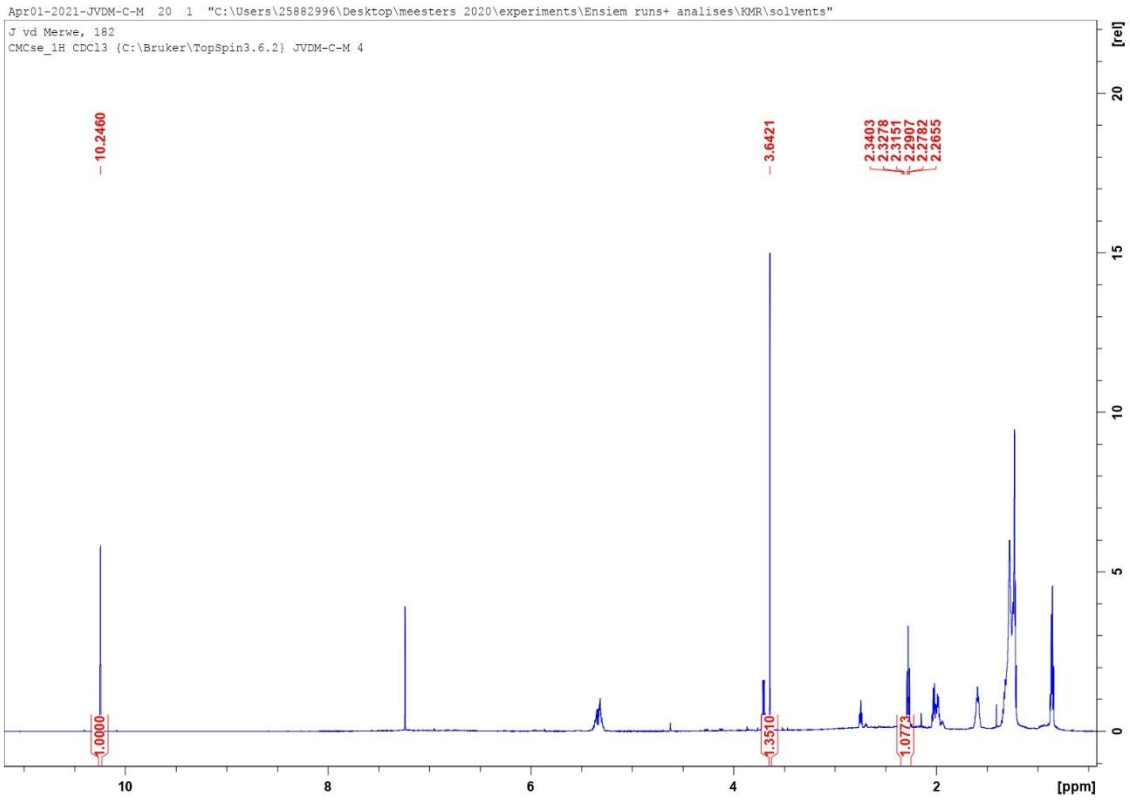

Figure D.36: NMR analysis of the biodiesel produced with recycled lipase (no-solvent fourth cycle), and an oil to methanol molar ratio of 1:3 at 30 °C

Table D.26: HHV of the biocrude oil produced at 30 °C with an oil to methanol molar ratio of 1:3

Run nr	HHV (MJ/kg)	H/C	O/C
1	35.22	1.67	0.18
2	34.20	1.66	0.20
3	35.44	1.63	0.17
Average	34.95	1.65	0.19
Standard deviation	0.66	0.03	0.02
Experimental error (%)	1.22	0.05	0.03